Graduate School of Energy Science, Kyoto University
Master Thesis in Socio-Environmental Energy Science

An Auto-multiscopic 3D Display using Light Diffusion within 3-dimensionally positioned Micro Regions

Supervisor： Prof. Hiroshi Shimoda

Author： Takuya Fujii

Submission： February 10th, 2016

Abstract

Title:

An Auto-multiscopic 3D Display using Light Diffusion
within 3-dimensionally positioned Micro Regions
（3次元配置した微小領域での光拡散を利用した多視点裸眼立体視ディスプレイの開発）

Shimoda Laboratory, Takuya Fujii

Abstract:

With the introduction of IT devices such as tablets, educational materials are becoming more dynamic with animations and touch interactions. By developing an auto-stereoscopic display in which the 3D contents can be observed from any surrounding viewpoints, such dynamic educational materials can be interacted with more effectively. Although many auto-stereoscopic displays have been reported in the past, there remain some challenges in the displays to be applied for above-mentioned educational interface.

Thus, in the present research, an auto-multiscopic 3D display using light diffusion within 3-dimensionally positioned micro regions is proposed, in order to overcome the challenges of existing auto-stereoscopic displays. The proposed 3D display, which is referred to as *LuminantCube*, consists of display body made of glass cuboid with numerous internally processed micro voids, a laser projector to project light towards the display body and a computer to control the projection. By projecting laser light into the micro voids, each void would emit a corresponding colour and brightness to the projected light. Thus, arbitrary 3D images and animations can be presented with a group of emitting points by controlling the projection for each individual micro voids. LuminantCube is able to present 3D contents with spatial effect to any number of simultaneous viewers at any viewpoint, without the requirement for the viewers to wear any kind of special glass-like equipments.

Additionally, an experiment to subjectively evaluate the specifications of LuminantCube was conducted. Here, the specifications of which were measured are the accuracies of representation of 3D solid shapes, spatial effects and 3D animation, as well as the levels of induced visual fatigue and sickness, respectively. The experimental results indicated that, the 3D solid shapes were presented with an accuracy in which the participants were able to recognize the shapes at a size of 35 [mm] with the percentage rate of 65 [%]. Moreover, the spatial effect can be presented with an accuracy of which the error being 2 [mm] or less with 85 [%] probability. The levels of visual fatigue and sickness induced by the observation of LuminantCube with an average duration of approximately 15 [min.] were either low or none.

CONTENTS

List of Figures

List of Tables

Chapter 1 Introduction

In recent years, many researches related to the proposal of various auto-stereoscopic displays have been reported. Many of these displays are aimed to be applied to educational interface, as well as for entertainment and exhibition usages. Specifically, certain types of educational tasks can be performed efficiently and effectively with auto-stereoscopic displays, in other words displays in which the viewers can perceive spatial effect with the naked eyes from any viewpoint around the display. One example would be the 3D representations of molecular structure which are generally shown using sphere blocks. Such methods have a number of limitations such as having to assemble and reassemble the blocks for different structures, as well as not supporting animations namely transitions during a chemical reaction. By using auto-stereoscopic displays, any kind of structures or reactions can be presented realistically in animations without the need of assembly. However, existing auto-stereoscopic displays are not capable of such applications due to the challenges namely, limitations of viewing angle and difficulties in supporting animations.

Thus, in the present research, an auto-multiscopic 3D display using light diffusion within 3-dimensionally positioned micro regions is proposed, in order to overcome such challenges. This display is referred to as *LuminantCube*. Here, auto-multiscopy represent the ability of the display in being able to present 3D contents with spatial effect that can be perceived from any viewpoint and number of simultaneous viewers with naked eyes. LuminantCube consists of a display body, a laser projector and a computer. The display body is made of glass cuboid with numerous micro voids processed internally in a 3D configuration, and the projector is used to project laser light into those micro voids. When light is projected in such manner, an emission is caused by the diffusion of the projected light upon contact with the micro voids. By controlling the projection for each individual micro voids, LuminantCube is able to present arbitrary 3D images and animations with groups of emitting points.

LuminantCube can be observed with multiple viewers simultaneously from any viewpoint. Moreover, viewers can perceive stereoscopy with their naked eyes. Since accommodation and the degree of convergence do not contradict, visual fatigue and sickness commonly induced while observing other 3D applications are expected to be reduced.

To successfully present 3D contents using LuminantCube, the projection must be adjusted for each individual micro voids precisely. Thus, calibration algorithm which can adjust the position of the projection by investigating the correspondence between

each projector pixel and micro voids are developed. Additionally, a middleware which is able to convert standard 3D model format into an optimal data for LuminantCube to present 3D solid model is also developed.

Finally, an experiment to subjectively evaluate the specifications of LuminantCube was conducted.

The present thesis consists of 5 chapters including Introduction. In chapter 2, the background, purpose and applications of the present research are explained. In chapter 3, the principle and hardware construction of LuminantCube are explained. In chapter 4, the details of the experiment for subjective evaluation and results of the experiment are explained, followed by descriptions of future works. The experiment was conducted in order to measure the specifications of LuminantCube such as the accuracies of representation of primitive shapes, 3D animations and spatial effect, as well as the levels of induced visual fatigue and sickness, respectively. Finally, in chapter 5, the research is summarized.

Chapter 2 Background and Purpose of the Present Research

In this chapter, the principles of how depth cues are used by human brains to gain depth perception are explained. Next, existing displays capable of providing depth cues to achieve auto-stereovision are reviewed. Finally, the purpose and the possible applications of the present display are stated.

2.1 Principles of Perceiving Spatial Effect

The human brain processes various informations gained from our visual system in order to perceive the spatial effect. One of the major categories of these information are physical depth cues, which are accommodation, binocular parallax and motion parallax[1]. These cues are commonly used in existing 3D displays with auto-stereovision, which are types of displays that do not require any special equipment such as glasses in order to achieve spatial effect. Details of each cues are mentioned below.

Accommodation

The principle of perceiving the distance to a physical object by accommodation is shown in Fig. 2.1. Here, t_n shows the thickness of the eyes' lenses when observing a physical object in close distance, t_f shows the thickness of the eyes' lenses when observing a physical object in far distance, d and D both show the distances from the eyes to the physical object, respectively. When our visual system observes a physical object, it sends a signal to our eyes to adjust the thickness of the eyes' lenses according to the distance to that physical object in order to focus[2]. In other words, as shown in the figure, the lens would be thicker at shorter distances and thinner at farther distances. In this way, each thickness of the eyes' lenses will indicate the corresponding distance, hence, the distance to that physical object can be perceived[3].

Binocular parallax

The principle of perceiving the distance to a physical object by binocular parallax is shown in Fig. 2.2. Here, L_n shows the image of a physical object in close distance observed by the left eye, L_f shows the image of a physical object in far distance observed by the left eye, R_n and R_f show the images observed by the right eye in the same

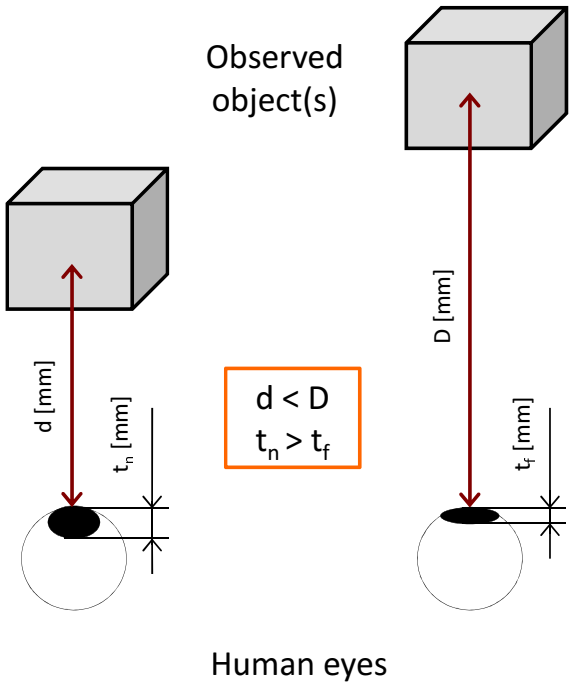

Fig. 2.1: Depth acquired from accommodation.

manner, d and D both show the distances to the physical object, respectively. Human eyes do not observe discrete objects simultaneously, instead they always observe one single object[4]. However, as each eye is placed in a certain distance apart form each other, the viewpoint of each sight differs slightly, causing an inconsistency between the images observed by each eye. In addition, the magnitude of this difference increases and decreases according to the distance to the object which the eyes are observing. Specifically, the magnitude increases as the distance shortens and decreases as the distance lengthens. Hence, the distance to that object can be perceived from the magnitude of the differences of each image accordingly.

Moreover, the angular difference in which the two viewing directions of each eye form changes accordingly to the distance to the physical object. This angular difference is called the degree of convergence, which is shown by θ_n and θ_f in Fig. 2.3. Here, the former shows the degree of convergence when the observed object is in close distance and the latter shows that of when the observed object is in far distance. As can be seen from the magnitude relationship from the two, the degree of convergence expands as the distance to the observed object decreases. Hence, the distance to the observed object can be perceived from the degree of convergence.

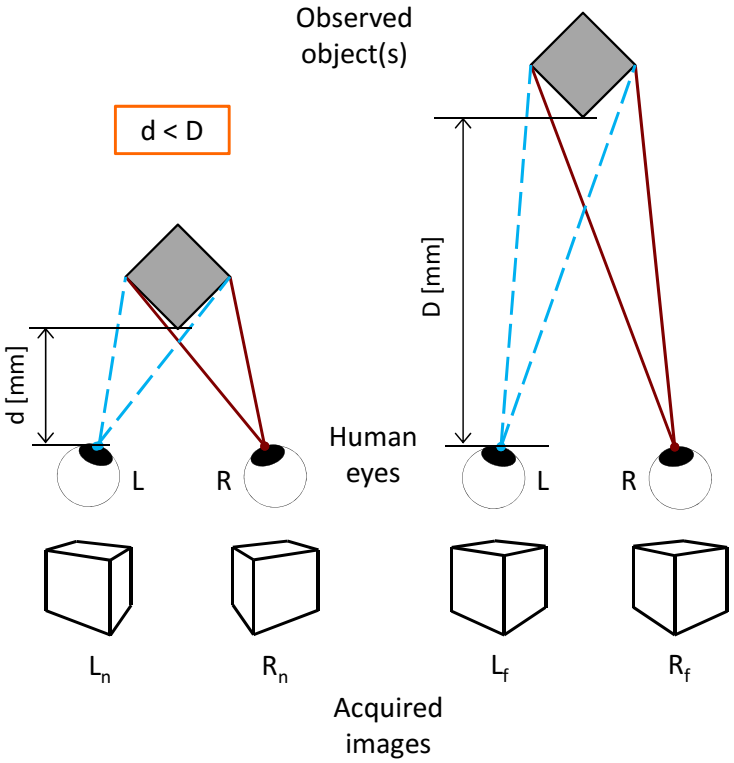

Fig. 2.2: Depth acquired from binocular parallax.

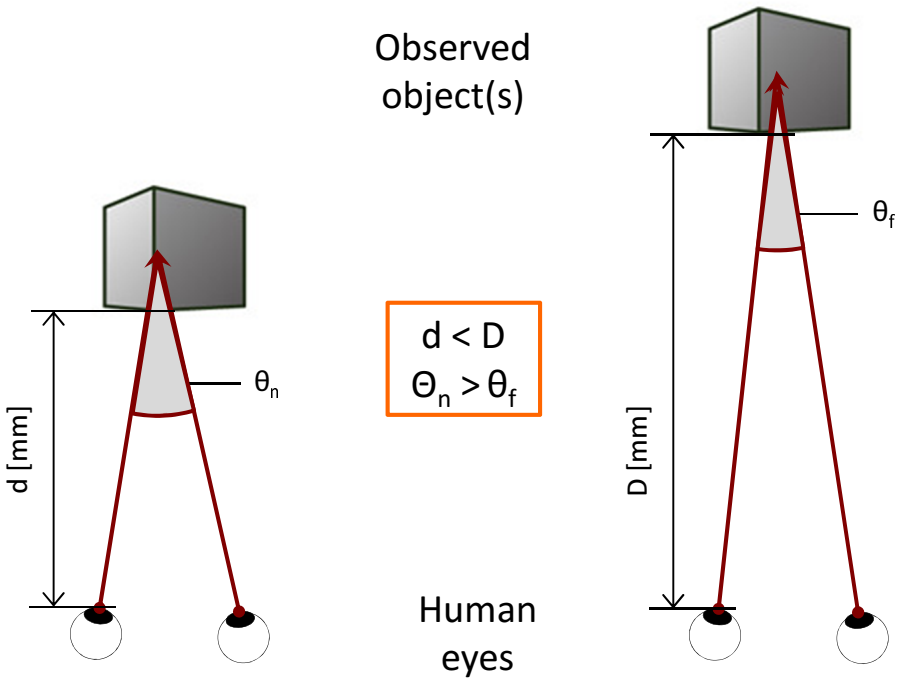

Fig. 2.3: Depth acquired from convergence.

Motion parallax

The principle of perceiving the distance to a physical object by motion parallax is shown in Fig. 2.4. Here, the upper side of the figure shows three observed objects aligned lengthways, [1], [2] and [3] show acquired images when observed from viewing positions indicated by [L], [M] and [R], respectively. Motion parallax is represented by the differences of the motions caused by moving the viewpoint or the observed object. As shown in Fig. 2.4, as the viewpoint moves to right and left, the objects also move sideways accordingly. In particular, objects that are placed closer are visually perceived by the human eyes to move more dominantly, resulting in the furthermost object to be more visible[5]. As shown in this example, the magnitude of the motion difference increases as the distance to the observed object decreases. Hence, the distance to the observed object can be perceived from motion parallax,

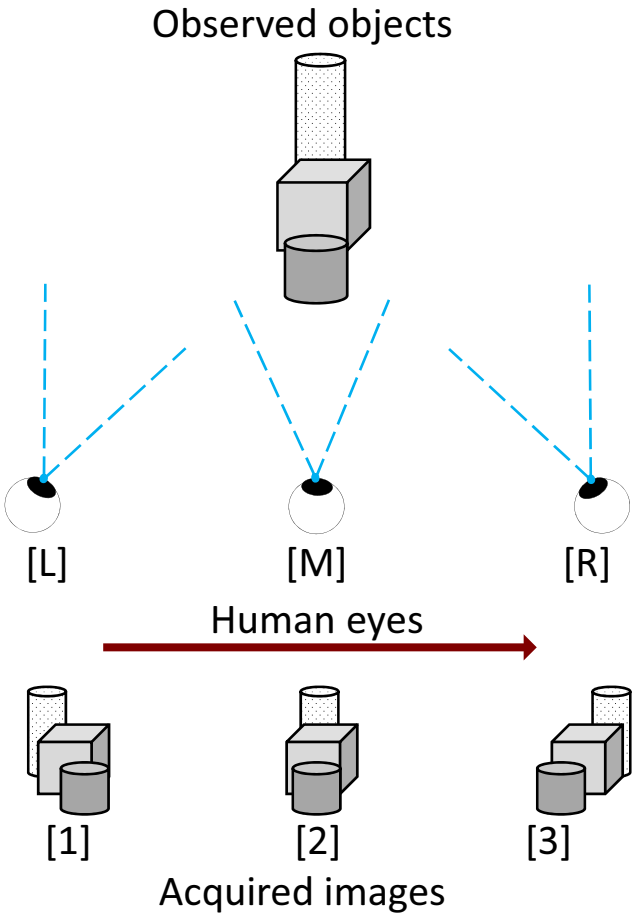

Fig. 2.4: Depth acquired from motion parallax.

Here, binocular parallax and motion parallax are reported to be the most dominant physical cues in the range of viewing distance of general displays, in addition to the fact that the dimensions of the spatial effect perceived from each cues vary according

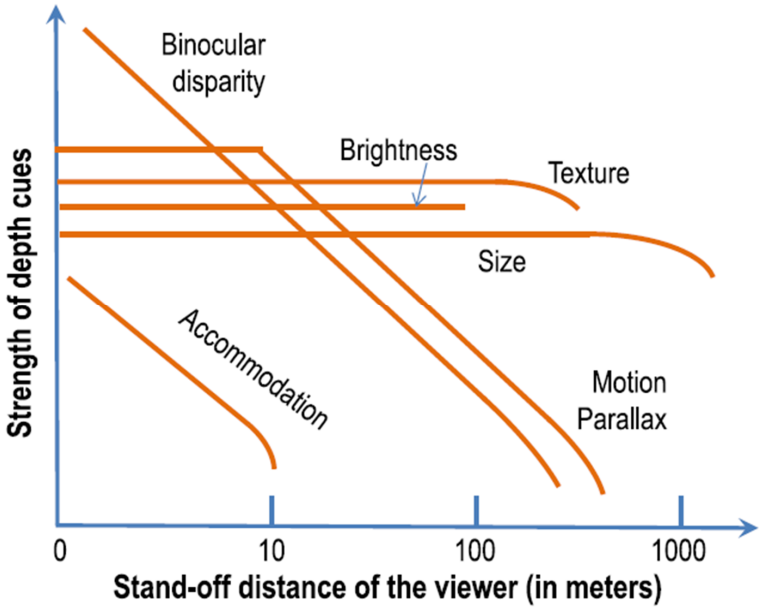

Fig. 2.5: Differences of depth perception between each depth cues[9].

to the distance to the observed object[6–11], as shown in Fig. 2.5[9].

It is reported that when watching a stereoscopic display incapable of replicating both cues of accommodation and degree of convergence simultaneously, the visual information perceived from that experience will not correspond to that of when observing the real world, therefore visual fatigue and 3D-sickness are induced[12–14].This problem is created when a virtual object is made to look like it was placed further away than the actual distance between the observer and the display itself, as shown in Fig. 2.6. Here, the accommodation is adjusted to focus both eyes on the display itself, therefore the distance perceived from accommodation indicates the distance to the display screen, or d in the figure. By contrast, degree of convergence is adjusted according to the distance to the virtual object placed in the virtual space inside the display, which will not always indicate equal distance as the display screen itself, especially when the 3D content to be shown in 3D-TVs is intended to have such difference in virtual distance. In this case, the distance perceived from the degree of convergence will indicate an alternative distance to d, as shown by D in the figure. Thus, each cue will have inconsistency in depth perception to one another resulting in an induction of visual fatigue and 3D-sickness. Therefore, in order to achieve an auto-stereovision on a 3D display with reduced visual fatigue and 3D-sickness, both accommodation and the degree of convergence must be in correspondence relation within the range shown in Fig. 2.7 which is known and described as $Percival's\ Zone\ of\ Comfort$ [15–17].

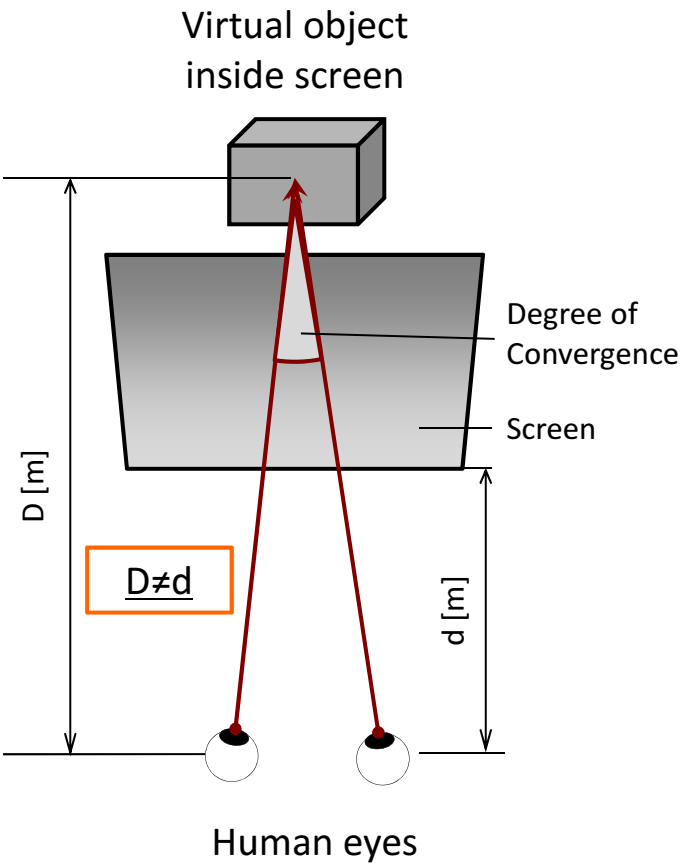

Fig. 2.6: Conflict between depth perception of each accommodation and binocular parallax when using a general flat panel 3D display.

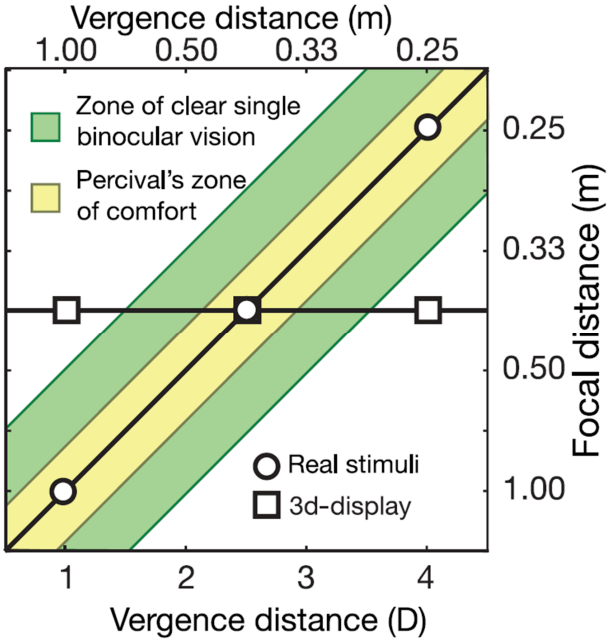

Fig. 2.7: Relationship between focal distance and vergence distance to achieve Percival's zone of comfort[15].

2.2 Existing Researches on Auto-stereoscopic 3D Displays

In recent years, many researches on various 3D displays for achieving auto-stereovision have been reported[18−20].These displays are categorized into representative methods, namely; $SinglepanelMethod$, $LayeredPanelMethod$, $SweptVolumeMethod$ and $Auto-multiscopicMethod$. Characteristics and challenges for each methods are described below.

Single Panel Method

One of the main examples of displays to be categorized in Single Panel Method is the multi-vision display proposed by Iwasawa et al.[21], Yamada et al.[22], Xue et al.[23], Zhao et al.[24] and Brar et al.[25], respectively. These displays use sets of projector arrays and Fresnel/lenticular lens or slitted panels, with the former to be placed behind and the latter to be placed in front of the display screen to output individual sets of screen images to each viewpoint around the front side of the display[26, 27]. Schematic view of such display is shown in Fig. 2.8. As the observer moves sideways in parallel to the display, different sets of screen images would be presented to the observer according to that viewpoint, namely motion parallax is replicated by the differences in acquired images in each viewpoint. However, the main challenge for this display is that the

range of the observer's positions in which motion parallax would be present is limited around the front side of the display. Moreover, as one or more image output equipments are required for each viewpoint, the cost and the complexity of the entire apparatus will increase as the number of the observers or the observable viewpoints increases, accordingly. Other example of Single Panel Method is the display proposed by H. G. Choo et al.[28], which uses pupil tracking in order to present corresponding images to the viewers position. This display requires an array of cameras to track the viewer's position, hence, the entire apparatus will become complicated and the total number of simultaneous viewers are limited to 1-4.

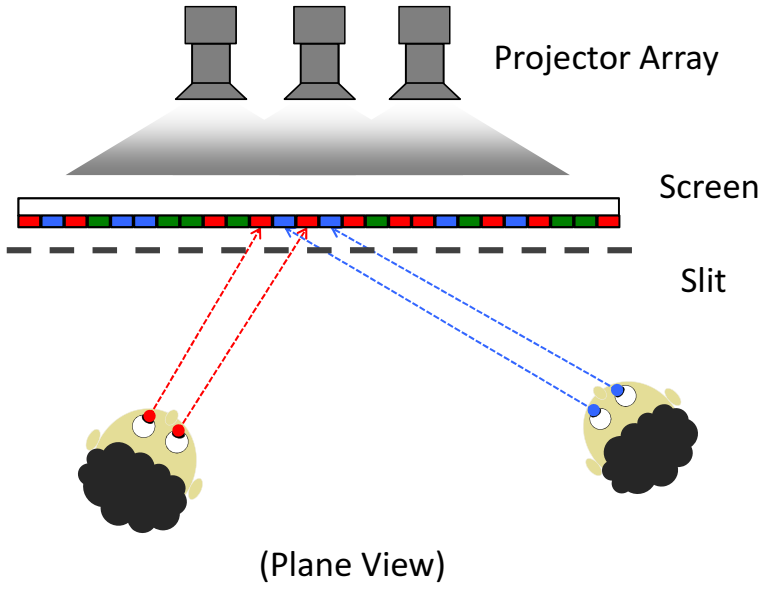

Fig. 2.8: Schematic view of a general Single Panel Method display.

Layered Panel Method

Barnum et al.[29] and Gotoda[30] each proposed a layered 3D display, which uses multiple flat-panel displays layered in longitudinal direction each showing individual screen images based on their distances to the observer. A schematic view of an example of a layered panel method display is shown in Fig. 2.9. Individual displays on each layer are not sterescopic, however stereovision is achieved by observing the layered screen images as a set of a single output image. This is due to each screen image being slightly different to one another while maintaining the distance relationship of corresponding distance between the observer and each layer of the displays. However, the observable area of which the observer can achieve stereovision is limited around the front side of the display in a similar manner as the Single Panel Method. Also, the

cost and the complexity of the entire apparatus increases accordingly with the increase of the number of layers.

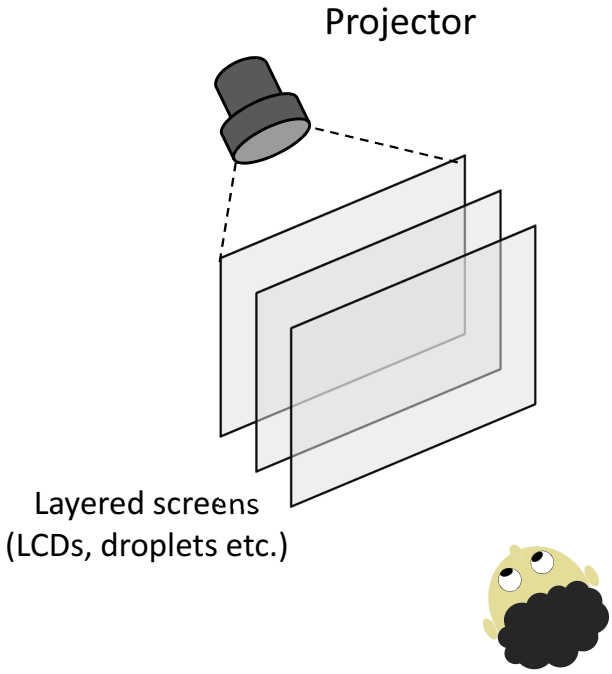

Fig. 2.9: Schematic view of a general Layered Panel Method display.

Swept Volume Method

Swept Volume Method, which uses afterimage to achieve pseudo-volumetric video presentation, can be categorized into spinning array displays proposed by Sun et al.[31], Teng et al.[32], Yendo et al.[33] and Gately et al.[34], and spinning mirror/lens displays proposed by Jones et al.[35] and Takaki et al.[36], respectively. These displays rapidly spin a planar array of LED or a single panel of mirror/lens which reflect light from the projector, while refreshing the image output simultaneously according to the angle of which the plane is facing, in order to present corresponding images for every viewpoint around the entire horizontal perimeter of the display. Thus, the observer will be able to walk around the display freely while being presented with corresponding perspectives of the 3D content for any viewpoint, in other words motion parallax is replicated, resulting in a perception of spatial effect. Displays that are categorized within Swept Volume Method have an advantage of being able to be observed from any horizontal direction. However, as the display needs to be spinning at high-speed, its size is limited. Furthermore, the images flicker even with high refresh rates. For this reason, these displays have difficulties in supporting video output which requires even higher refresh rates.

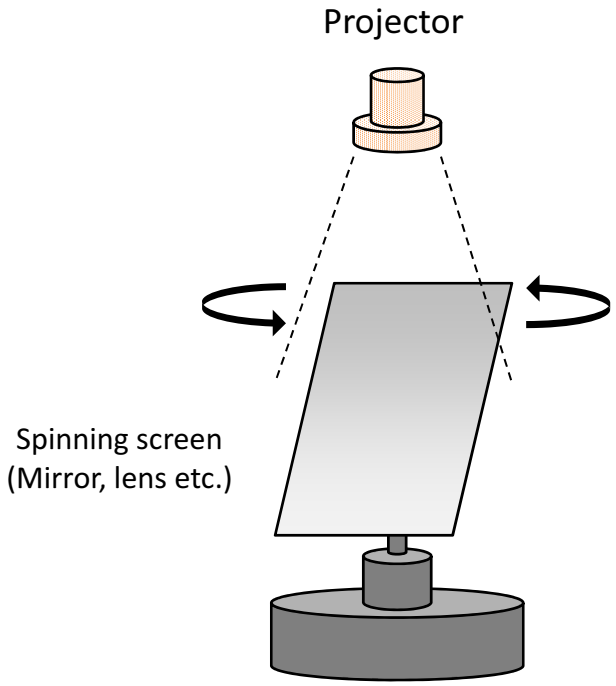

Fig. 2.10: Schematic view of a general Swept Volume Method display.

Auto-multiscopic Display Method

Displays for achieving an auto-multiscopy, in other words auto-stereovision with omnidirectional viewpoints, is represented by the so-called volumetric voxel displays, namely; droplet display proposed by Eitoku et al.[37] and laser plasma display proposed by Ishikawa et al.[38, 39], respectively. Droplet display uses sets of droplets in grid configuration to be dropped in constant frequency in order to form a cubic aligned voxel. Then, a projector placed below is used to project corresponding images to each individual droplet to form a volumetric imagery. This display is able to present volumetric imagery at low cost with a relatively simple structure. However, the resolution and the refresh rate of the presented volumetric imagery is low, making the display inadequate for video presentation. On the other hand, laser plasma display uses a principle of which plasma emission is produced when a high-power laser is focused at a certain point in mid-air. Each plasma emission only lasts for an instant, thus it is repeatedly generated rapidly to present an object image usign saccade-induced afterimage[40, 41]. Schematic view of the display is shown in Fig. 2.11[38]. By producing sequential points of plasma emission, a silhouette of an arbitrary 3D shape can be presented by moving those sequential points to trace the silhouette unicursally. However, as the number of points of plasma emissions that can be produced per certain amount of time is limited, the resolution and the refresh rate of the display will be difficult to increase. Hence, this proves as a challenge for the display to support complex shapes and animations.

Other examples of volumetric voxel displays, such as volumetric LED-array display proposed by Hirayama et al.[42] and vortex display proposed by Tokuda et al.[43], each have similar difficulties in increasing the resolution and supporting animations as the above mentioned displays.

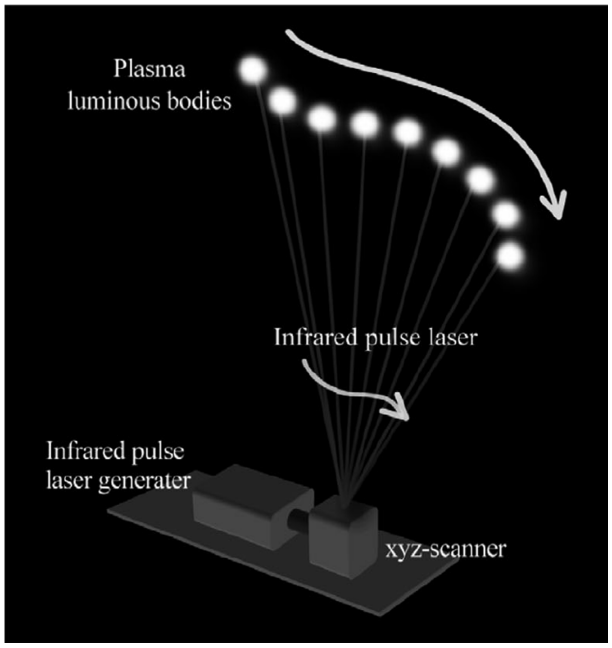

Fig. 2.11: Schematic view of laser plasma display[38].

Altogether, there have been many displays designed to achieve auto-stereovision reported in the past, whereas, a method which overcomes all of the above mentioned challenges simultaneously has not yet been reported[44, 45].

2.3 Purpose and Applications of the Research

In the present research, a new auto-multiscopic 3D display using light diffusion within 3-dimensionally positioned micro regions (hereinafter referred to as *LuminantCube*) is proposed, in order to overcome the existing challenges mentioned in section 2.2 as the ultimate purpose. LuminantCube consists of a cuboid shaped display body made of glass, a laser projector placed next to the display body to project images and a computer to control the projection. It uses the principle of which an emission to every direction is caused by a diffusion of light from the projector when the light hits a micro void processed numerously in 3-dimensional configuration inside the glass cuboid.

LuminantCube can be observed from any direction around the display with any number of simultaneous viewers without any need of special equipments to be worn. It

is also capable of achieving auto-stereovision with correspondence of accommodation and the degree of convergence, resulting reduction of visual fatigue and 3D-sickness.

Main examples of applications for LuminantCube are as follows:

A Truely-3D CAD/Educational Interface for Collaborative Operation

An application to a Computer-aided Design (CAD) and/or an educational interface intended for simultaneous observation and collaborative operation with multiple users can be achieved. Examples of 3D contents to be used in such interface include, a completed 3D model of a design proposal for a complex machinery or a 3D animation for a transition of molecular structure during a chemical reaction. In general, sphere models in various colours are used to replicate molecular structures. However, to show different structures, these models need to be assembled and disassembled every time by hand, as well as having difficulties showing transitions. By using LuminantCube, various kinds of structures can be supported and will be able to present reactions and transitions between multiple substances.

3D Telecommunication Interface

LuminantCube can be used for a 3D telecommunication interface. By installing into the system a depth camera as represented by Microsoft Kinect, which is capable of acquiring depth information in addition to RGB information, it would be able to detect the user's face and facial expressions and present a replication of the person in remote location.

Chapter 3 Development of LuminantCube

In this chapter, the principle, advantages and disadvantages of LuminatCube are explained. Then, the required specifications for achieving auto-multiscopy using the present principle are discussed. Finally, the definitive hardware and software specifications to satisfy the above requirements are described.

3.1 Principle and Characteristics of LuminantCube

In the present research, an auto-multiscopic 3D display using light diffusion within 3-dimensionally positioned micro regions, referred to as LuminantCube, is proposed. As shown in Fig. 3.1, light is projected from a projector towards micro voids which are numerously processed in a 3D configuration inside a light permeable material made cuboid, in order to diffuse light into every direction. Here, by projecting light with various colour and brightness into the micro voids, each projected micro void would emit light with the corresponding colour and brightness. If the projection is controlled for each individual void, each projected micro void would become visible with the intended colour and brightness, with the remaining micro voids invisible. Hence, any image or animation with full colour can be presented by a group of luminous points represented by those emitting micro voids. In this manner, light diffused to every direction would make the emission visible from any viewpoint, namely auto-stereovision with correspondence of accommodation and the degree of convergence as shown in Fig. 3.2 is achievable.

LuminantCube has the following advantages and disadvantages.

Advantages

- Detection of the viewer's position is unnecessary, therefore the entire apparatus can be simplified and there are no time lags in the images even if the viewer's viewpoint is moving.
- Observation with multiple simultaneous viewers is possible.
- The hardware structure of the display can be maintained at low cost while supporting observation with any number of simultaneous viewers.
- While observing the display, viewers can walk around the display freely as it doesn't require them to wear any kind of special equipment.

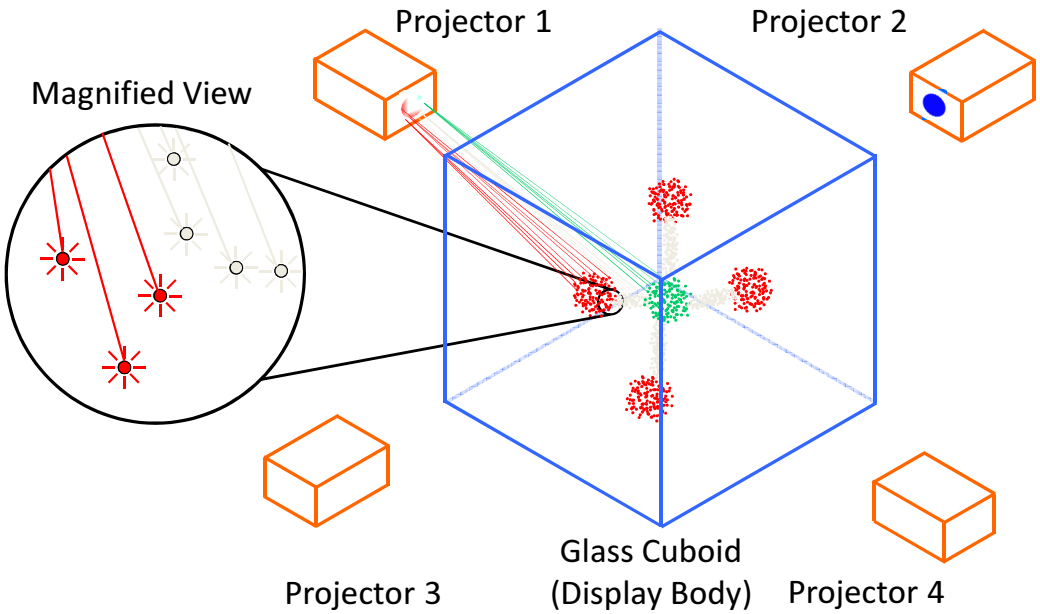

Fig. 3.1: Principle of LuminantCube.

- The entire apparatus is easily transportable, due to the hardware construction being small and simple.
- Visual fatigue and 3D-sickness are expected to be reduced as the correspondence of accommodation and the degree of convergence is maintained at all times.

Disadvantages

- Resolution and contrast ratio are relatively low compared to standard stereoscopic displays used for 3D-TVs.
- The adjustment of the projected image's position need to be done precisely.

3.2 Comparison with a Similar Principle

Nayar et al.[46] proposed an auto-multiscopic 3D display using optical scatterers which the principle in use is similar to that of LuminantCube. Nayar's display uses a projector with high-pressure mercury vapor lamp as a light source in order to project light on to physical cracks processed inside a block of glass by a processing method of laser induced damage[47]. Here, a set of Fresnel lens is used with the projector to reflect the projection into parallel rays when entering the glass block. Also, the size of the glass block is 70 [mm] in height and 200 [mm] for both width and depth. Different number of points are processed internally for each representative 3D contents namely,

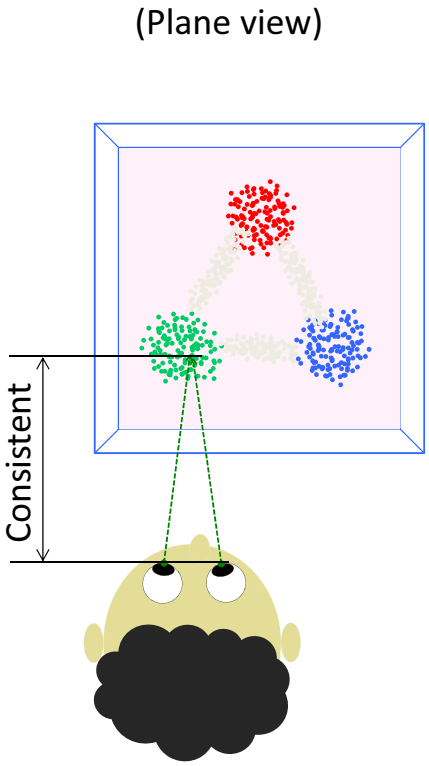

Fig. 3.2: Consistency between accommodation and the degree of convergence.

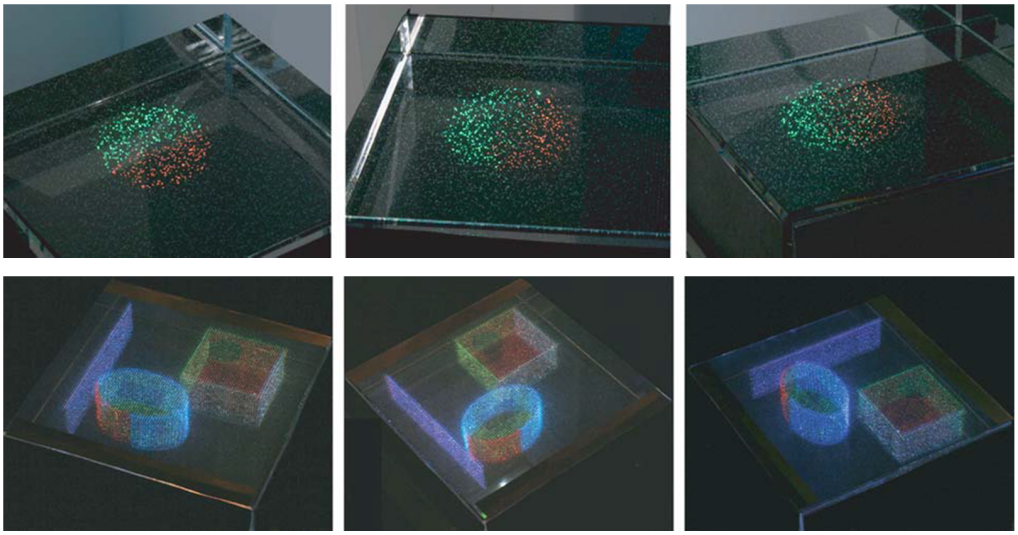

Fig. 3.3: Projection result of an arbitrary sphere and extruded objects on Nayar's display[46].

10000 points for presenting spheres with an arbitrary diameter and colour, and 190500 points for presenting extruded objects with arbitrary colour and cross-sectional shape, which are shown in Fig. 3.3 respectively. Here, by extruded objects, it means that the 3D solid shape shown in the lower row of Fig. 3.3 can only be shown in 3D with translational symmetry in height direction, in other words, the cross-sectional shape cannot be changed. The sphere can be presented in an arbitrary diameter, however the density of the points cannot be increased. On the other hand, if the density of the points is increased, only extruded objects can be presented since the projection cannot be adjusted accurately enough not to project the unintended points.

To project light correctly on to each point, Nayar's display uses a manual calibration method which adjusts the XY grid of the projection to match the correspondence of the projector pixels and the intended point. This procedure does not detect the correspondence of every point, instead only the representative points are detected, and is required to be repeated for each colour channel, thus, the entire calibration procedure takes 6 hours to complete. Also, since the individual errors for each point are not corrected, the accuracy of this calibration method is lower than that of the calibration method used in LuminantCube, which is mentioned in section 3.5. The disadvantages of Nayar's display are that it is difficult to increase the density of the physical cracks due to the low accuracy of calibration method. As a result, in order to present an arbitrary shape, Nayar's display can only increase the density of the points to 3.6 [-/cm^2]. Moreover, as the calibration method requires the projection to be a parallel ray by using Fresnel lens in a set with the projectors, the placement of the projectors will be limited.

In contrast, LuminantCube uses an automatic calibration method which can detect the correspondence between every individual micro voids and the projector pixels, with high accuracy. Consequently, the density of the points of LuminantCube, which is 15 [-/cm^2], is higher than that of Nayar's display which is 3.6 [-/cm^2]. hence, LuminantCube is able to present more detailed 3D content to the viewers.

3.3 Required Specifications of LuminantCube

In order to achieve auto-multiscopy using the principle mentioned in section 3.1, the following requirements must be satisfied:

- Material used for the display body is light permeable.
- Processing method applied for the above stated material is capable of processing micro voids in arbitrary 3D configuration in a non-destructive manner.

- The above-mentioned processing method is also capable of processing micro voids in arbitrary shape and size which can diffuse projected light into every direction uniformly with brightness at a visible level.
- Projector is able to project the projection in focus to any distance in between the range of thickness of the display body in order to increase the contrast.

To satisfy these requirements, the specifications of the material and processing method to be used for the display body, the light source of the projector and the shape and size of the internally processed micro voids are considered in the following manner, respectively:

Material and Processing Method for Display Body

Options of light permeable material to be used for the display body include, glass and 3D-printed transparent resin. For the former, a processing method called *High Power Laser Engraving Method*[48] which focuses high-power laser at an arbitrary 3D coordinate to create a microscopic crack can be used to process micro voids internally. For the latter, by using a certain 3D-printer capable of outputting two materials simultaneously, where the first being the light permeable resin for the base and the second being the opaque resin, display body of an arbitrary design can be achieved. In the present research, two cuboid shaped display body samples with each material processed with the above-mentioned processing methods went under comparative review for the optimal choice to be used for LuminantCube. By projecting identical light towards each sample, as shown in Fig. 3.4, it showed that glass processed with high-power laser had a higher light permeability and showed higher brightness as well as colour reproducibility when projected with light. Thus, glass with high-power laser processing method was decided as the optimal choice of the material and it's processing method.

Light Source of the Projector

There are mainly two types of light sources that are used in standard projectors, which are light bulb type and laser type. The former requires a set of lens to be installed inside a projector in order to adjust the focus of the projection, and the focus changes according to the distance to the projected surface. On the other hand, the latter doesn't require such lens nor any focusing, in other words it is always in focus regardless of the distance to the projected surface. Consequently, laser type projector is optimal for the case of LuminantCube. Specifically, picopro (Celluon Inc.) is used for LuminantCube as it was the only commercially available laser type projector with HD resolution. Here, the throw ratio of picopro is 1.3.

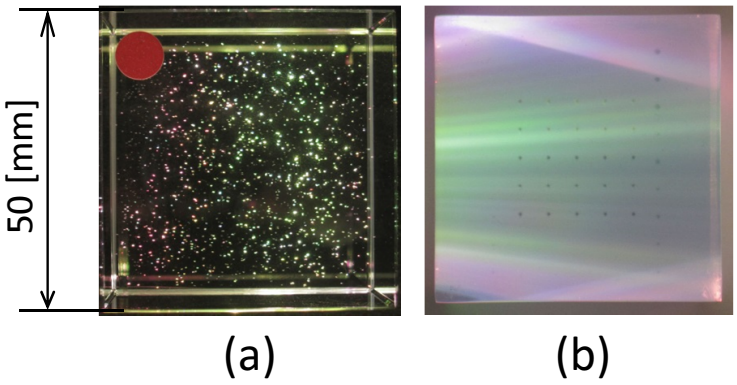

Fig. 3.4: Comparison of the appearance between (a) glass cuboid with laser processing and (b) 3D-printed transparent resin, when light is projected.

Shape of Micro Voids

The shape of each micro void was set to a sphere so that the light projected to the voids would diffuse uniformly in any direction.

Size of Micro Voids

The size of each micro void was decided using a simple test of which diameter would emit light with a brightness above visible level with a single pixel projection. Here, the number of pixels to be used for each projection wasn't considered at this point, since the laser diameter of a single pixel projection would differ according to the distance between the voids and the projector. Note that, it is desirable to keep the diameter of the micro voids as small as possible, in order to be able to process a higher number of voids inside the cuboid to increase the resolution. Since the minimum diameter which *High Power Laser Engraving Method* can process a sphere is ϕ 0.1 [mm], a series of micro voids from a diameter of ϕ 0.1 [mm] to ϕ 0.9 [mm] in every 0.05 [mm] was processed inside a sample to be used for the above-mentioned test. The smallest diameter of which a diffused light with a brightness above visible level was ϕ 0.2 [mm]. Thus, the diameter of the micro voids was set to ϕ 0.2 [mm].

Taking the above-mentioned specifications into account, other specifications of LuminantCube are considered in the following manner, namely the display body size, light source of the projector, position of the projector, configuration of the micro voids and total number of micro voids to be processed.

Display Body Size

The display body size is set to a height of 140 [mm] and both width and depth of 80 [mm], respectively. This is the largest size of glass cuboid which is commercially available which can be processed with *High Power Laser Engraving Method*. Here, the largest size was chosen in order to reduce the effects of the relative error caused by the machinery when processing the voids inside the display body to a minimum.

The display body is divided into two areas; the processing area and the margin area, as shown in Fig. 3.5. The former is the area of which the micro voids will actually be processed and the latter is the area with no micro voids. The margin area is added in order to reduce the occurrence of unintended emissions of micro voids caused by total reflection at inner surfaces of the cuboid. The processing area is set at the centre of the display body with a height of 80 [mm] and both width and depth of 50 [mm], with margins of 15 [mm] to the sides and 30 [mm] up and down. The margins are set to these measurements due to the fact that, in order to eliminate the projected light from re-entering the processing area by total reflection, a margin with a length of 24 % of that of the processing area is required for every dimension, in view of the projector's throw ratio being 1.3.

Position of the Projector

The projector is placed to the side of the display body in a portrait orientation. The position is set to the side for ease of assembling, however, it is ideal to place it below the display to allow the viewers to observe from any direction. The orientation is set in portrait in order to match the aspect ratio of the landscape-oriented projection screen to that of portrait-oriented display surface. Additionally, in order to be able to project light from the projector to every single micro void processed inside the display body, the distance between the projector and the display body was set at 120 [mm], in view of the projector's throw ratio being 1.3.

Here, it should be pointed out that, the position and orientation of the projector will include some errors against the above-mentioned specifications. Therefore, the relative position and orientation of the projector, and the 3D coordinates of each micro voids must be estimated by a calibration algorithm, which the details are mentioned in section 3.5.

Positioning and Total Number of Micro Voids to be Processed

The positioning and total number of micro voids must be carefully determined since the projected light partially penetrates the micro voids at contact. In other words,

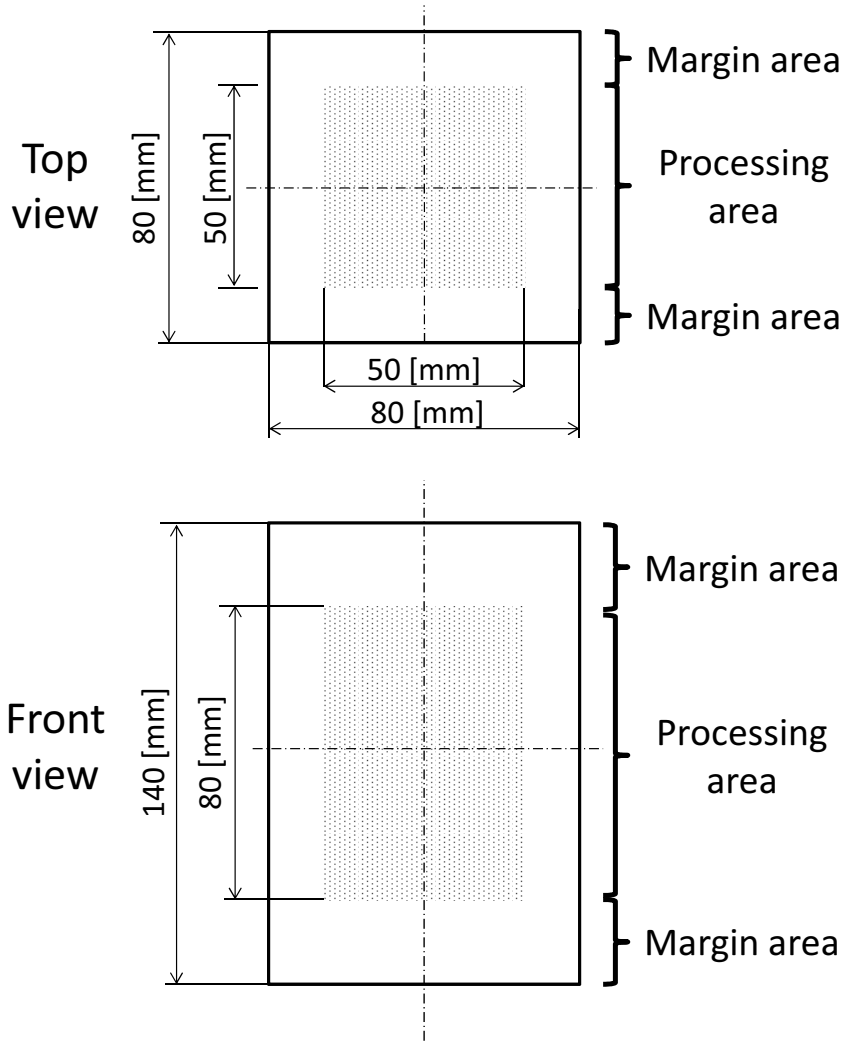

Fig. 3.5: Schematic view of the divided areas inside display body.

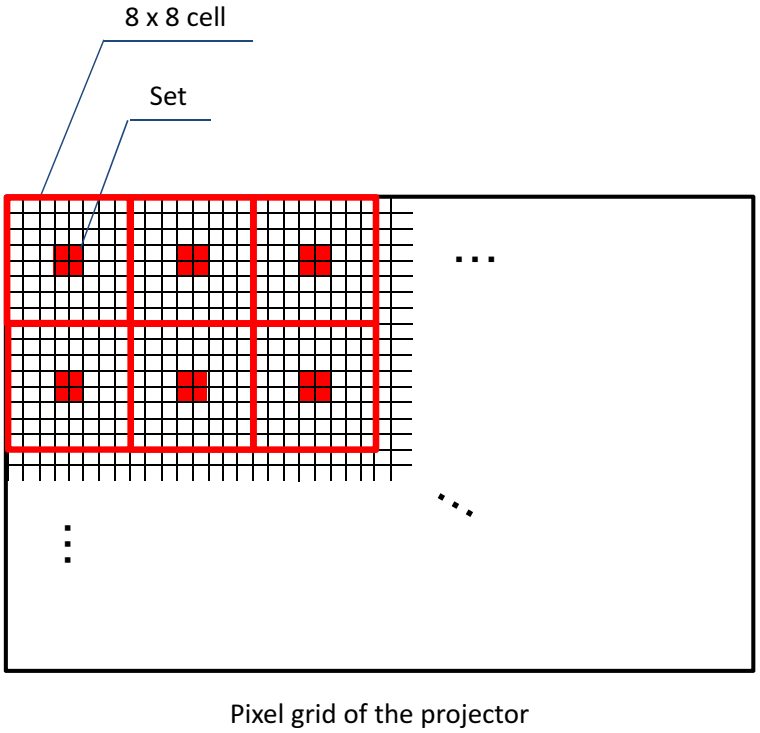

Fig. 3.6: Division of the pixel grid of the projector explained in Step 1 of the void positioning.

if more than one micro void is placed on the pathway of a single projector pixel, unintended emission of micro voids would occur. To reduce the occurrence of multiple micro voids being placed over the routes of the laser projected from single pixel of the projector, a certain distance is maintained in between each micro void. This distance is set to 3.5[mm] and is referred to as the *threshold* when determining the number of micro voids to be processed inside the display body. The threshold of 3.5[mm] was chosen for this distance as it was the smallest distance, in every 0.5 [mm], which can affectively reduce the above-mentioned occurrence. Additionally, the total number of micro voids are determined from 0 and up in every 250 until the below-mentioned algorithm did not converge. The precise position of each micro void was determined using the following algorithm.

Step 1: As shown in Fig. 3.6, the pixel grid of the projector is divided into cells of 8 $\times$ 8, with each four pixel in the centre of each cell being referred to as the *Set*. Then, each set is given a random number between one to the maximum number of sets created. The subsequent procedures are done in ascending order of this number.

Step 2: Pathway of each pixel represented by the sets are calculated according to the

projector's throw ratio, position and orientation relative to the cuboid, respectively.

Step 3: Each set is given a random number between 0 to 50 which is referred to as a depth value. Then, a single micro void is tentatively created at a point on the pathway calculated at Step 2, with a depth distance equal to the given depth value away from the processing area's surface nearest to the projector. Here, depth distance indicates the distance in the direction equal to the axis of the projection's traveling direction.

Step 4: The distance between the void tentatively created at Step 3 and the closest void out of the ones already positioned is calculated. Then, the calculated value is compared with the threshold, in order to determined whether to save the coordinate of the tentatively created micro void if the value is higher, or not to save if the value is lower. If the latter is chosen, the procedure for the present set is canceled and will be started over from Step 3. If this procedure fails for 10 consecutive times for the same set, that set is excluded from the list and the corresponding micro void will not be positioned. By setting the threshold for the number of allowed failures to 10 times, the distribution of the micro voids would become visually uniform.

Step 5: Above procedures are repeated until all sets that are not excluded are done and a database of a correspondence table for void coordinates to projector pixel coordinates is created.

The result of a simulation performed under the above-mentioned algorithm is shown in Fig. 3.7. Here, the wire frame model in the centre shows the cuboid display body, the smaller cuboid placed next to that wire frame model shows the projector and each line connecting the rectangle and the dots inside the wire frame model shows the projectile of the projected light, respectively. In this manner, if the projector is placed 120 [mm] away from the surface of the display body, a total of 3000 micro voids can be configured inside the display body. Thus, the identical number and position of micro voids are processed for the present version of LuminantCube. In addition, 16 voids with a diameter of ϕ 0.3 [mm] which are referred to as *markers* are processed inside the display body, which the details of the position are explained in section 3.4. These markers are used for the calibration algorithm which the details are mentioned in section 3.5.

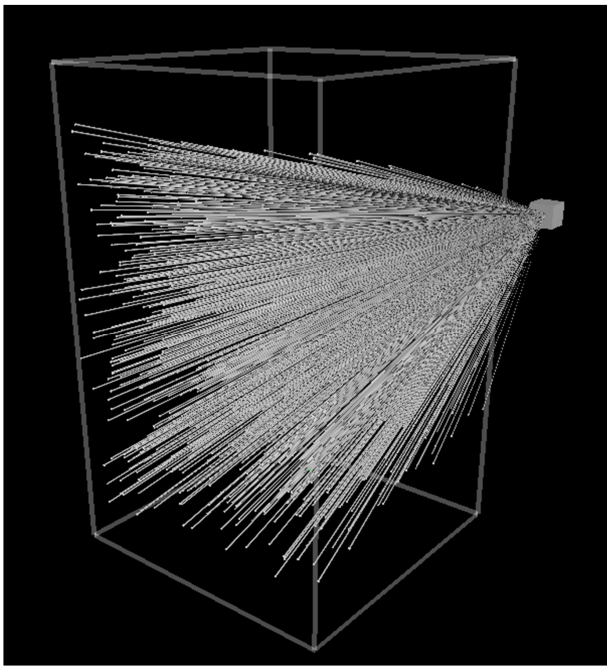

Fig. 3.7: Simulation of projection with multiple projectors.

3.4 Hardware Construction

Schematic view of LuminantCube designed under the consideration of the specifications discussed in section 3.3 is shown in Fig. 3.8. LuminantCube consists of a display body made of a glass cuboid with a height of 140 [mm] and both width and depth of 80 [mm], a laser projector placed in distance of 120 [mm] away from the display body and a computer to control the projection and to output the images of the contents. Detailed descriptions for each component are as follows:

Display Body

The specifications of the display body used in the present research is shown in Table 3.1. As stated in section 3.3, glass is used for the material and *High Power Laser Engraving Method* is used for the processing in order to make the display body for the present research. Inside the display body, there are a total of 3016 micro voids processed in a spherical shape with a diameter of ϕ 0.2 [mm]. 16 of these micro voids are processed with a diameter of ϕ 0.3 [mm], which are referred to as the *markers*. A detailed design of the cuboid is shown in Fig. 3.9. Here, [A] indicated by 4 larger dots is the upper marker section, [B] indicated by the patterned rectangular area is the central micro void section and [C] indicated by 4 large dots is the lower marker section, respectively. Markers are used for estimating the positions and orientations of

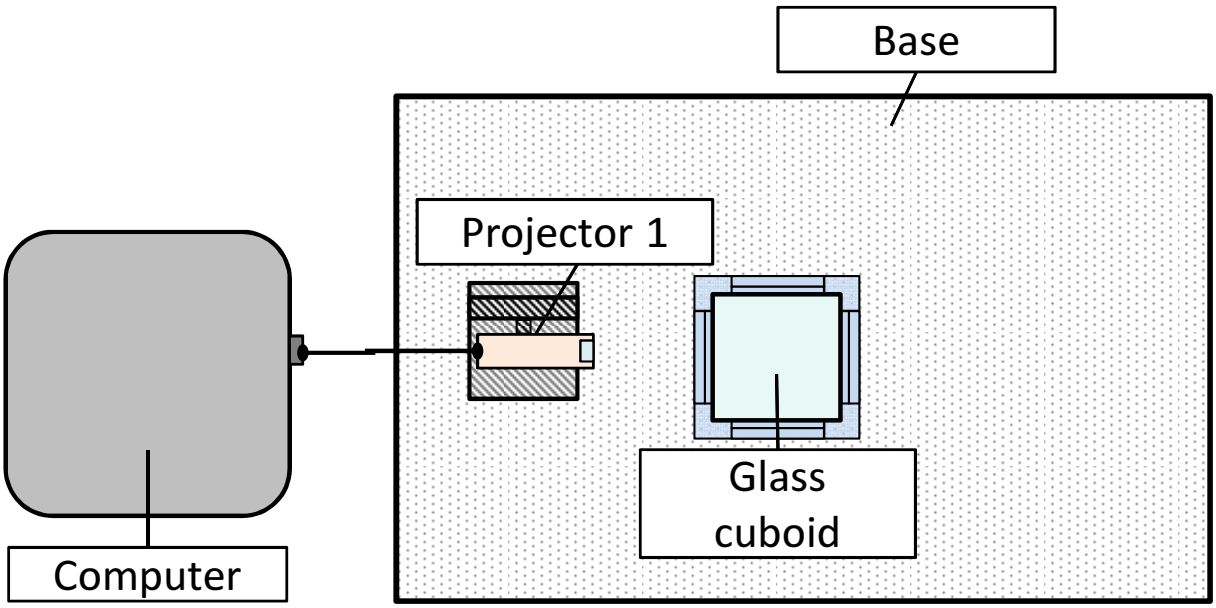

Fig. 3.8: Schematic view of LuminantCube.

the projector and camera, respectively. Details of each purpose of the above-mentioned markers and the estimation method are stated in section 3.5.

Table 3.1: Specification of display body

External Size	H130 × W80 × D80 [mm]
Weight	Approx. 2.3 [kg]
Number of voids	3016
Material	Crystal glass
Processing Method	High-power Laser Engraving Method

Laser Projector

As each micro void is placed in different distances away from the projector, a laser projector (Celluon Inc., picopro) which doesn't require focusing is used for LuminantCube. The specification of the laser projector is shown in Table 3.2. Here, as the emission at micro voids are caused by diffusion of laser light projected from the projector, the refresh rate of the 3D content shown on LuminantCube is identical to that of the laser projector, which in this case is 60 [Hz].

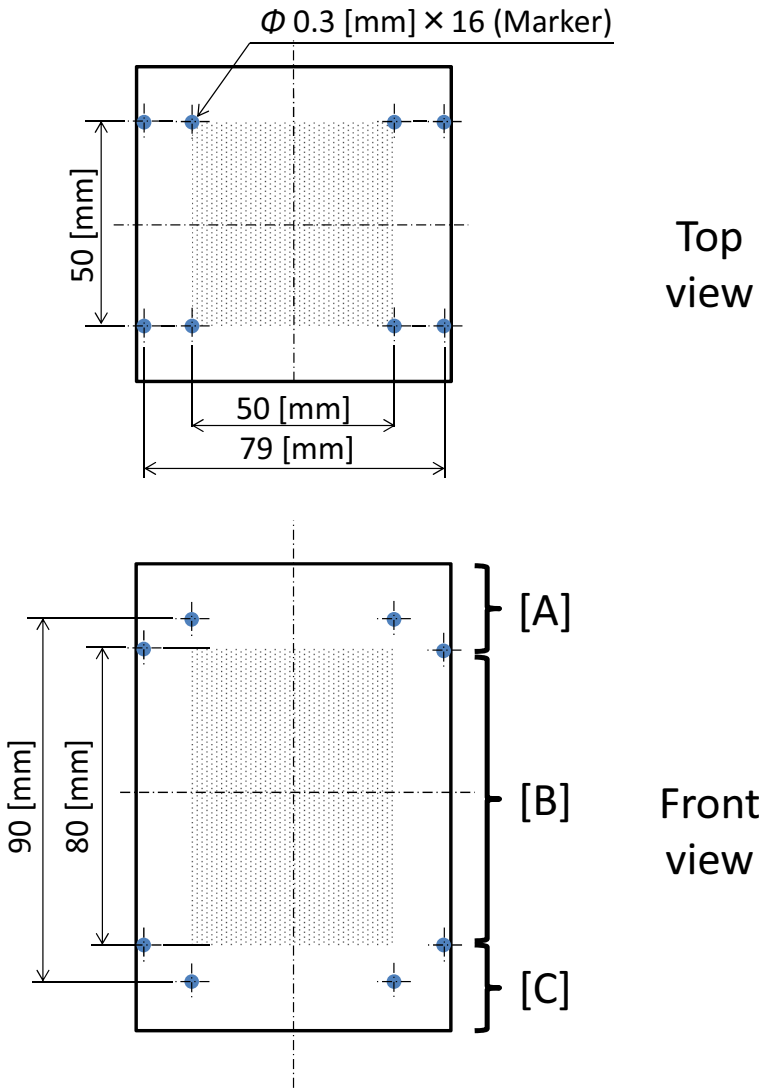

Fig. 3.9: Design of the glass cuboid.

Table 3.2: Specification of laser projector

Display Method	Laser
External Size	H150 × W73 × D13.4 [mm]
Weight	181 [g]
Resolution	1280 × 720 [Pixel]
Brightness	32 [ANSI Lumens]
Contrast ratio	80000:1
Colour Depth	RGB 24 [Bit]
Throw Ratio	1.3
Focus	Focus free (always in focus)
Laser Pulse Frequency	60 [Hz]

Computer

The projector is connected to a computer which is responsible for generating the output images and controlling the projection. The specification of the computer is shown in Table 3.3.

Table 3.3: Specification of computer

OS	Windows 7 Professional, 64 bit
CPU	Intel Core i7-3770 3.40 GHz
GPU	Intel(R) HD Graphics 4000
RAM	16 GB

Here, it should be pointed out that, there are a few disadvantages when using LuminantCube in its present stage consisting of the above-mentioned hardware construction, mainly;

- Usable only in dark environments, namely a blacked-out room with light shielding from the external light, due to low contrast and maximum brightness.
- The outlines and vertices may be ambiguous when presenting 3D contents consisting of solid models with complicated shapes, due to low resolution.

However, the latter drawback caused by low resolution is not considered as a major drawback, as Ye et al.[49] reported that, if a certain amount of correct visual information is acquired, missing or incorrect information would be complemented within the human brain, and would result in a sound perception of an image. Moreover, the above-mentioned drawback are expected to be able to be improved by increasing the number of projectors to be used. The details of the above improvements are mentioned in section 4.4.

3.5 Calibration Algorithm

To project to individual micro voids accurately, the position of the projection must be adjusted with the refraction caused at the surface of the display body taken into account. Thus, in the present research, calibration algorithms aiming to perform the adjustment automatically by investigating the correspondence between each pixel of the projector and the voids are developed. To perform the procedures of the calibration, a camera (Ximea, MQ013CG-E2) is used to detect the emission of the micro voids when individual pixels of the projector are projected, which is placed facing the display body as shown in Fig. 3.10. The specifications of the camera are shown in Table 3.4.

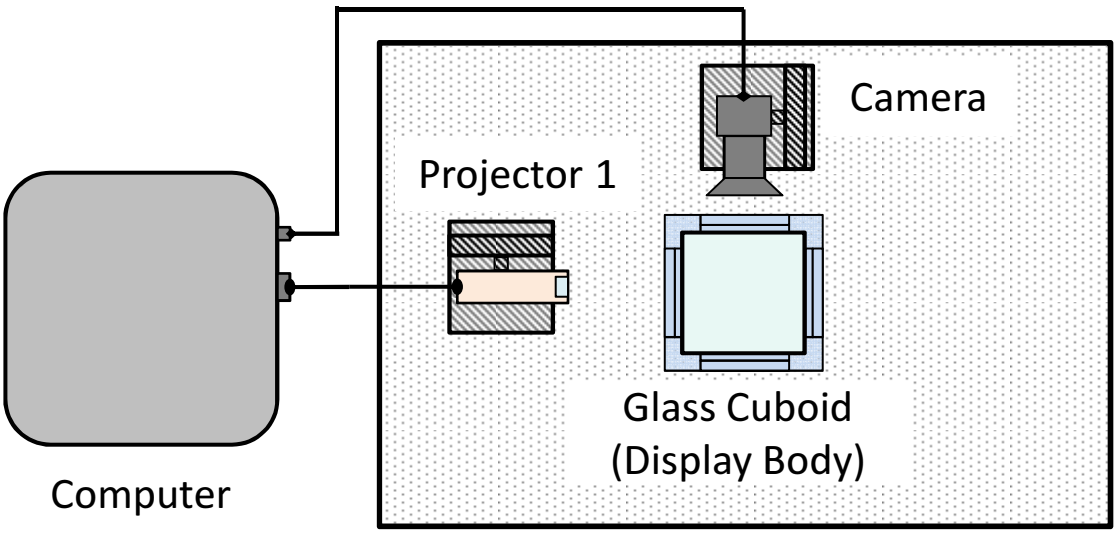

Fig. 3.10: Schematic view of apparatus for calibration.

Table 3.4: Specification of camera used in calibration

Resolution	1.3 [MP] (1280 × 720) [Pixel]
Sensor type	CMOS RGB Bayer Matrix
Sensor size	1/1.8”
Sensor active area	6.9 × 5.5 [mm]
Pixel size	5.3 × 5.3 [um]
Bits per pixel	8 [Bit]
Dynamic range	60 [dB]
Frame rates	60 [fps]
Image data interface	USB 3.0
Lens mount	C or CS Mount
Weight	26 [g]
External size	H26 × W26 × D26 [mm]

A brief description of the procedure which is performed repeatedly for the calibration is as follows:

1. Relative positions and orientations of the projector and camera to the display body are estimated, respectively.

2. Arbitrary pixel(s) of the projector is(are) projected towards the display body. Here, based on the position and orientation of the projector and the known 3D coordinates of the micro voids, the area of which the voids may emit are estimated.

3. An image of the display body is acquired using a camera while projecting , and the presence or absence of any emitting micro void is detected from the estimated area in the acquired image.

4. If present, the 3D coordinate of that emitting micro void is calculated based on the position and orientation of the camera, the camera's pixel coordinate of which that emitting micro void was acquired and the known 3D coordinates of the micro voids .

5. Based on the above informations, a correspondence table of projector pixel coordinate of which is projected to micro void's 3D coordinate of which is detected is created.

Here, the above-mentioned procedure is repeated until every pixel of the projector is detected whether it corresponds to any of the micro voids. Moreover, in the case of the present research, the projection is adjusted for every 2×2 projector pixels in the second step of the procedure in order to shorten the processing time, since the adjustment of single projector pixel was confirmed to be too fine from a preliminary test. The details of each step are mentioned below.

The respective position and orientation of projector and camera to the display body are required in order to calculate the positions of the detected emitting micro voids. They are estimated by solving a PnP (Perspective-n-point) problem[50], which is shown in Fig. 3.11. This is performed by acquiring an image containing n points with known 3D-coordinates and investigating the coordinates of the pixels in which those points are acquired. A function to solve PnP problem which is provided along OpenCV library is used to solve PnP problem in the present research. In the case of LuminantCube, markers that were mentioned in section 3.4 are used for the above-mentioned known points. Since PnP problem requires at least 4 points and the accuracy of the estimation increases accordingly to the increase of the number of points, a total of 16 markers were processed inside the display body. The camera is placed so that all 16 points are framed in, and the position and orientation of the camera are estimated by solving PnP problem

with these 16 points. The internal parameters of the camera, which are required when solving PnP problem, are obtained using a camera calibration software (Graphics and Media Lab, GML C++ Camera Calibration Toolbox)[51]. Additionally, since projectors can be considered as an opposite device against cameras in terms of both having similar internal parameters such as resolution and viewing angle/throw ratio, the position and orientation of a projector can be estimated in the above-mentioned manner.

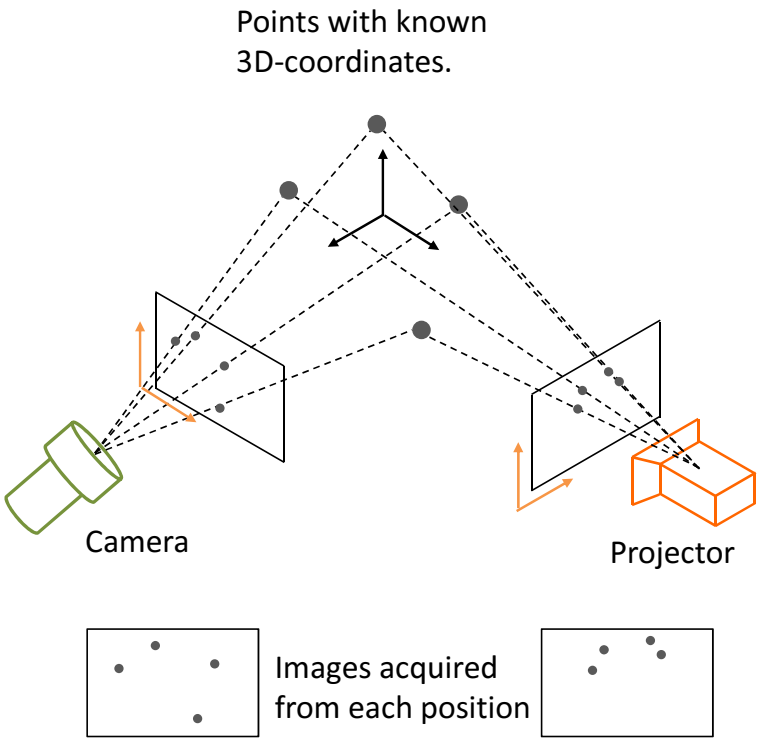

Fig. 3.11: Principle of PnP problem.

In order to detect the emission using a camera at the third step of the above-mentioned procedure, an adequate amount of contrast or brightness is required between emitting and non-emitting voids. If the contrast is too low, the shutter speed or the sensitivity of the camera must be increased to improve the conditions. However, increasing these components would also result in an increase of image noise and decrease of the accuracy of image processing. Therefore, in this research, a noise reduction procedure shown in Fig. 3.12 is performed. Here, [A] is the image acquired with projection, [B] is the image acquired with no projection, [C] is the differential image acquired by subtracting [B] from [A], [D] is the image acquired by adding median filter to [C] and [E] is the image acquired by processing binarization to [D]. Generally, if no noise reduction is performed, an image similar to [A] is acquired and since the difference between pixels that are indicating either luminous voids or image noise is very small, it is almost indistinguishable. However, by acquiring [C] in the above-mentioned

manner, most of the noise can be eliminated from [A] with the pixels that are indicating luminous voids remaining. As there are a slight amount of image noise remaining, a 3 × 3 median filter is performed to reduce such noise. Here, a 3 × 3 median filter replaces the brightness of the centre pixel of 3 × 3 pixel grid with the median of that of all 9 pixels, which levels the brightness of the entire image. Generally, noise appear on single individual pixel, where as the pixels which indicate the emission of the micro voids extend across multiple pixel, therefore the median filter is able to eliminate the noise. In addition, binarization process is performed in order to separate the pixels which indicate the emission of the micro voids from the background. As a result, only pixels with a certain brightness or higher is remained, as shown with [E] in Fig. 3.12. By performing the above-mentioned process, accuracy of image processing during the procedure of calibration is improved.

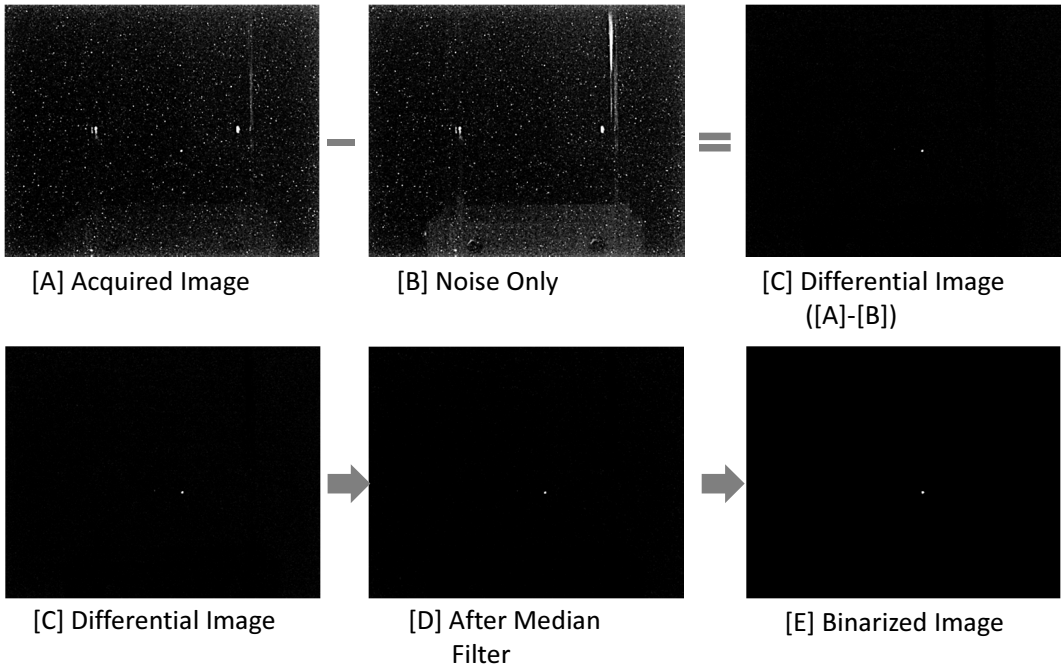

Fig. 3.12: Noise reduction used during the detection of emission.

Based on the estimation of the position and orientation of the projector and camera, the pathway of the projection and the area inside the display body in which the emission is most likely to occur can also be estimated, as shown in Fig. 3.13. By limiting the area in which the detections of the emission are to be performed, which is referred to as the scanning area, the possibilities of causing errors such as detecting unintended emissions outside the area can be reduced.

One kind of method to perform the above-mentioned procedure is to project a single projector pixel for each procedure, starting from the upper-left corner to the bottom-

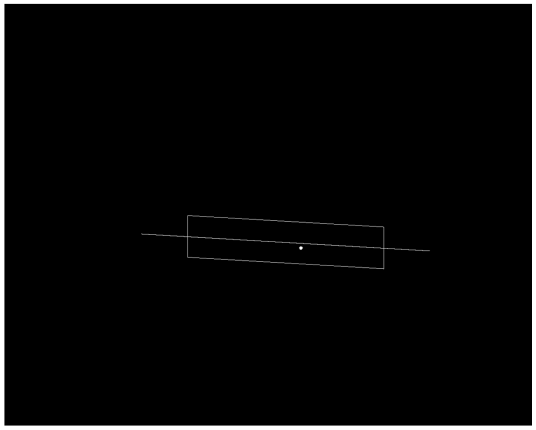

Fig. 3.13: Estimated scanning area and pathway of projection.

right corner, which is referred to as *Pixel Scan Method* in the present research. This method requires the procedure to be repeated for the total number of times equal to the projector's resolution. Since the projection is adjusted for every 2×2 projector pixels, the procedure is repeated for 230400 in the case of the present research. As an image must be acquired and processed for noise reduction for each procedure, which is repeated for the above-mentioned number of times, this method consumes a vast amount of time.

In order to shorten the total processing time of the calibration, the repeat count of the procedure must be decreased. Thus, in the present research, calibration methods which projects multiple projector pixel simultaneously for each procedure to decrease the processing time are proposed, which are referred to as *Line Scan Method* and $Structured - Light\ Method$.

As shown in Fig. 3.14, Line Scan Method projects a single line of pixels, both horizontally and vertically for each procedure from edge to edge, with the height or width of the line being 2 pixels, and acquires an image of the display body respectively. The purpose of projecting in line of pixels is to increase the number of pixels to be projected simultaneously, in other words decrease the number of images to be acquired in total, in order to shortened the processing time accordingly. As shown in Fig. 3.15, the detection of an arbitrary pixel can be performed by calculating the product of the two acquired images correspondent to the respective input images with the according horizontal and vertical lines to that pixel's horizontal and vertical position. The detection for all projector pixels can be performed only with the number of acquired images equal to half of the sum of rows and columns of the projector's resolution, which in the case of the present research is 1000. Here, the total number of acquired images would be 2000 which is the sum of rows and columns of the projector's resolution if

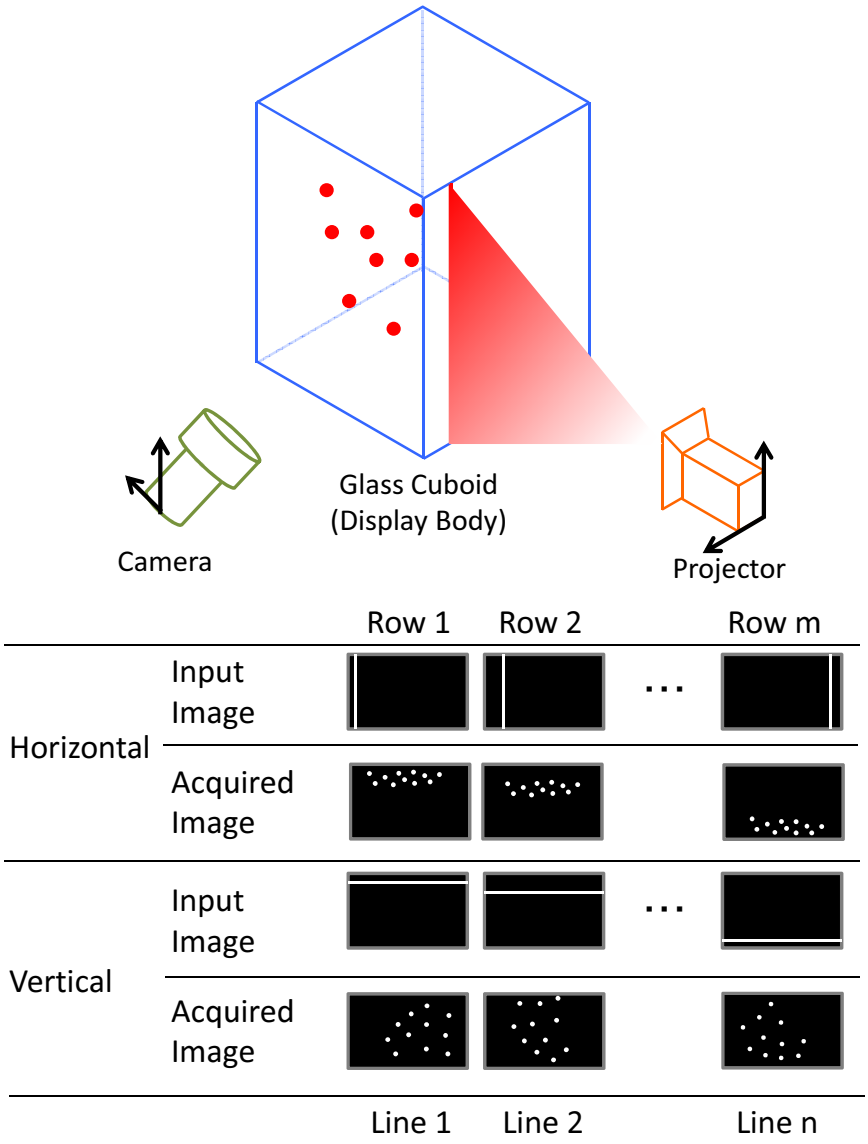

Fig. 3.14: Positional relation of each component and procedure of image acquisition for Line Scan Method.

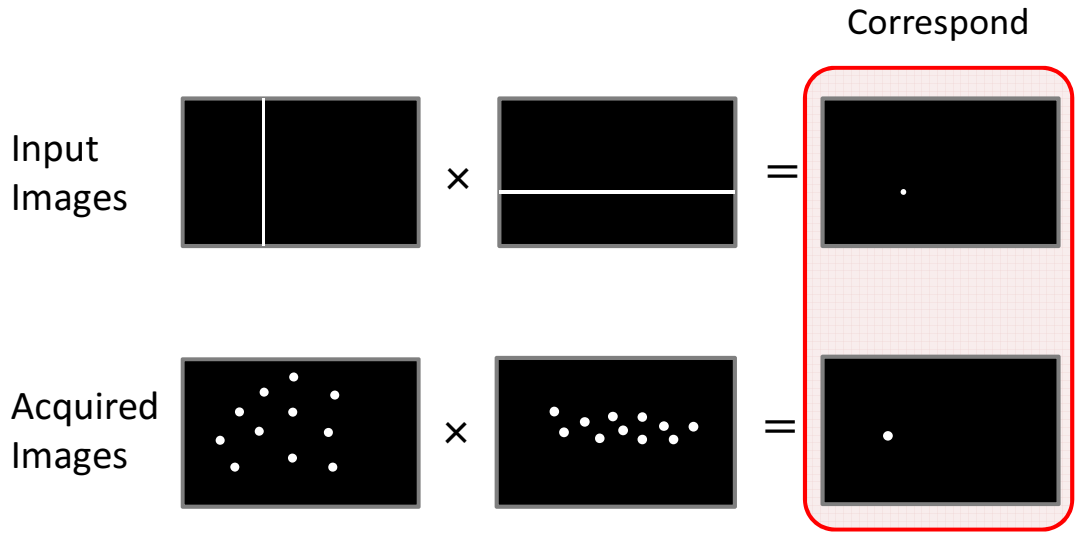

Fig. 3.15: Principle of Line Scan Method.

the height or width of the projected line was set to 1 pixel. Since the total number of repeat count of the procedure is equally reduced, the total processing time for the calibration can also be shortened as compared to Pixel Scan Method.

On the other hand, as shown in Fig. 3.16, Structured-Light Method projects a combination of arbitrary striped patterns of pixels and acquires an image of the display body respectively. Here, the numbers written above each image indicate the the total number of pixels in width or height for each black and white stripes. The white stripe is the area that is projected and the black stripe is the area that is not projected. The height and the width of the pattern are varied for each time so that the detection of an arbitrary pixel can be performed in the same manner as Line Scan Method, by calculating the product of a certain combination of the input images. Here, the height and width of the projected pattern start at exactly half of the resolution in either direction and are halved each time until it is repeated for 5 times, then the number of pixels are reduced from 18 to 2 by 2 at a time. This is also repeated for the identical patterns with the projecting pixels inverted, as shown in left and right side of Fig. 3.16. Here, the total processing time can be shortened to an order of logarithm of the projector's resolution, which in the case of the present research is 392.

The total processing time and the concordance rates of each calibration method are shown in Table 3.5, respectively. Here, concordance rate indicates how the results of the correspondence table detected with Line Scan Method and Structured-Light Method concord with that of Pixel Scan Method, respectively. As can be seen from Table 3.5, the total processing time of Line Scan Method and Structured-Light Method decrease compared to Pixel Scan Method.

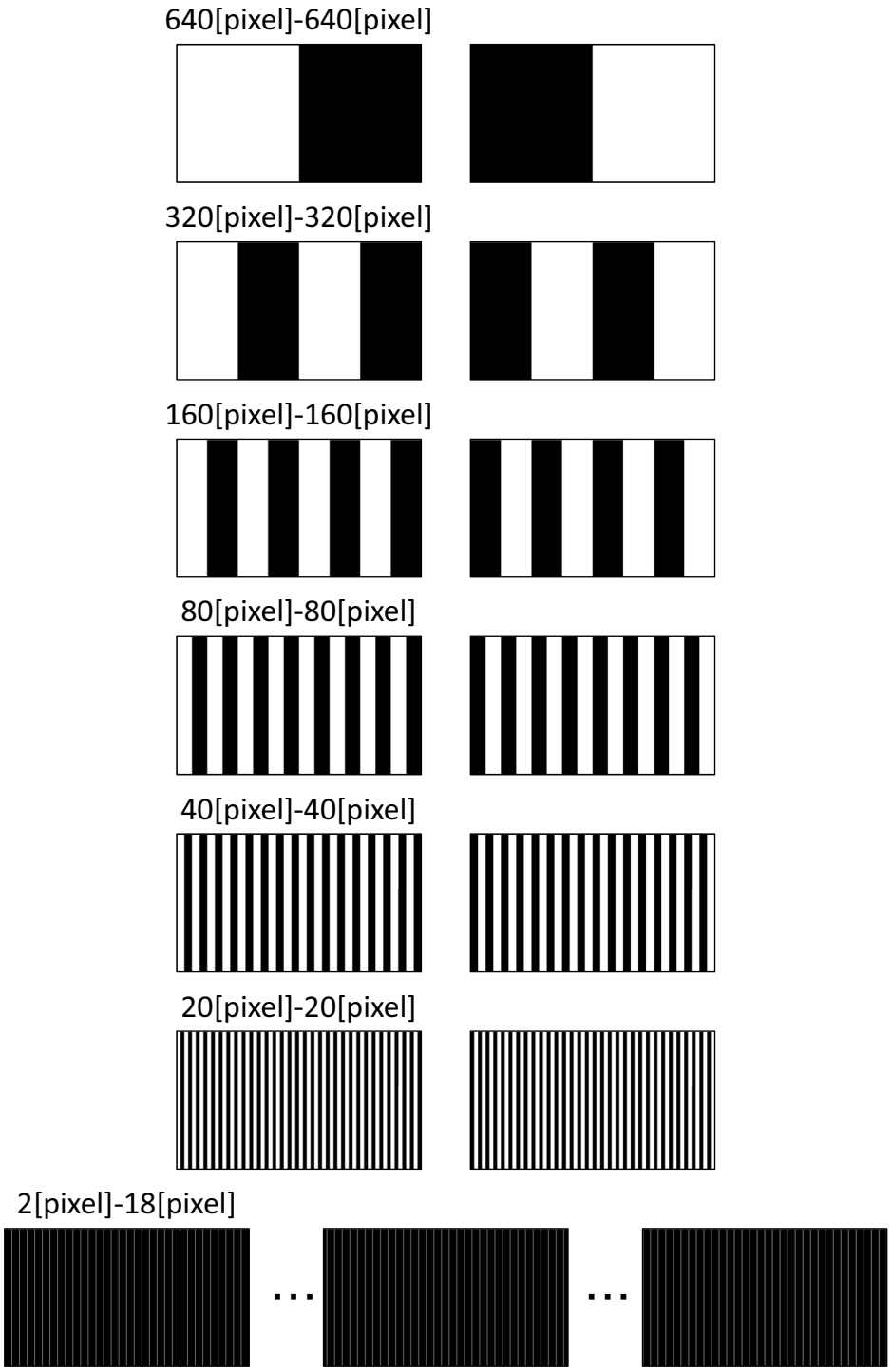

Fig. 3.16: Principle of Structured-Light Method.

Table 3.5: The total processing time and the concordance rates of each calibration method

	Pixel-Scan Method	Line-Scan Method	Structured-Light Method
Processing Time	10.2 [hr.]	392 [sec.]	236 [sec.]
Concordance Rate	-	95.2 [%]	92.9 [%]

The results of presenting primitive shapes based on Pixel Scan Method, Line Scan Method and Structured-Light Method are shown in Fig, 3.17, respectively. Here, the shapes that are presented from left to right are; sphere, cube, cuboid, pyramid, cone and cylinder. As can be seen from Fig. 3.17, unintended visible voids tend to increase towards the lower images. This indicates that the accuracies of Line Scan Method and Structured-Light Method may be lower compared to Pixel Scan Method. Therefore, the differences in how the viewers are able to perceive the 3D contents using each of the calibration methods need to be evaluated.

3.6 Middleware for 3D Content Rendering

To make LuminantCube easy to use for any user, it is desirable for it to be able to show any 3D content using standard 3D model format, such as STL format, without the need of being fully aware of the detailed structure of the display such as the number and the configuration of each projector, as well as the voids inside the display body, and the design of the 3D content to be shown. Here, STL format, is written with coordinates of vertices of polygons which are formed when dividing the surface of the 3D model into minute triangles. Note that, since STL format only possess the coordinates of the surface of the 3D model, it does not contain data of the solid part, as well as any of the RGB information. In the case of presenting a 3D model on a standard 2D flat panel display, the surfaces of the model are filled with an arbitrary colour with no gap. hence, the 3D model would look as if it is a solid model even though the interior is empty. In the case of presenting a 3D model on LuminantCube, since there are gaps in between the micro voids, the empty interior will be visible which would make the 3D content difficult to perceive. In order to reduce these gaps, the solid part of each model need to be filled. Therefore, in the present research, a middleware capable of calculating RGB and brightness information for the solid part of the 3D model to fill the interior is developed. Below is the description of a process of the middleware which converts a standard STL format 3D model data into a data which enables LuminantCube to present 3D solid model.

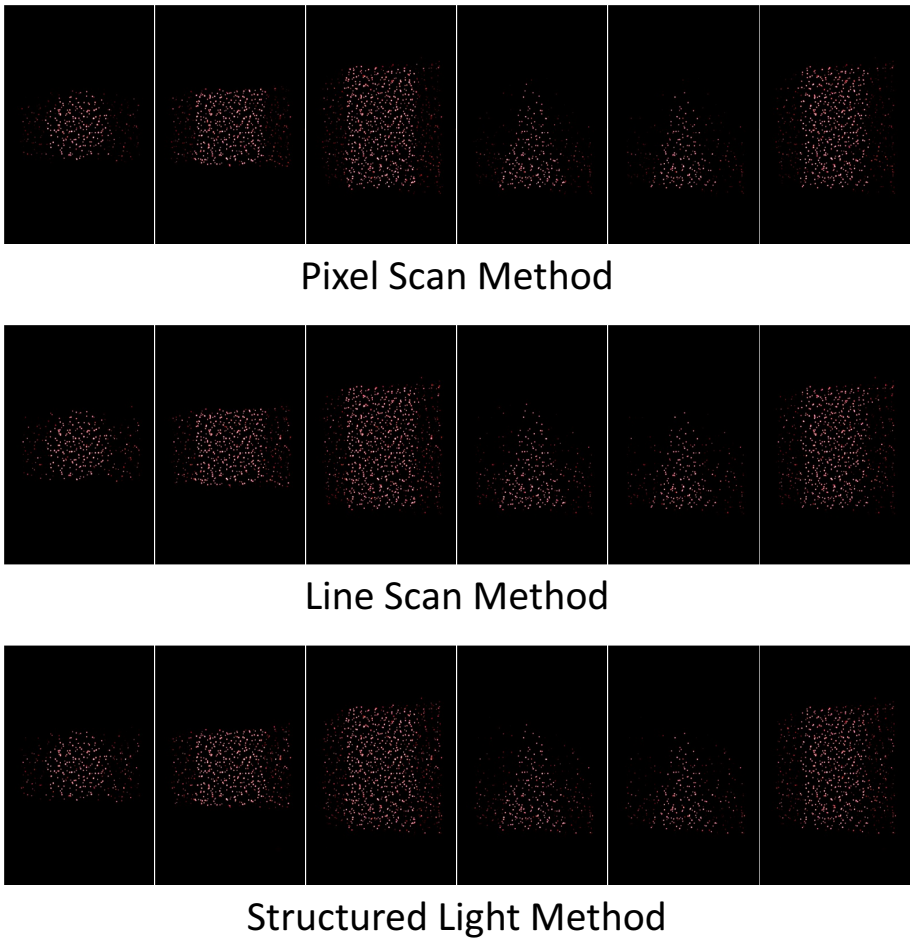

Fig. 3.17: Comparison of represented primitive shapes based on each calibration method.

In the present middleware, the 3D model is put in a cubic lattice with a partition number of n and are detected whether which cell in each grid interferes with each surface of the 3D model, as shown in Fig.3.18, in order to fill the inner part of the 3D model. The details of the procedure is described in each step, namely *Step*1 to *Step*5 in the following:

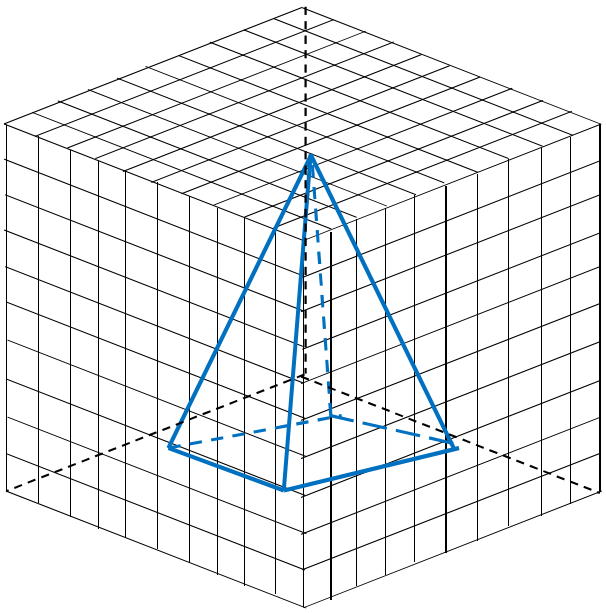

Fig. 3.18: Cubic lattice structure to be used with the middleware.

Step 1: The cubic lattice is divided into horizontal layers. Here, each horizontal layer is referred to as the *Grid*. Then, lines of intersection between the 3D model and the grid are detected. Here, on the present layer, a shape framed by multiple lines of intersection is formed, as shown in Fig. 3.19.

Step 2: For each line of the grid, each cell from left to right is scanned to detect whether the centre line of each cell intersects with the outline of the shape formed in Step 1. Here, when a cell is detected as so, the number of the occurrence of that intersection is recorded. This is to record the cells that are in between each set of odd and even number of the occurrence, as shown in Fig. 3.20. Here, one or more cells that are recorded in this manner will be stated as the internal part of the 3D model.

Step 3: Step 2 is repeated for every line on the grid until all cells on the grid are determined either as blank or as a part of the 3D model, as shown in Fig. 3.21. Then, each cell that are detected as a part of the 3D model will be recorded as regions to be projected.

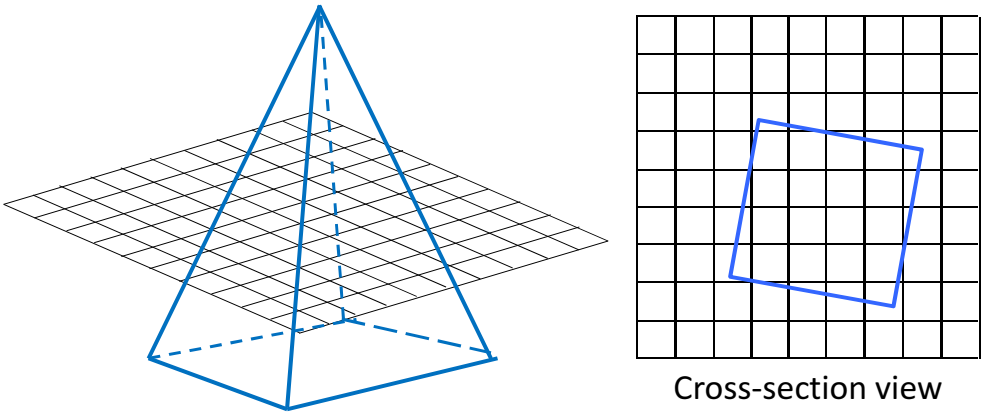

Fig. 3.19: Step 1 of middleware procedure.

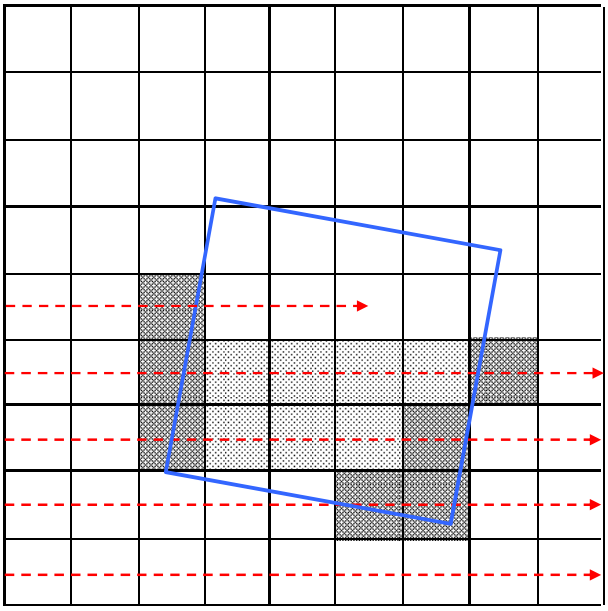

Fig. 3.20: Step 2 of middleware procedure.

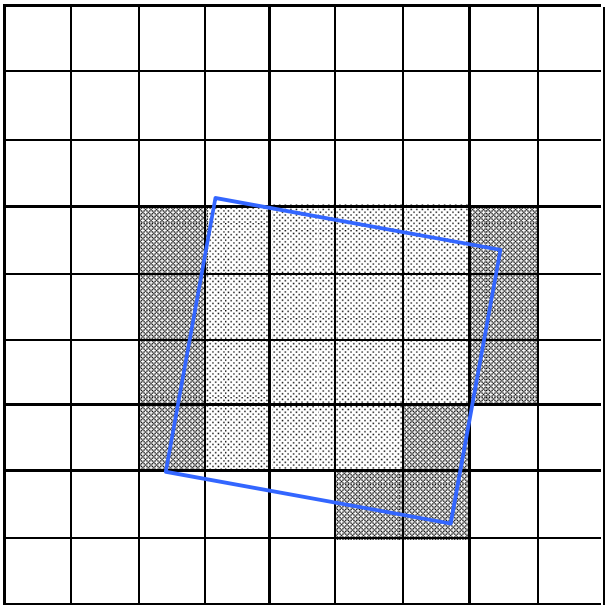

Fig. 3.21: Step 3 of middleware procedure.

Step 4: Step 3 is repeated for every grid. Then, an arbitrary RGB and brightness data is added to every cell inside the cubic lattice that are recorded to be projected. As a result, a correspondence table for RGB and brightness informations to cell coordinate is created, as shown in Fig. 3.22.

Step 5: As the correspondence table of which voids are inside which cell can be calculated from the design diagram, the correspondence table created in Step 4 is matched with the projector-pixel to void-coordinate conversion database to make an output image to be projected, as shown in Fig. 3.23.

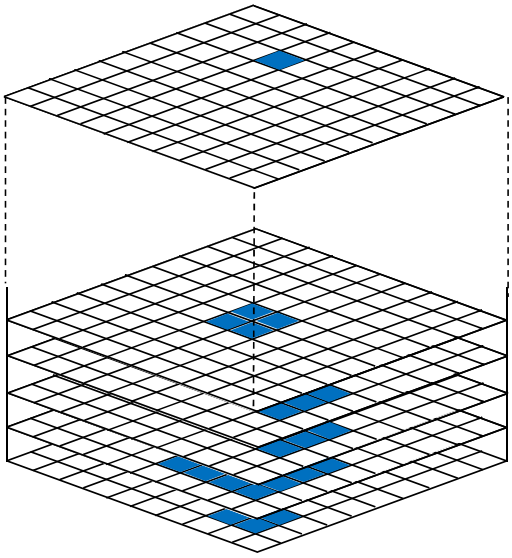

	Layer 1				Layer 2				...	Layer n			
Row \ Column	1	2	...	n	1	2	...	n	...	1	2	...	n
1	0	0	...	0	0	0	...	0		0	1	...	0
2	1	1		0	0	1		1		1	1		0
⋮	⋮		...		⋮		...		...	⋮		...	
n	0	0	...	0	0	1	...	0		0	1	...	0

Arbitrary RGB Information

Fig. 3.22: Step 4 of middleware procedure.

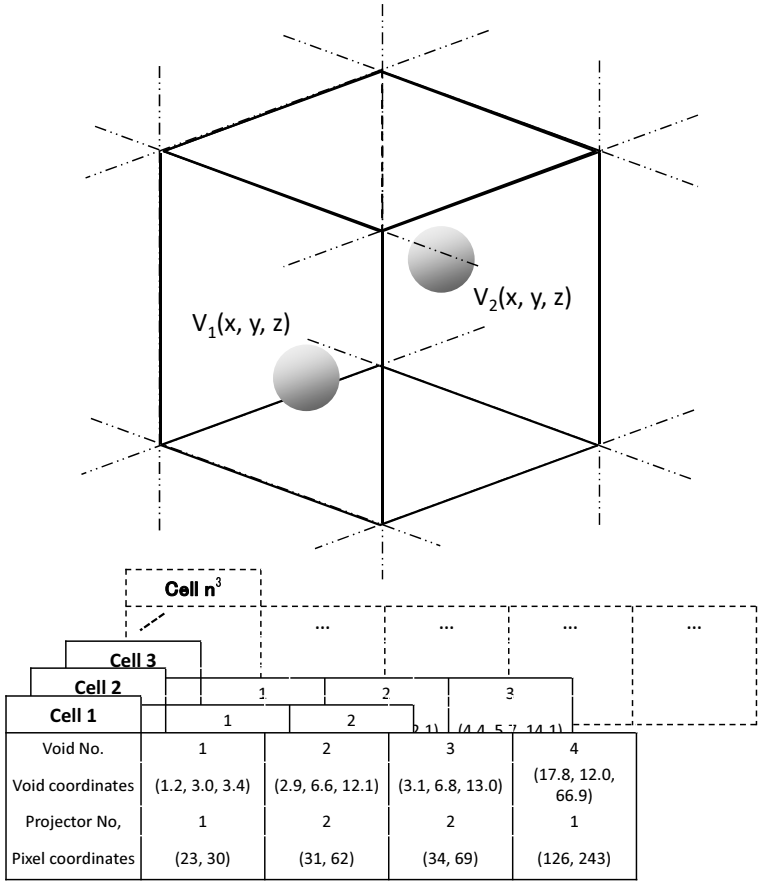

Fig. 3.23: Step 5 of middleware procedure.

Chapter 4 Evaluation of LuminantCube

In this chapter, the purpose of the experimental evaluation for LuminantCube is mentioned. After which, the details of the experiment such as the conditions, the protocols, the questionnaire and the 3D contents used for the evaluation are explained, respectively. Finally, the results of the experiment are analyzed, followed with future works.

4.1 Purpose of Experimental Evaluation

As mentioned in section 3.1, the ultimate purpose of the present research is to solve the problems of existing auto-stereoscopic displays by proposing an auto-multiscopic 3D display, which is referred to as LuminantCube. In other words, the specifications shown on the left side of Fig. 4.1 must be confirmed at minimum. In order to do so, the factors that are shown on the right side of the figure have to be evaluated experimentally. Since [2-A], [2-B], [4-B], [5] and [6] are self-explanatory either from the previous chapter of from preliminary experiment, only [1-A], [1-B] and from [2-C] to [4-A] are evaluated. In addition, as mentioned in section 3.5, the the differences in how the viewers are able to perceive the 3D contents using each of the calibration methods must also be evaluated

Thus, the purpose of the experimental evaluation is to measure the following specifications qualitatively. Here, the numbers of each measurement show the corresponding factors shown in Fig. 4.1.

[1-A] The accuracy of representation of 3D solid shapes in terms of the minimal size in which the viewers can recognize those shapes.

[1-B] The accuracy of representation of 3D solid shapes in terms of the differences in percentage rate of correct recognition for each shapes that will be shown to the viewers.

[1-A,B] The accuracy of representation of 3D solid shapes for each 3 calibration methods, namely; Pixel Scan Method, Line Scan Method and Structured-Light Method.

[2-C] The presence and the accuracy of the depth perception achieved by binocular parallax.

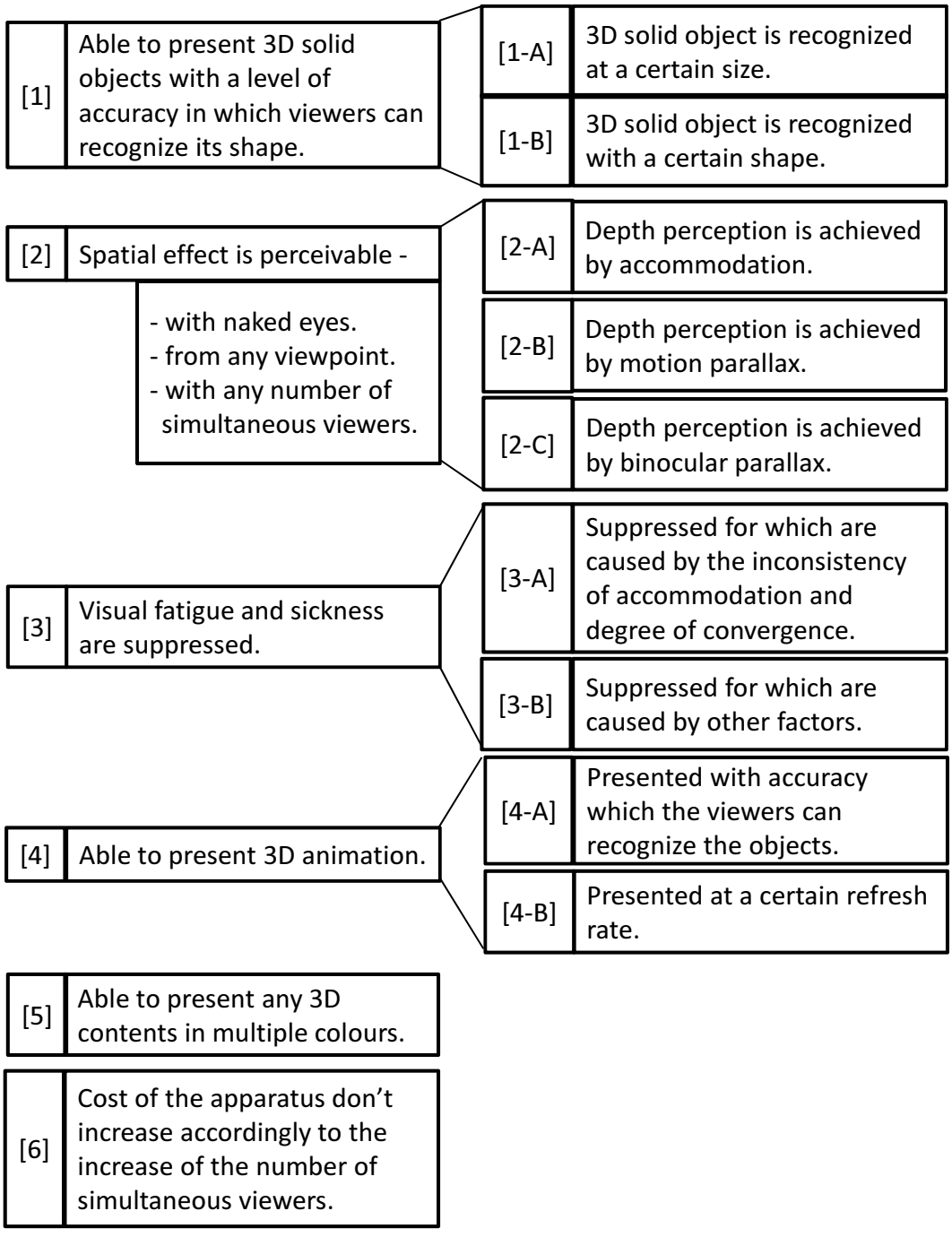

Fig. 4.1: Requirements of LuminantCube and their factors.

[3-A,B] The respective magnitudes of visual fatigue and sickness with their possible cause, and their subjective assessment.

[4-A] The accuracy of the representation of a 3D animation in terms of whether the viewers are able to recognize the objects included.

4.2 Experimental Evaluation

In order to evaluate the specifications mentioned in section 4.1, a subjective evaluation was conducted. Each of the 10 participants underwent an experiment with an approximate duration time of 40 [min.], which includes some observation of 3D contents and answering questionnaires.

4.2.1 Experimental Conditions

Participants

The experiment was conducted with a total of 10 participants, with 9 male and 1 female, aged between 22 to 26, and each participant was recruited from students of Kyoto University. The participants were chosen under conditions of having no prior experience of observing LuminantCube and having no issue of eye sight with daily activities. Any kind of interaction or communication between the participants that are relevant to the content of the experiment were restricted.

Environment of Experiment Room

The experiment was conducted in a blacked-out room with light shielding from external light. The illumination intensity was below 0.1 [lx] which was measured using a chroma meter (Konica Minolta Optics Inc., CL-200A). The plane view of the room is shown in Fig. 4.2 and the detailed measurements around LuminantCube and observer's position are shown in Fig. 4.3. Here, the distance between LuminantCube and the participants while observation was kept to approximately 400 [mm]. This is to place LuminantCube within the range of 10 [deg] around the centre of the field of view of the viewer as that range is indicated as the area to have a correlation with shape identification and attentiveness[52]. However, the participants were allowed to move their viewpoints freely if the above-mentioned distance is maintained, which was ensured by instructing them to keep their arms and waist in touch with the chair.

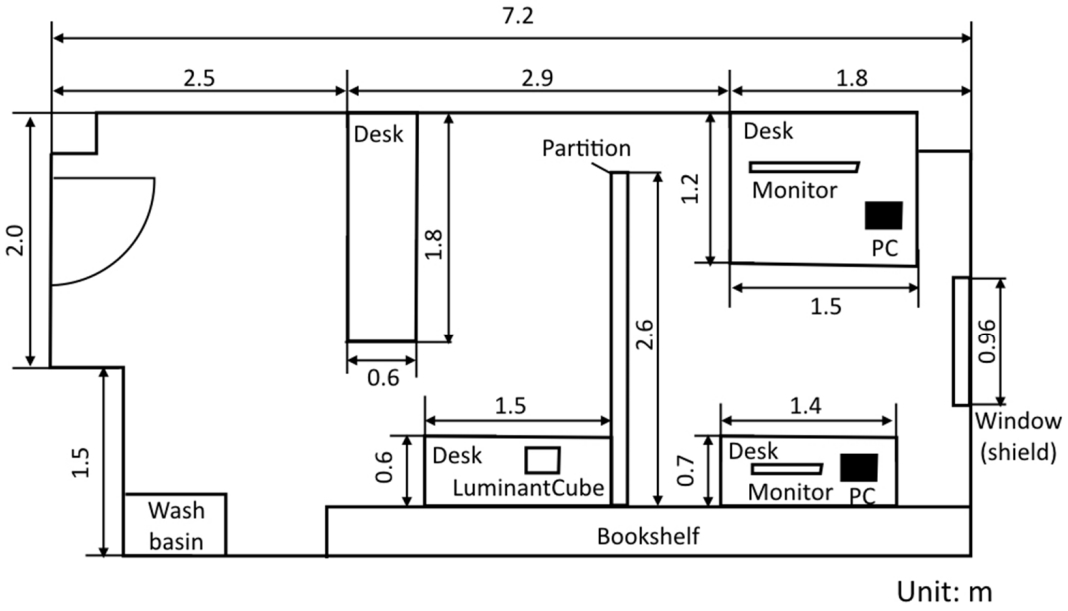

Fig. 4.2: Plane view of the room for conducting the experiment.

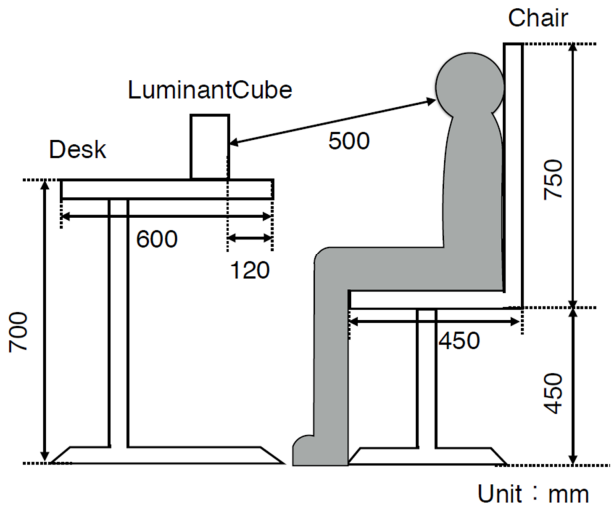

Fig. 4.3: Schematic view of the measurements around the observing position.

4.2.2 Experimental Protocol

Each experiment was conducted with a single participant at a time under the protocol shown in Table. 4.1. Each participant was called in at different hours in order to eliminate any kind of interaction or communication between the participants that are relevant to the content of the experiment. All of the explanations and questionnaires were conducted in Japanese since all of the participants were residents of Japan.

Table 4.1: Experimental protocol for each participant

Step No.	Procedure Description	Duration
1	Explanation & consent	10 [min]
2	Waiting time for dark adaptation	10 [min]
3	Observation of demo content	4 [min]
4	Observation of 3D content & questionnaire for Q1	8 [min]
5	Observation of 3D content & questionnaire for Q2	<4 [min]
6	Questionnaire for Q3	<3 [min]
7	Observation of 3D content & questionnaire for Q4	1 [min]
8	Questionnaire for Q5	1 [min]

Prior to the observation, each participant underwent an explanation and consent. This procedure includes explaining the details and cautions about the experiment, namely; the purpose of the experiment is to evaluate how the 3D contents are perceived when they are presented using LuminantCube, there will be no reward to be paid to the participants, some visual fatigue and sickness may occur during the observation, any information related to the research and experiment are confidential, the details of the experimental protocol, personal information will be kept secure and only to be used for experimental purposes only, and participants are allowed to abort the experiment at any time with no inconvenience to occur to them. If the participants are to confirm and accept the content of the above-mentioned explanations about the experiment, they were instructed to sign a consent form.

After the explanation and consent, the light of the experiment room was turned off for the participants to adapt their vision to the dark environment. The waiting time for dark adaptation for the participants was set to 10 [min.] as the sensitivity of the area of retina which is used for the observation will reach its maximum at approximately

10 [min.] after changing from bright to dark environment[53]. The waiting time was fixed at this duration in order to confirm that every participant has fully adapted to dark environment which will eliminate the possibilities of causing differences in how the participants would perceive the 3D content during the observation.

Lastly, the participants underwent a procedure of observation of 3D contents, which is highlighted in gray in Fig. 4.1. During the observation, the participants were asked to answer the questions which the details are mentioned in section 4.2.3.

4.2.3 Questionnaire and 3D Contents

The purpose and content of each questions included in the questionnaire are explained, followed by the description of the 3D contents to be presented to the participants.

Questionnaire

The original Japanese copy of the questionnaire is shown in APPENDIX A. There are 5 questions in the questionnaire, and Q1, Q2 and Q3 are related to the observation of 3D contents that are described in section 4.2.3. Each question was asked in order to measure the following factors shown in Table 4.2:

Table 4.2: Measurements and scales of each question in the questionnaire

In	Measurement	Scale
Q1	The level of accuracy of 3D solid shape representation, measured by the minimal size of when the participants are able to recognize the shape.	Correct/Incorrect 9 levels
Q2	The level of accuracy of depth perception achieved by binocular parallax, measured by how close participants can align 2 spheres in depth direction.	25 levels
Q3	The respective levels of visual fatigue and sickness caused during the experiment and their possible causes, measured by subjective assessment.	4 levels and free description
Q4	The accuracy of 3D animation representation, measured by the content of the participants' free description about the animation.	Free description
Q5	Free comments and feedbacks about the experiment.	Free description

Q1 This question is aimed to measure the level of accuracy of 3D solid shape representation using LuminantCube, by measuring the minimal size of which the participants were able to recognize the presented shape, which correspond to [1-A] and [1-B] in Fig. 4.1. Here, 6 primitive shapes and 3 calibration methods mentioned in section 3.5 are used for Q1, respectively. The shapes are shown in 9 different sizes and the answers will be evaluated whether the answered shape is correct or incorrect and the size of the shape in which it was correctly recognized, thus, the scales for Q1 are set to correct/incorrect and 9 levels. The results for each shape and calibration methods are compared to evaluate the differences of the above-mentioned accuracy for different shapes and calibration methods.

Q2 This question is aimed to measure the levels of accuracy of depth perception achieved by binocular parallax, measured by the distances in depth direction between the centres of 2 spheres, which correspond to [2-C] in Fig. 4.1. Two spheres are presented to the user, which one is static and the other is dynamic, and the participant is instructed to control the position of the dynamic sphere to be aligned with the static sphere in depth direction. With the centre of the display being 0 [mm], the dynamic sphere can be moved in the range of ± 12 [mm] with a resolution of 1 [mm] in depth direction, thus, the scale for Q2 is set to 25 levels.

Q3 This question is aimed to measure the respective levels of visual fatigue and sickness caused by the observation of 3D contents using LuminantCube and their possible causes, which correspond to [3A] and[3-B] in Fig. 4.1. The levels of visual fatigue and sickness are subjectively evaluated in 4 levels, namely; "no visual fatigue/sickness at all", "yes, felt a little", "yes", and "yes, felt very much".

Q4 This question is aimed to measure the accuracy of 3D animation representation based on the content of the participants' free description about the animation, which correspond to [4-A] in Fig. 4.1. An animation which lasts for approximately 30 [sec.] will be presented to the participants and they will be instructed to describe the content or the behavior of the animation freely in 30 [sec.].

Q5 This question is aimed to receive any general comments and feedbacks about the experiment and LuminantCube.

The English translation of the questionnaire is as follows:

Q1 A 3D content of a primitive solid shape with stepwise size increase will be shown at the center of the display. Observe that shape until it disappears. Answer the name of the solid shape as soon as you recognize it. You may change your answer

numerous times within the period until the image disappears. This process will be repeated 6 times with 1 second intervals between each time. The shape will be chosen randomly every time, with a probability of choosing the same shape more than once during the entire process.

Q2 Two spheres with different diameters and depth distances will be shown on either side of the horizontal surface at the centre of the display. Here, the left sphere will be fixed and the right sphere will move frontward for a constant distance if "UP" key on the keyboard is pressed , and backward for a constant distance if "DOWN" key is pressed. Move the right sphere using both keys so that the centres of the two spheres line up sideways with the identical depth distances. This procedure is repeated twice for each case of which the right sphere is larger and smaller than the left sphere. The default position and the relative size of the right sphere are chosen randomly every time, with a probability of the default position to be lined up sideways with the left sphere. Time limit for each procedure is 1 [min.].

Q3 During the observation of the 3D contents, did you feel any visual fatigue (sickness)? Answer from the following four options. (1) Not at all. (2) Yes, a little. (3) Yes. (4) Yes, very much. If you picked (2), (3) or (4), explain the reason(s) for your answer.

(This question was asked once for each visual fatigue and sickness, respectively.)

Q4 Describe the content or behavior of the 3D animation shown using the display.

Q5 If you have any comments or feedbacks for the experiment or the observation, please explain.

3D Contents

All of the 3D contents were shown in red colour as it was confirmed to be the most visible by a preliminary experiment. Additionally, all of the 3D contents are designed based on a single or combinations of multiple primitive shapes, as such shapes with less vertices are reported to be relatively easy to be perceived with low resolution displays, compared to the shapes with the opposite dimension[54, 55]. One or more 3D content was used for Q1, Q2 and Q4. Descriptions for each 3D content are as follows:

Demo A demo content which shows 10 different primitive solid shapes repeatedly are presented for 4 [min.] for the participants to familiarize to the 3D content presentation using LuminantCube. The 10 shapes presented are namely; hemisphere, sphere, cube, cuboid, cylinder, pyramid, cone, regular tetrahedron, regular octahedron and spheroid. The size of each shape is chosen randomly within the range

of 40-50 [mm] in width, with an aspect ratio of 1:1.6 for cuboid, cylinder, cone, pyramid and spheroid. Each shape is shown for 8 [sec.] each time and is shown for a total of 3 times during the 4 [min.], which is a total of 30 times for the 3D solid shape to be presented to the participants. Due to this, each participant's level of proficiency against the observation of 3D content using LuminantCube was eliminated for the experience. The images of each shape at its maximum size and the sequence of which the shapes are presented are shown in Fig. 4.4, respectively.

Q1 6 primitive solid shapes were used for Q1 which are represented in Fig. 4.5, namely a sphere, a cube, a cuboid, a pyramid, a cone and a cylinder. Each shape was presented in 9 steps with each step representing a stepwise size increase of 5 [mm] in width, starting from 10 [mm] to 50 [mm]. The aspect ratios of each shape except the sphere and the cube were set at 1:1.6 which is equal to that of the processing area of the display body. For each question, the shape and its calibration method are chosen randomly, in a certain manner in which each shape is chosen only once and each calibration method is chosen twice for each participant. Here, the participants are instructed that each shape may appear more than once in order to reduce the possibilities of the participants answering the shape using the elimination method. The images acquired at each step of the 6 shapes are shown in the following:

Sphere: Images acquired at each step are shown in Fig. 4.6.

Cube: Images acquired at each step are shown in Fig. 4.7.

Cuboid: Images acquired at each step are shown in Fig. 4.8.

Pyramid: Images acquired at each step are shown in Fig. 4.9.

Cone: Images acquired at each step are shown in Fig. 4.10.

Cylinder: Images acquired at each step are shown in Fig. 4.11.

Note that, Fig. 4.6 to Fig. 4.11 are based on Pixel Scan Method. Images of the above-mentioned shapes based on Line Scan Method and Structured Light Method are shown in APPENDIX B

Q2 3D contents including a set of two spheres placed 12.5 [mm] away to the sides from the centre, with diameters of 20 [mm] for the smaller sphere and 25 [mm] for the larger sphere were shown to the participants for Q2. The reason the diameters were set to a different value is to prevent the participants from aligning the spheres by matching the size of the outline. The images acquired at each position of the right sphere are shown in Fig. 4.12 and Fig. 4.13. Here, Fig. 4.12 shows the case

of the right sphere being smaller than the left sphere and Fig. 4.13 shows the case of the right sphere being larger. Every projection performed in this question is based on the calibration of Pixel Scan Method.

Q4 An animation of a snowman is shown for Q4. This animation contains a snowman wearing a red hat, which is placed 10 [mm] to the left from the centre of the display, with snowfall from the top and accumulating snow at the bottom half. The images acquired from every 10 frames of the animation are shown in Fig. 4.14. Here, the frames start from the left top image to the right bottom image, ascending from left to right. The solid shapes that are included in this animation include 2 white spheres with diameters of ϕ 30 [mm] and ϕ 20 [mm] for the snowman, a red sphere with a diameter of ϕ 12 [mm] for the hat, flickering of white points projected to the remaining areas of the display for the snowfall and a white cuboid with incremental height increase from the bottom for the accumulating snow, respectively. Every projection performed in this question is based on the calibration of Pixel Scan Method.

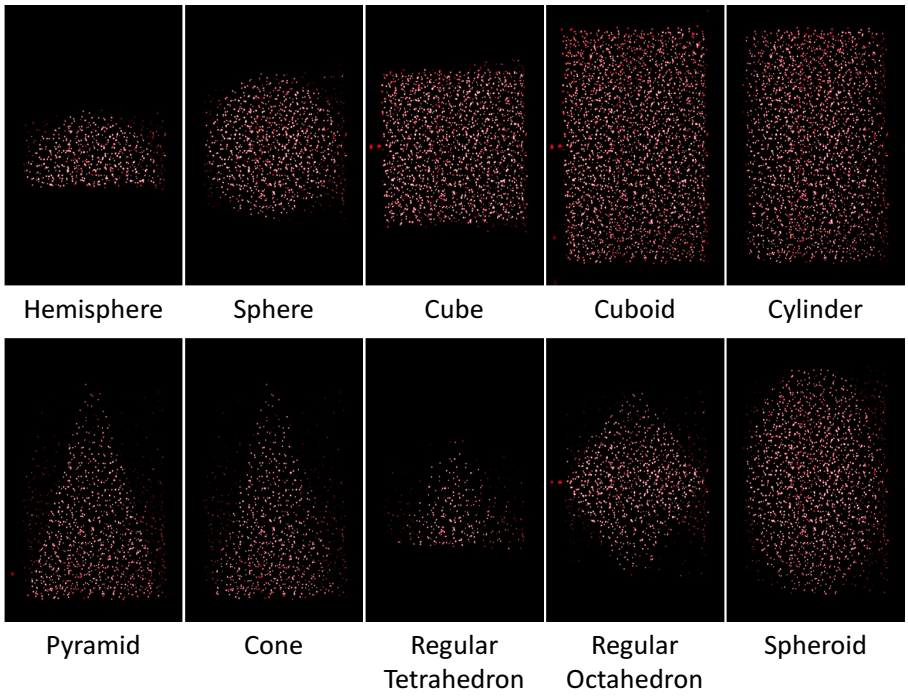

1	2	3	4	5
Cuboid	Pyramid	Regular Octahedron	Cylinder	Sphere
6	7	8	9	10
Cone	Hemisphere	Regular Tetrahedron	Spheroid	Cube
11	12	13	14	15
Cuboid	Regular Octahedron	Hemisphere	Spheroid	Pyramid
16	17	18	19	20
Cube	Cone	Sphere	Cylinder	Regular Tetrahedron
21	22	23	24	25
Cube	Hemisphere	Pyramid	Cone	Cylinder
26	27	28	29	30
Cuboid	Regular Tetrahedron	Spheroid	Regular Octahedron	Sphere

Fig. 4.4: Images of the 10 shapes used for the demo content and sequence of which they are presented.

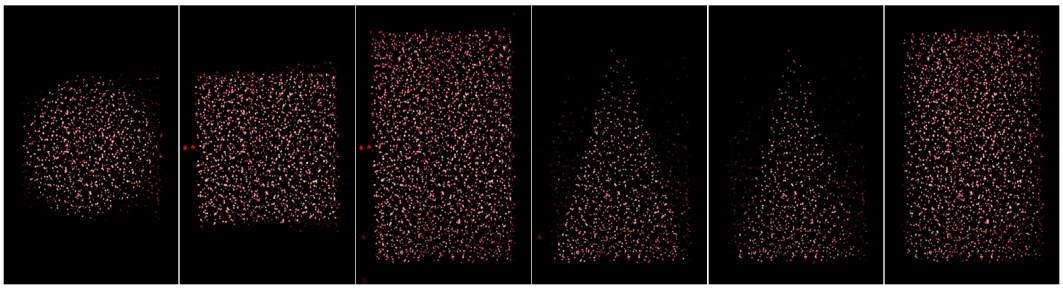

Pixel Scan Method

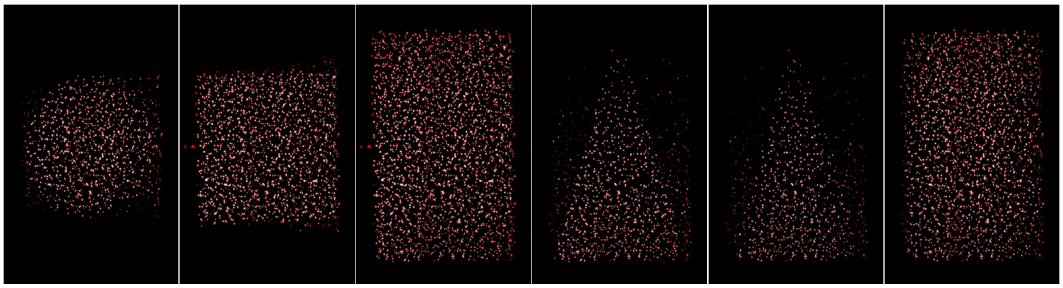

Line Scan Method

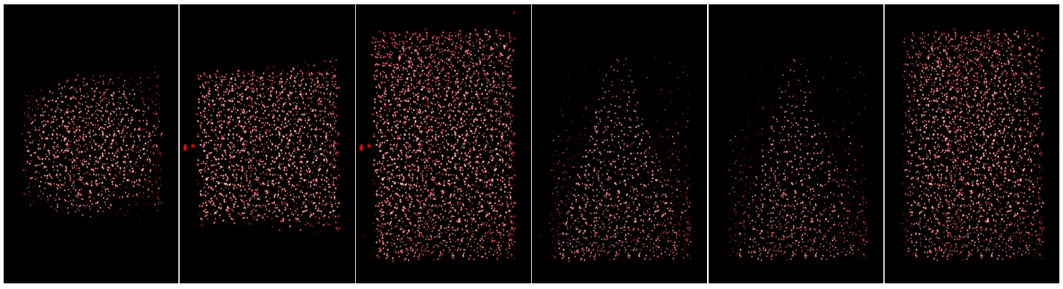

Structured Light Method

Fig. 4.5: Images of the 6 shapes used for Q1.

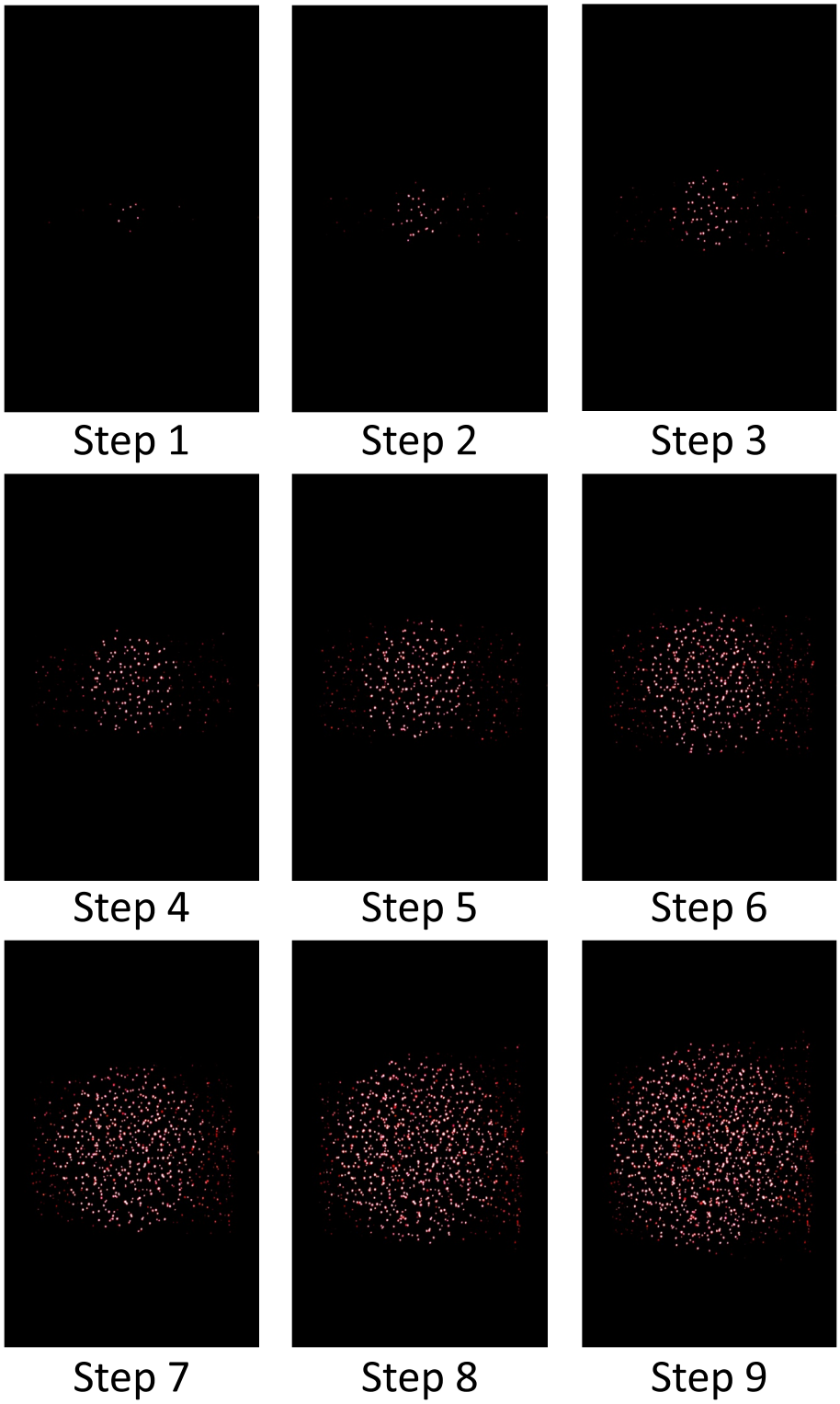

Fig. 4.6: Images acquired at each step of the size increase of a sphere using Pixel Scan Method.

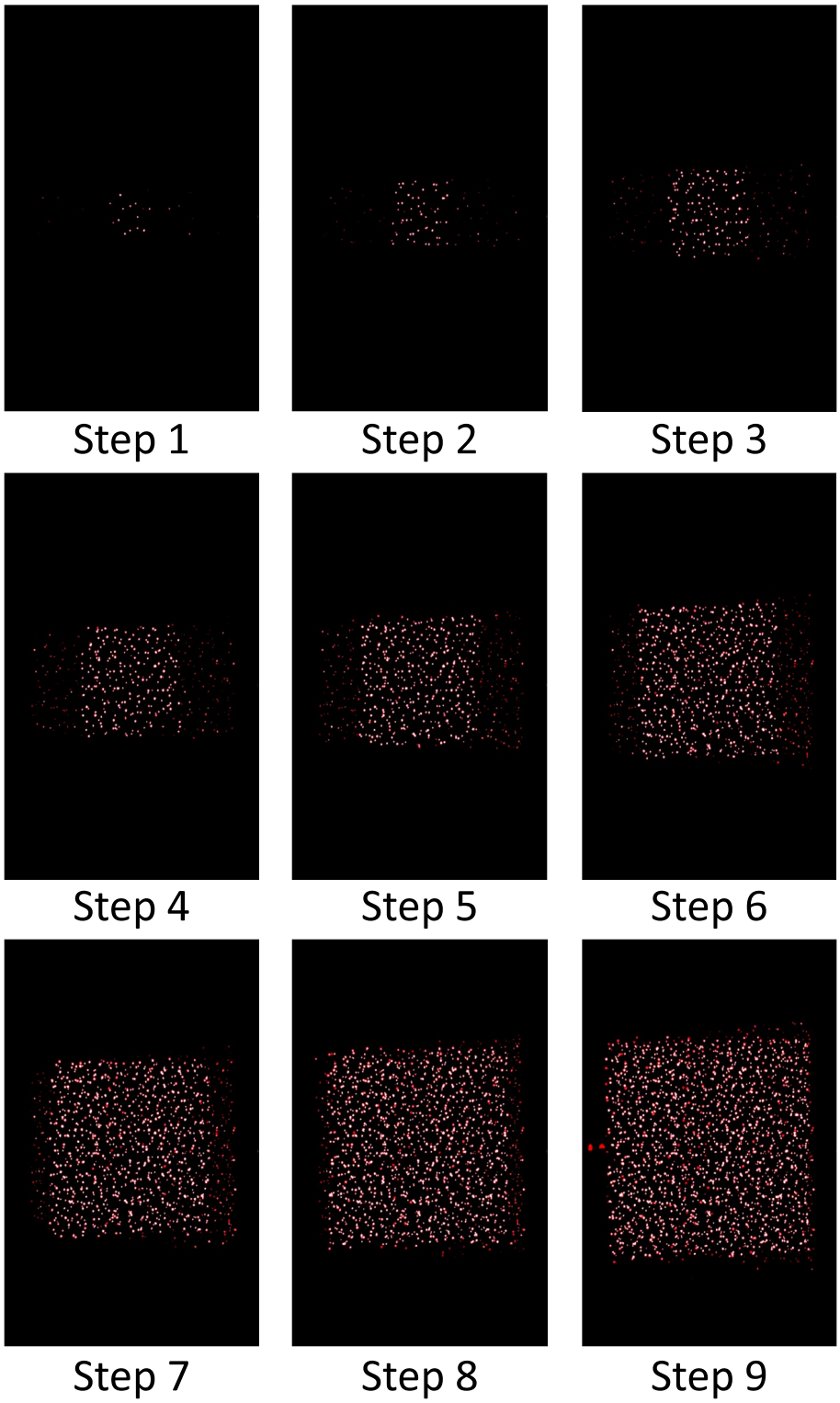

Fig. 4.7: Images acquired at each step of the size increase of a cube using Pixel Scan Method.

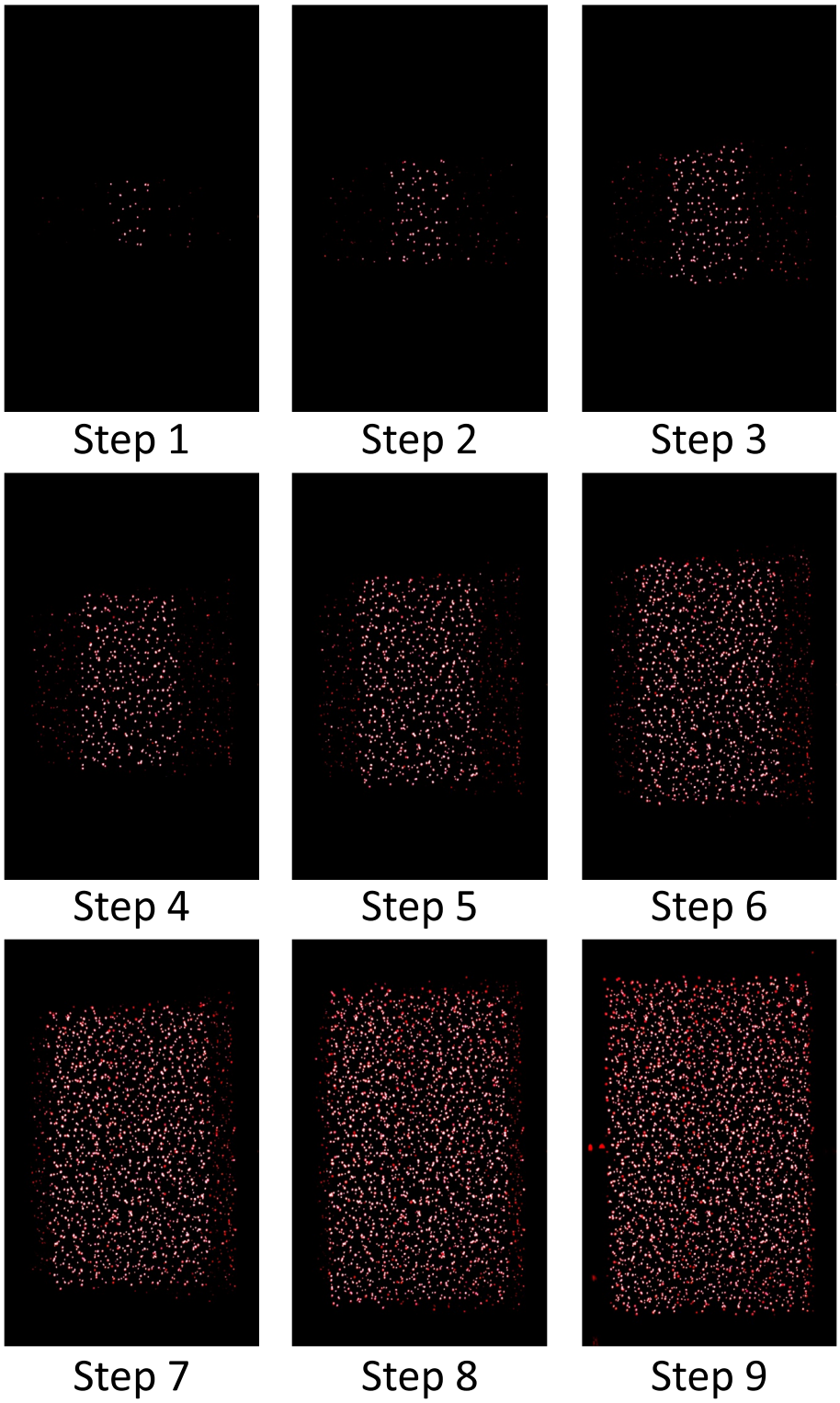

Fig. 4.8: Images acquired at each step of the size increase of a cuboid using Pixel Scan Method.

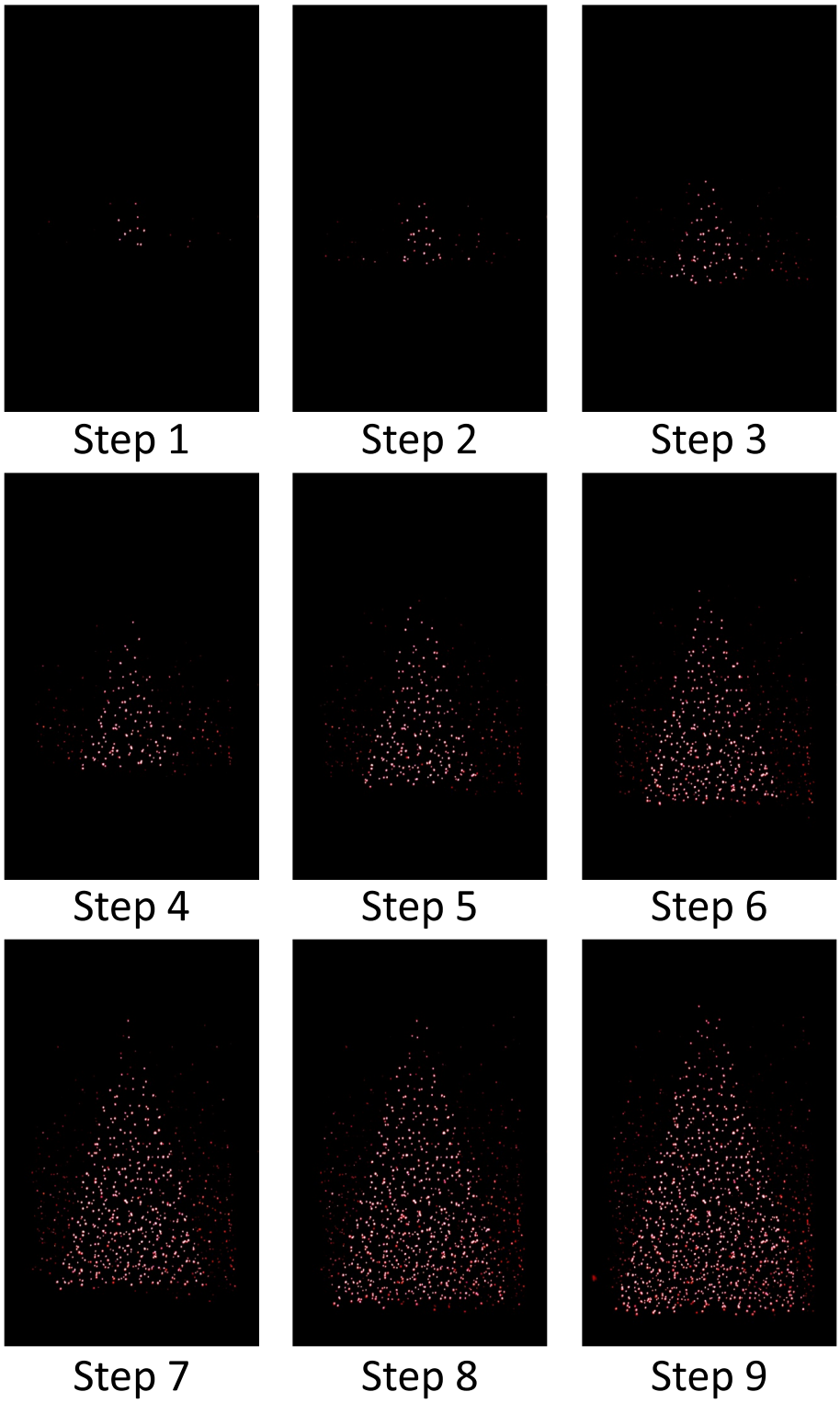

Fig. 4.9: Images acquired at each step of the size increase of a pyramid using Pixel Scan Method.

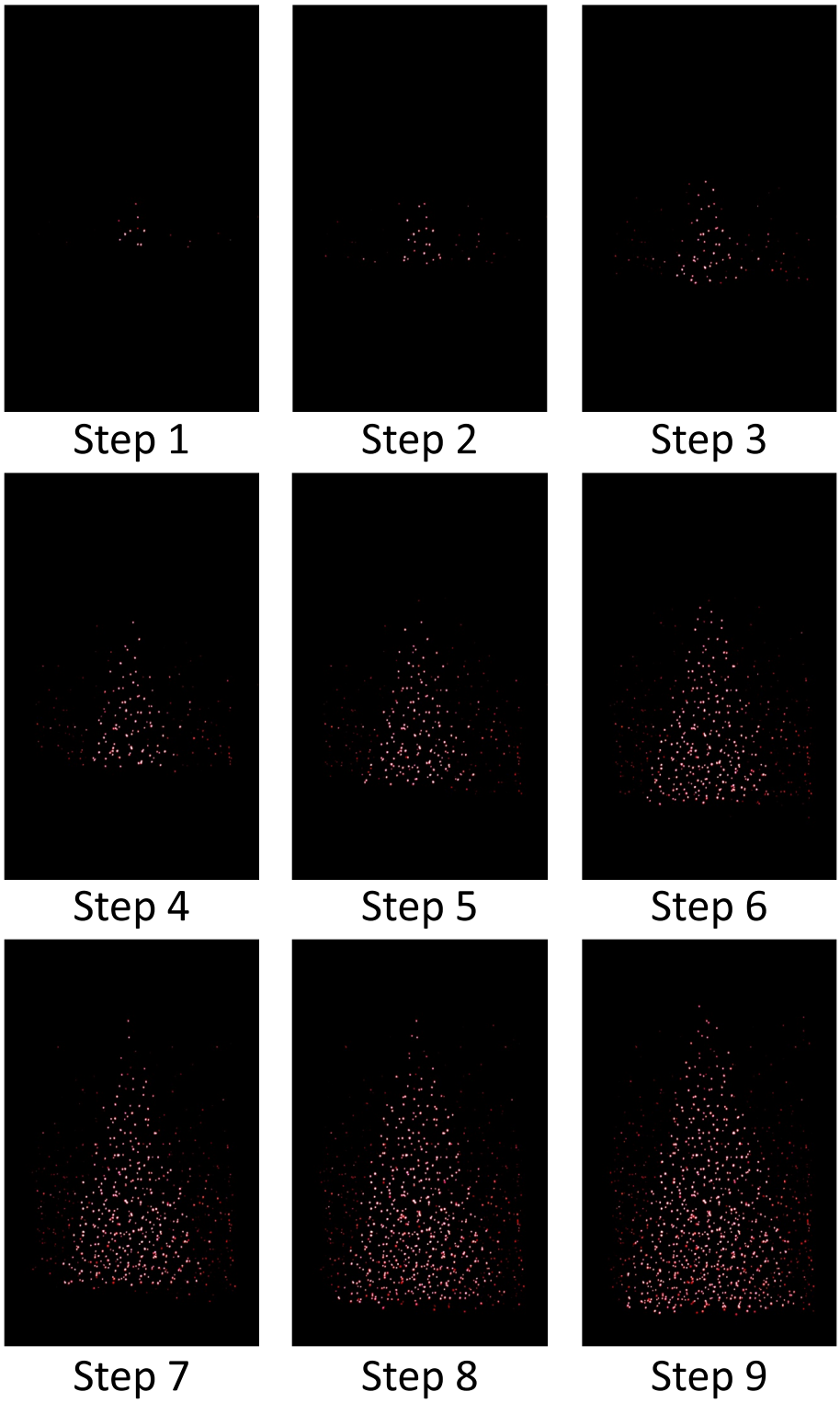

Fig. 4.10: Images acquired at each step of the size increase of a cone using Pixel Scan Method.

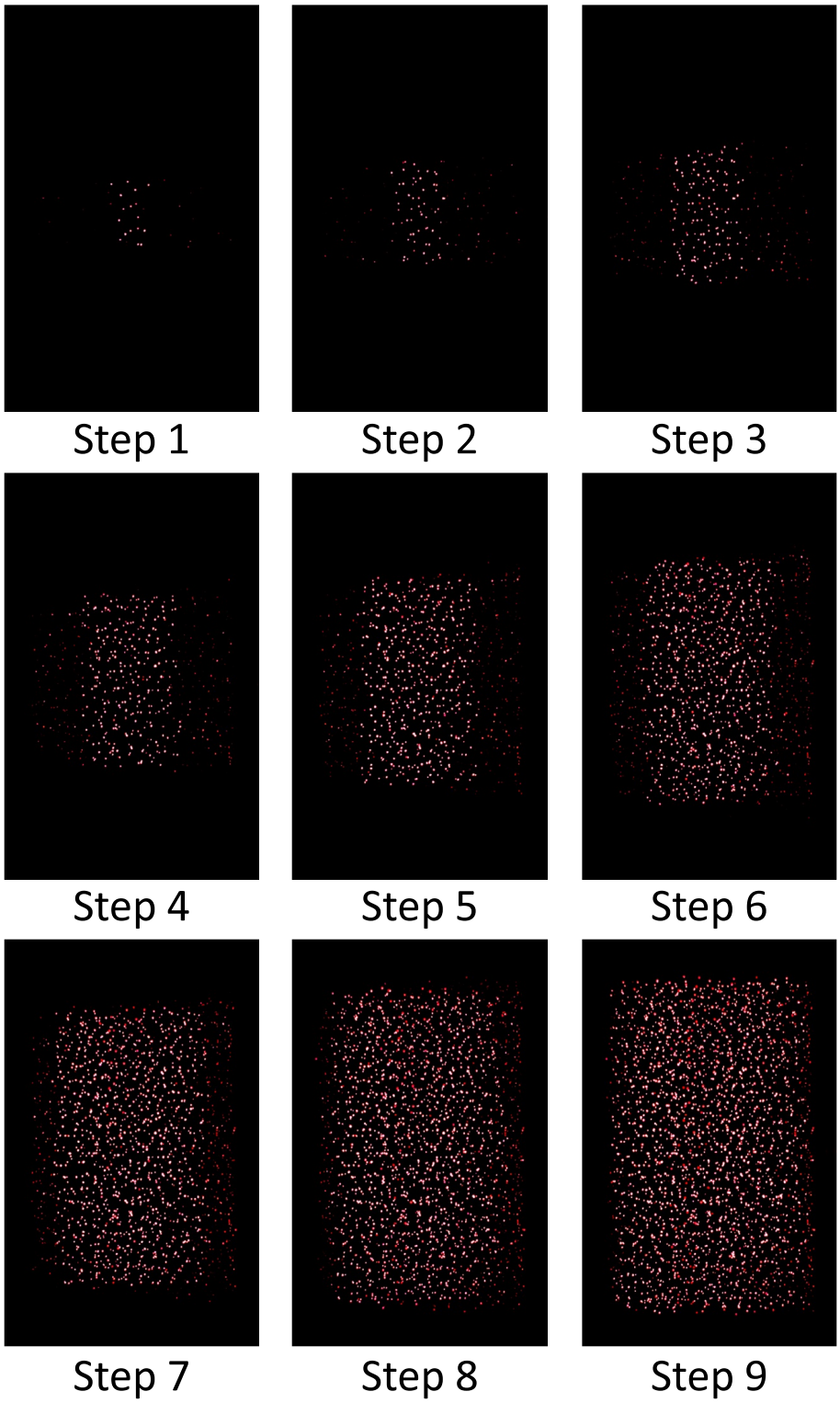

Fig. 4.11: Images acquired at each step of the size increase of a cylinder using Pixel Scan Method.

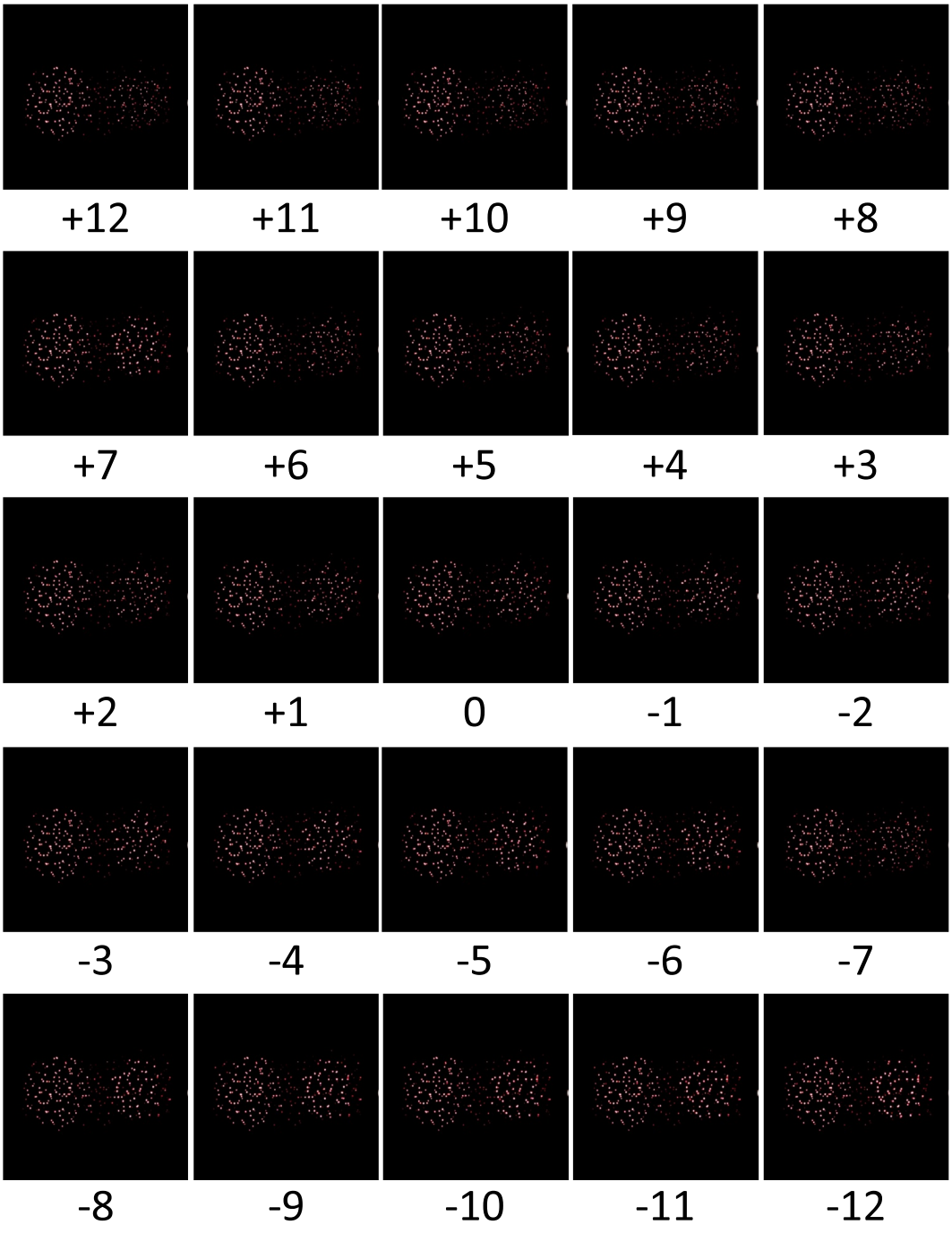

Fig. 4.12: Images acquired at each position of the right sphere, being smaller.

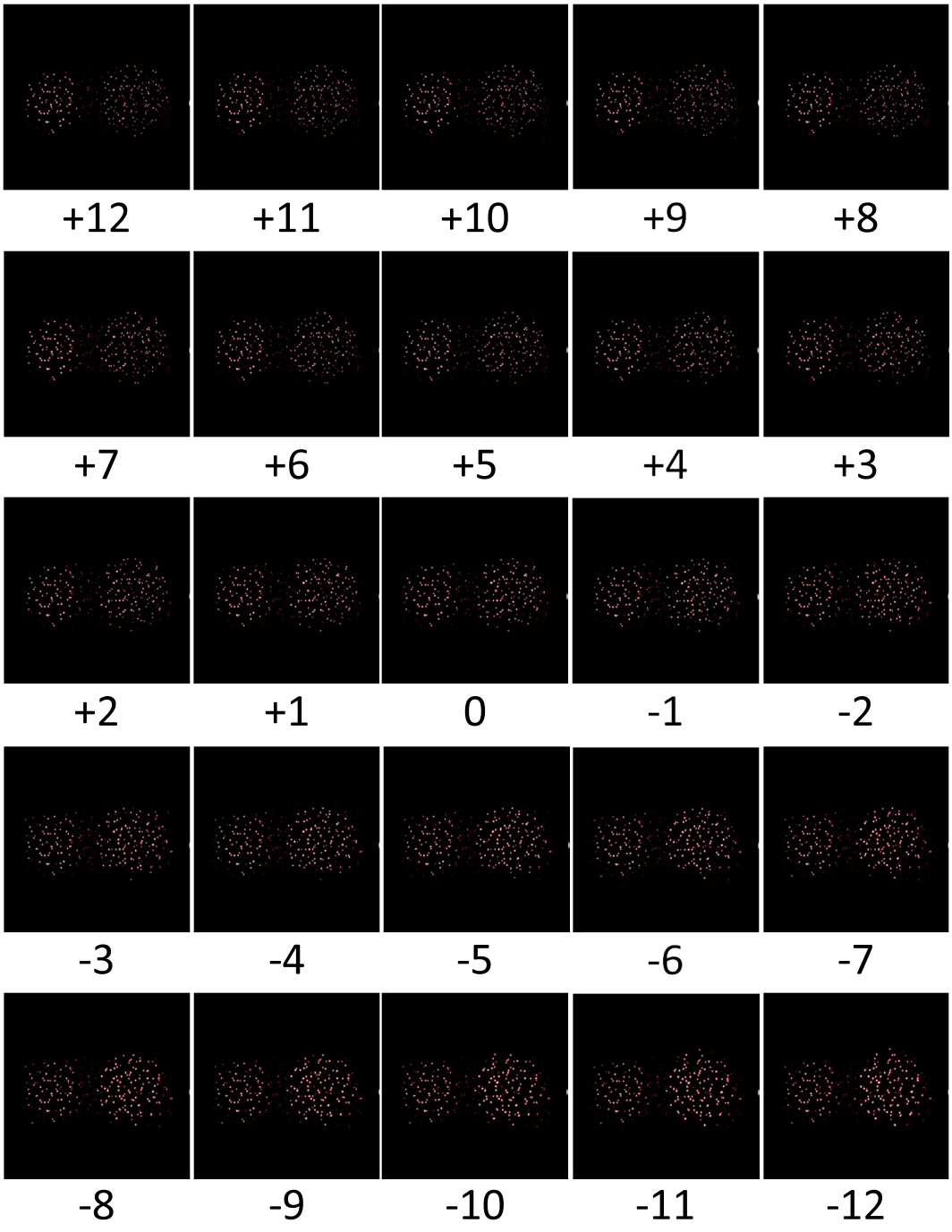

Fig. 4.13: Images acquired at each position of the right sphere, being larger.

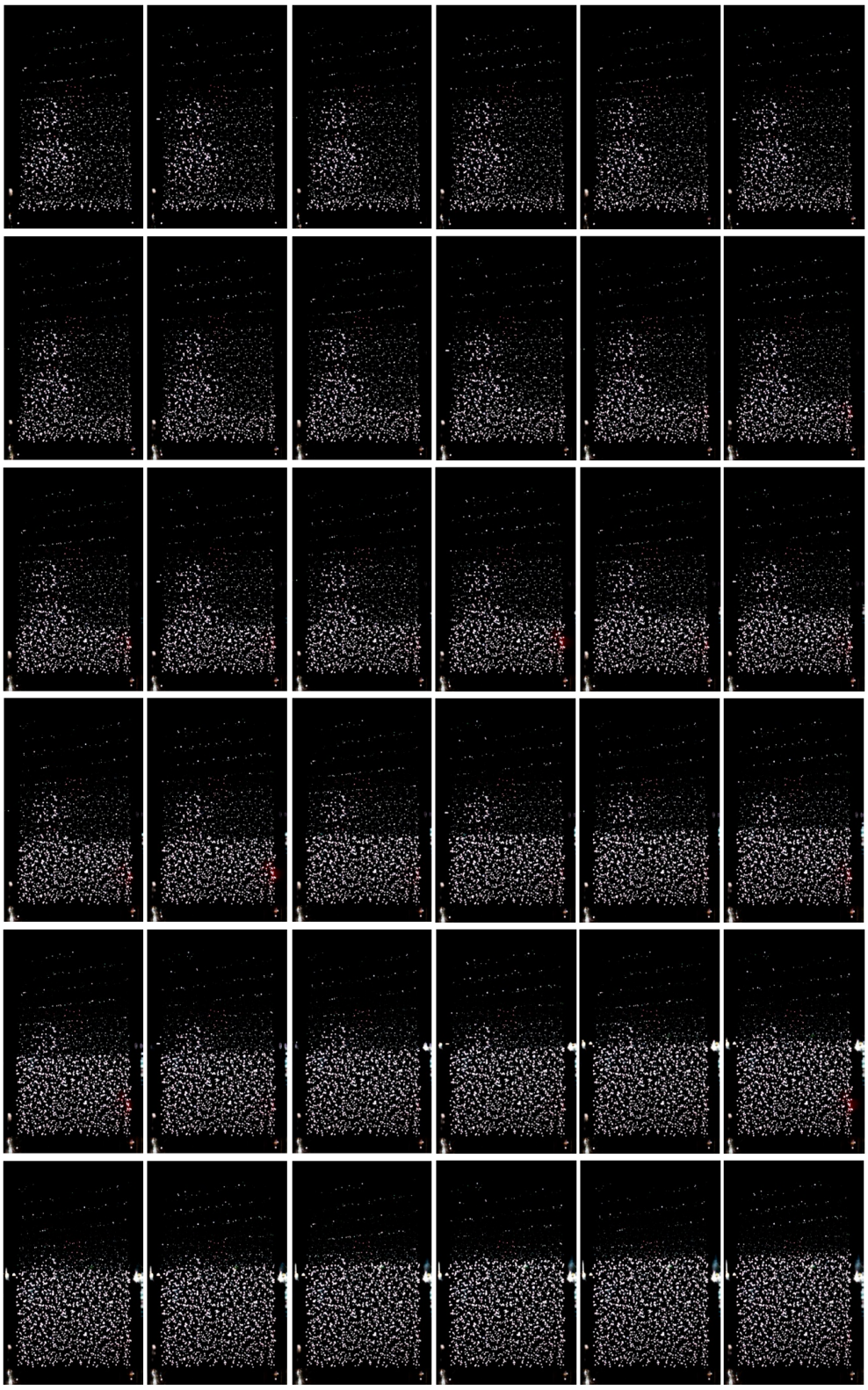

Fig. 4.14: Frames acquired from animation of a Snowman.

4.3 Experimental Results and Analysis

In this section, the results of the questionnaire are explained along with the analysis.

Q1: Accuracy of 3D Solid Shape Representation

This question was intended to measure the level of accuracy of 3D solid shape representation using LuminantCube, by measuring the minimal size of which the participants were able to recognize the presented shape. The cumulative percentages of questions answered correctly for Q1, along with the final percentage value at step 9, are shown in Fig. 4.15 for different calibration methods and in Fig. 4.16 for different shapes, respectively. Fig. 4.15 shows that while Pixel Scan Method and Line Scan Method both having an identical percentage, the former was answered correctly mostly from the early steps of each shape and the latter was answered mostly at step 4-6.

The root cause of the difference need to be investigated quantitatively in the future works. Note that, despite having the fastest calibration processing time, Structured Light Method showed a relative low percentage of correct answers.

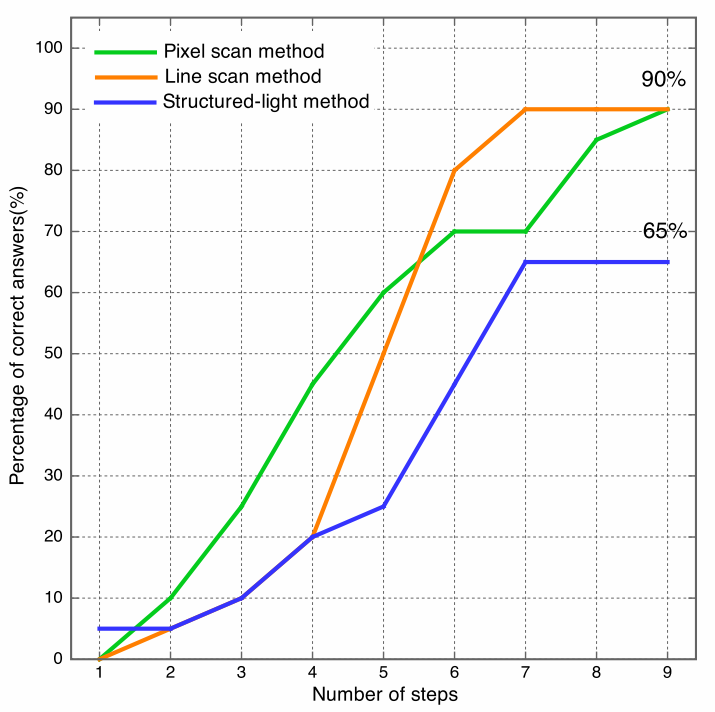

Fig. 4.15: Cumulative percentages of correct answers for Q1 for different calibration methods.

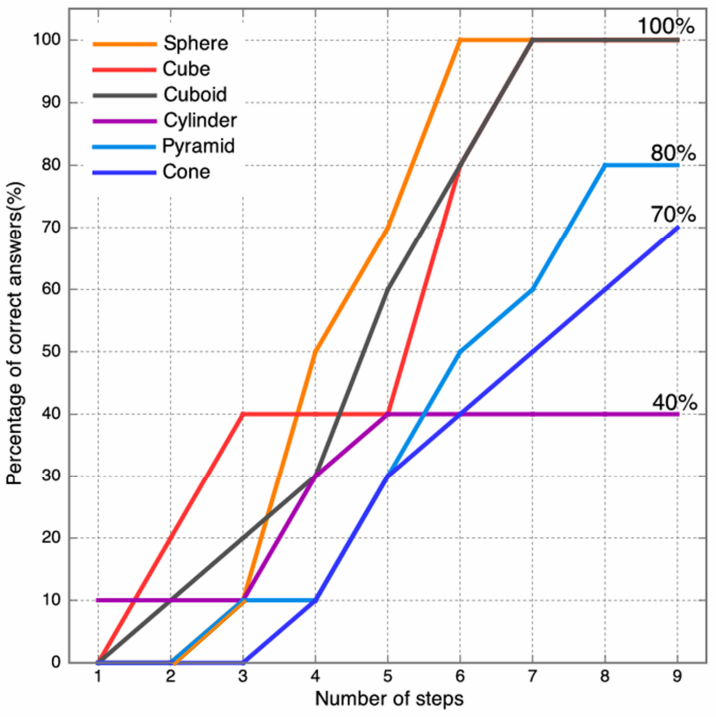

Fig. 4.16: Cumulative percentages of correct answers for Q1 for different shapes.

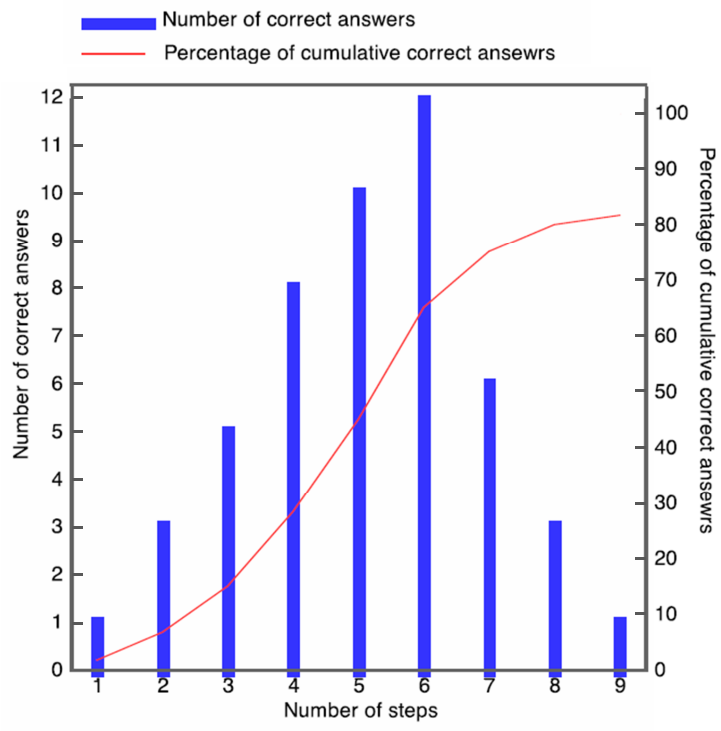

Fig. 4.17: Histogram of the total of correct answers for Q1 with the percentage of correct answers.

Fig. 4.16 shows that the percentages of questions answered correctly for cone, pyramid and cylinder were relatively low compared to sphere, cube and cuboid. Here, every incorrect answer while cylinder was shown were answered to cuboid and 50 % of correct answers while cuboid was shown were answered as cylinder before changing the final answer as cuboid. Also, every incorrect answers for questions showing a pyramid were answered as cone, and conversely. The above-mentioned results indicate that despite LuminantCube being able to present the outline of each shape, the corners and the edges cannot be presented clearly enough with adequate amount of voids.

The histogram of the total of correct answers for Q1 at each step is shown in Fig. 4.17, along with the percentage of the questions answered correctly. From Fig. 4.17 having the peak at step 6, it can be discussed that with the percentage rate of 65 % of being the correct answer, the 3D solid shape can be recognized at step 6, in other words at a size of 35 [mm] in width.

Q2: Accuracy of Depth Perception Achieved by Binocular Parallax

This question was intended to measure the levels of accuracy of depth perception achieved by binocular parallax, measured by the distances in depth direction between the centres of 2 spheres. Here, the diameters of the spheres were set to different values in order to prevent the participants aligning the spheres at the point where the apparent diameters match. The results of depth perception scaled in Q2 for each case of the right sphere being either larger or smaller than the left sphere are shown in Fig. 4.18, respectively. The overall result of depth perception is shown in Fig. 4.19.

Here, the minus side of the horizontal axis indicate the nearside of the display body and the plus side indicate the further side, respectively. As shown in Fig. 4.18, in the case of the right sphere being larger, the answers were distributed more to the plus side, in other words further side, with the peak at "1". In contrast, in the case of the sphere being smaller, the answers were distributed more to the minus side, in other words the nearside. Thus, it can be argued that the diameter of the right sphere caused the participants to perceive the sphere to be further away with smaller diameter, and closer with larger diameter, respectively, which may have worsened the participants to answer further from "0". On the other hand, the overall result shown in Fig. 4.19 indicates that by using LuminantCube, spatial effect can be achieved by binocular parallax with an accuracy of which the error being 2 [mm] or less with 85 [%]. probability.

Q3: The respective levels of visual fatigue and sickness, and their cause

The results of visual fatigue and sickness induced by observation of 3D contents are shown in Fig. 4.20, respectively. Here, the average observation time of all participants

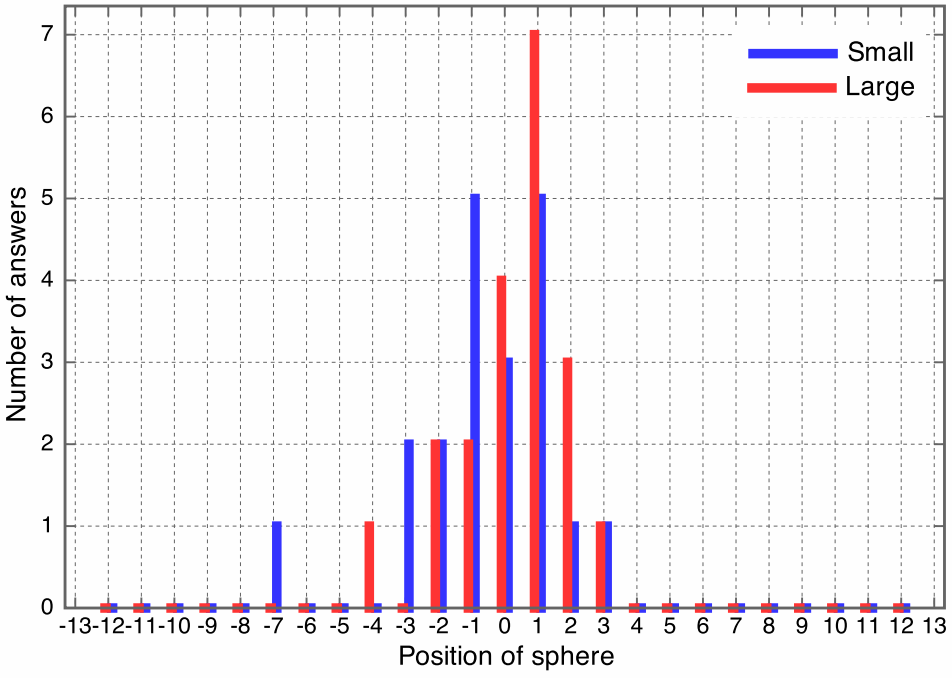

Fig. 4.18: Histogram of answers at each distance for Q2 with the right sphere being larger and smaller, respectively.

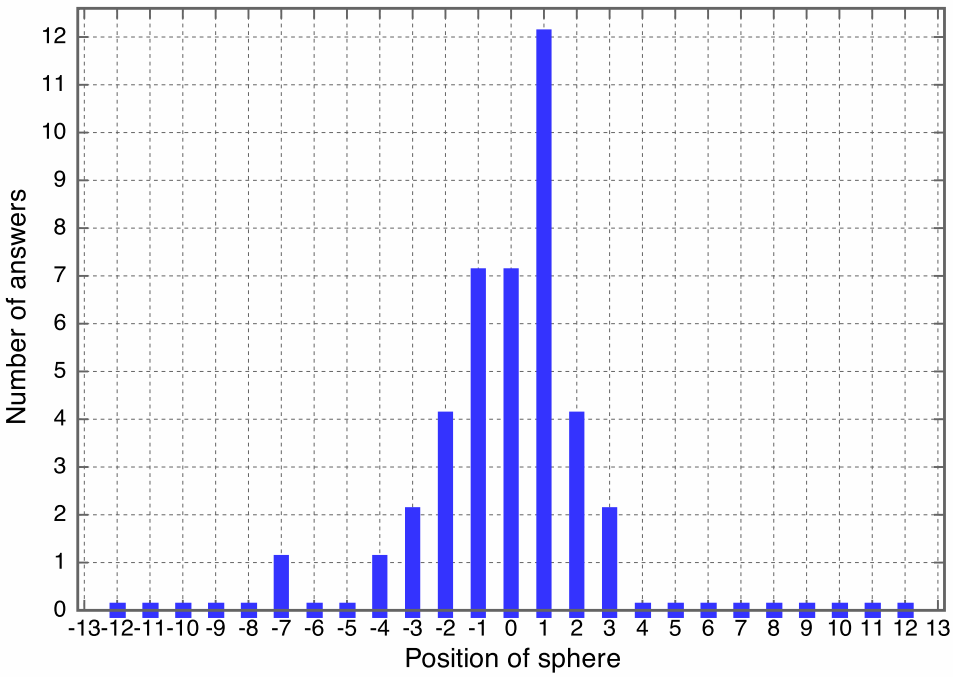

Fig. 4.19: Histogram of total number of answers at each distance for Q2.

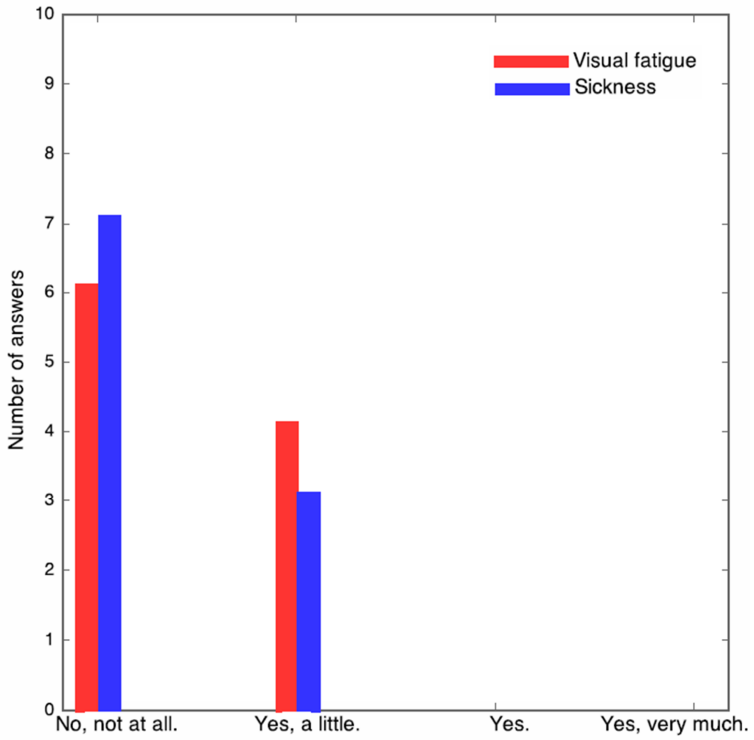

Fig. 4.20: Histogram of visual fatigue and sickness caused during the experience.

when Q3 was asked was approximately 15 [min.]. The majority of the participants did not have any visual fatigue nor sickness during the experience with a duration of 15 [min.]. There were some participants who felt a little visual fatigue or sickness, respectively, however none answered "Yes." or "Yes, very much" for either of visual fatigue and sickness. The subjective descriptions for the possible causes of each visual fatigue and sickness are shown in APPENDIX C. Considering that the possible applications of LuminantCube such as 3D-CAD or educational interface include a longer observation time, the effects against visual fatigue and sickness with a prolonged observation must be determined in the future works.

Q4: The accuracy of 3D Animation Representation

The descriptions of the answers of Q4 are shown in APPENDIX C. All of the answers for Q4 can be grouped into 2 kinds; (1)answers with only the names of primitive shapes and (2)answers with *things* and/or *sceneries*, such as snowman and snowfall. 6 out of 10 participants were able to recognize a snowman in the animation and 5 out of those 6 participants also recognized snowfall and/or accumulating snow. The answers from the above-mentioned participants are grouped in (2). As there are no participants who recognized snowfall or accumulating snow and not the snowman at the same time, it

is safe to say that the sceneries were complemented by the recognition of the snowman as well as having a prior experience of seeing a snowman in such sceneries. There are mainly 3 probable causes for 4 remaining participants to answer only with the names of primitive shapes such as "a white cuboid" or "a red sphere", which in this case are grouped in (1). The first is the instructions for Q1 causing a bias to the participants to answer in names of primitive shapes. The second is the appearance of unintended visible voids around the snowman. As can be seen in Fig. 4.14, which is based on Pixel Scan Method, there are some luminous points, which is referred to as the *noise*, around the right side of the snowman which were not intended to be visible for this content. This is due to the calibration error, in other words, some pixels of the projector which was intended to project at a certain void is either projected at a displaced direction or is also projected at other voids that are on the pathway of that projection, because of the inaccuracy of the adjustment during the calibration procedure. Since the colours of the snowman and the noise are identical and the contrast between the two are low, the participants who could not recognize the snowman may have recognized both snowman and the noise to be a single object, which in this case a white cuboid. The third is the stepwise height increase of the white cuboid representing the accumulating snow at the lower side of the display partially covering the snowman. Since the order of the areas of the display which the participants focused on during the observation of the animation vary according to different participants, there are possibilities which the snowman will be partially covered by the increasing cuboid. Therefore, it will be more likely to recognize the content as a white cuboid and not the snowman.

Q5: Comments and feedbacks about the experiment

The descriptions of the answers of Q5 are shown in APPENDIX C. There were 5 participants who answered that distinguishing the shape as being either a cuboid or a cylinder, and either a cone or a pyramid in Q1 were difficult due to the corners and lines being unclear. By contrast, 1 participant answered that identifying the snowman was relatively easier than identifying the shapes in Q1 since the content of Q4 was showing an object and scenery we see in real life, and the informations were complemented inside the head. Lastly, 2 participants mentioned about the possible improvements on LuminantCube, which were related to the increase of the display body size and the improvements on the resolution or the density of the voids along with the consideration of optimal viewing distance. The display body size was mentioned that if it was to be larger, the experience could have more impact. The resolution or density of voids and the optimal viewing distance are related to the comment which implied that perceiving spatial effect from a group of emitting points may have some difficulties, in terms

of the mechanism of the human visual system and not the mechanism of the display itself. Since screen images on standard LCD display are also represented with group of pixels, the only difference between such displays and LuminantCube is whether each point is small enough to be unrecognizable as individual points or is too large and are recognized discretely. In order to mitigate the viewers recognizing each emitting void as discrete points, the resolution of the display have to be increased to make the voids more dense in the future works. Furthermore, investigating the optimal viewing distance which can reduce the viewers from recognizing discrete voids as well as the viewer being able to observe the details of the contents need to be done in the future works.

4.4 Future Works

Future works for LuminantCube are considered, namely; resolution and contrast ratio improvements, alternative display body shape and size, and depth camera installation to the system.

Higher Resolution (Density of micro voids)

By using multiple projectors as shown in Fig. 4.21, the number of micro voids that will be able to be projected without conflicting other projection pathways can be increased. As a result of achieving such improvements in resolution, showing more complicated shapes with more vertices will be possible, meaning that there will be more options of applications to be considered in the future.

Higher Contrast Ration and Maximum Brightness

By projecting from multiple projectors against one single micro void as shown in Fig. 4.22, the contrast ratio and maximum brightness can be improved. The ultimate purpose of the improvement on the maximum brightness is to make LuminantCube able to be used in standard indoor lighting environment.

Alternative Display Shape

As can be seen in Fig. 4.23, the edges of the display body causes the 3D content to look distorted due to the refraction. This problem can be solved by using a cylinder or hemisphere shaped glass block as the display body. Alternatively, the projector(s) will be placed below the display body and projected into the bottom planar surface to reduce any distortion.

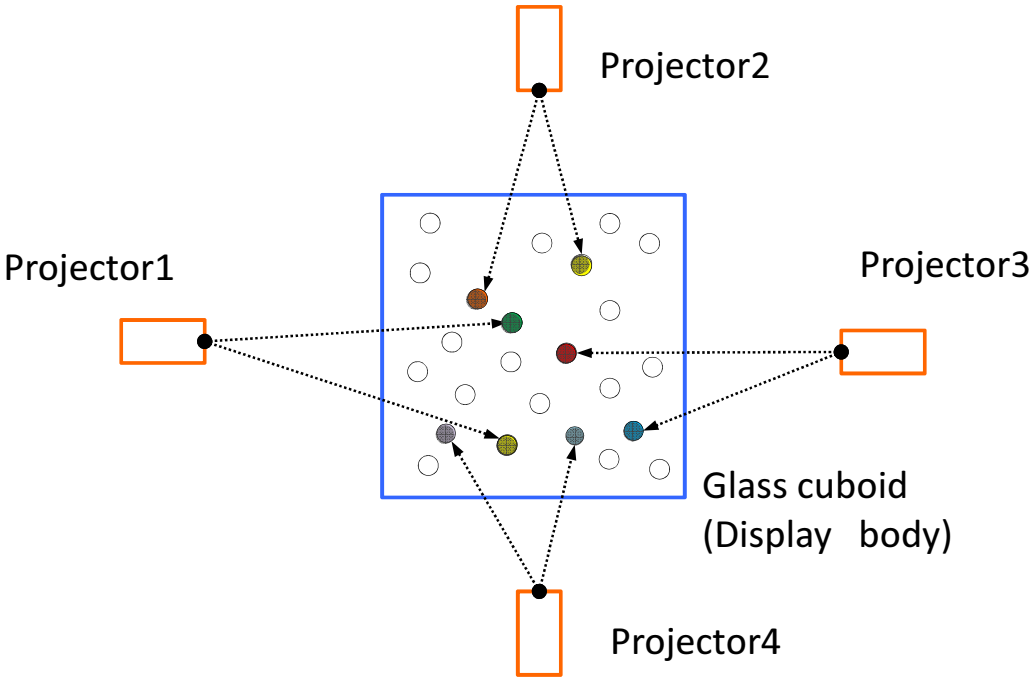

Fig. 4.21: Schematic view of the apparatus for resolution improvements.

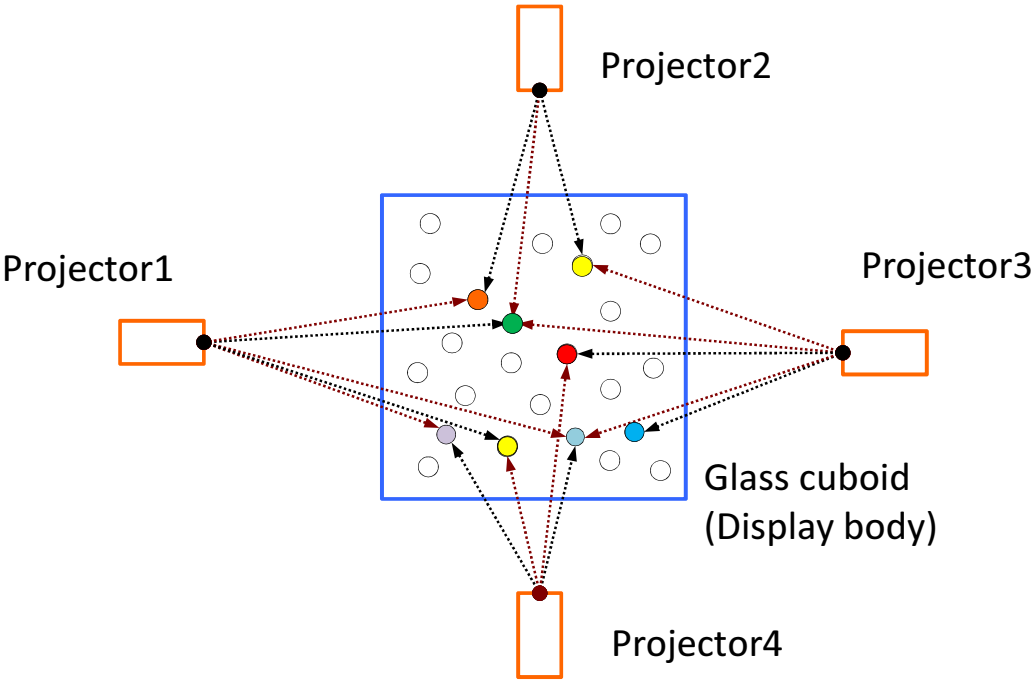

Fig. 4.22: Overlaying projections to improve maximum brightness.

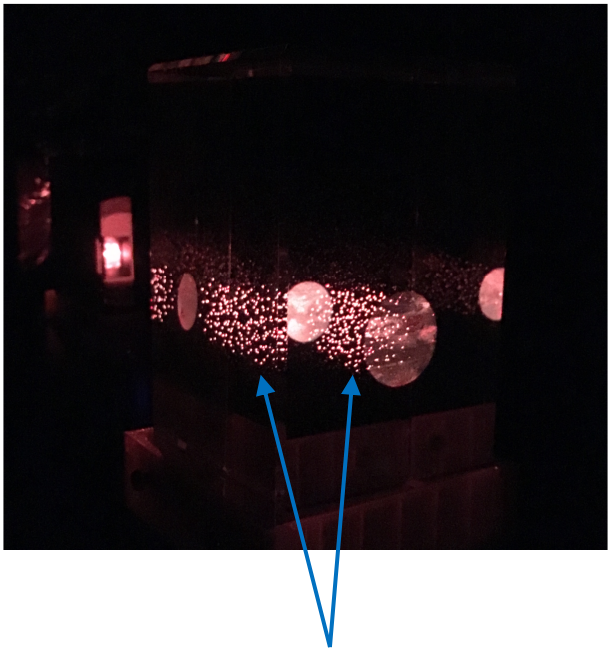

Fig. 4.23: Distorted view of the 3D content when observed around the edge of display body.

Larger Display Size

The display body is expected be able to be enlarged to a cube of approximately 600 [mm] in height in terms of transparency limits. As seen in common large scale aquariums, the thickest plates of acryl used for water tanks are approximately 600 [mm] in thickness, while maintaining the transparency high enough for the inside of the tanks to be visible. Achieving such large display body size can result in applications such as 3D digital signage.

Installation of Depth Cameras

As the middleware designed exclusively for this system is already in shape, the conversion from point cloud data acquired from depth camera to volumetric pixel coordinates is relatively easy. By installing multiple depth cameras placed to surround an arbitrary object or a person, a replication of that object or a person can be performed with no occlusion. Moreover, by reducing the processing time of the above-mentioned conversion, the data acquired from depth cameras can be reflected in real time with no time lag. Hence, the application of real-time 3D telecommunication introduced in section 2.3 can be achieved.

Chapter 5 Conclusion

In the present research, an auto-multiscopic 3D display using light diffusion within 3-dimensionally positioned micro regions referred to as LuminantCube is proposed. The purpose of this research is to overcome the challenges of the existing auto-stereoscopic displays, such as the limitations of observable viewpoints and simultaneous viewers. LuminantCube can be observed from any direction with any number of simultaneous viewers with the naked eyes. Moreover, the correspondence of accommodation and the degree of convergence is maintained during the observation, which may reduce the occurrence of visual fatigue and sickness.

LuminantCube consists of a display body made of a glass cuboid with numerous internally processed micro voids and a laser projector connected to a computer to control the projection. By projecting light with various colour and brightness into the micro voids from the projector, each micro void would emit the corresponding colour and brightness upon contact with the projection. Hence, an arbitrary image or animation can be presented by a group of emitting micro voids on LuminantCube by controlling the projection for each individual micro void.

To project light onto each individual micro voids accurately, calibration algorithms which adjusts the position of the projection automatically are developed, namely; Pixel Scan Method, Line Scan Method and Structured-Light Method. The adjustment is performed by detecting the correspondence between each projector pixel and the micro voids. This is performed by projecting either single pixel at a time (Pixel Scan Method) or multiple pixels simultaneously (Line Scan Method, Structured-Light Method), in which the latter can shorten the processing time for the calibration to complete. The processing times of Line Scan Method and Structured-Light Method were 392 [sec.] and 236 [sec.], respectively, which are significantly faster than 10.2 [hr.] of Pixel Scan Method.

A middleware capable of rendering 3D content from STL format files was developed in order to enable LuminantCube to present 3D contents using standard 3D model format.

In order to evaluate whether LuminantCube can achieve the ultimate purpose of overcoming the challenges of existing auto-stereoscopic displays, a subjective evaluation with 10 participants was conducted. The evaluation was performed by asking the participants a questionnaire related to the 3D contents which they were instructed to observe. The specifications that were measured in the present experiment were namely;

the accuracies of representation of 3D solid shapes, animations, depth perception and the respective magnitudes of visual fatigue and sickness caused by the observations of 3D contents.

The results related to the accuracies of representation of 3D solid shapes showed that, despite Line Scan Method being faster than Pixel Scan Method for the calibration, the percentage rate of correct recognition were identical. Moreover, the 3D solid shape can be recognized at a size of 35 [mm] with the percentage rate of 65 [%]. The detailed results indicated that despite LuminantCube being able to present the outline of the shapes, the corners and edges cannot be presented clearly enough with adequate amount of voids.

The results related to the accuracy of depth perception showed that, by using LuminantCube spatial effect can be achieved by binocular parallax with an accuracy of which the error being 2 [mm] or less with 85 [%] probability.

For the evaluation of induced visual fatigue, 6 participants did not feel any visual fatigue at all, while 4 felt a little fatigued. As for the evaluation of induced sickness, 7 participants did not feel any sickness at all, while 3 felt a slight sickness. However, none of the participants reported the feeling of great visual fatigue and/or sickness.

The descriptions by the participants about the 3D animation indicated that prior knowledge and experience related to the content complemented the perceived information which helped some participants to recognize the content. However, 4 participants could not recognize the content which were partially caused by the inaccuracy of the representation disturbed by the unintended emission of micro voids.

For future works of the present research, the resolution and contrast ratio are to be improved by increasing the number of projectors and overlaying multiple projections on each micro voids. Additionally, the display body size and shape may be altered to a cylinder or a hemisphere with a larger volume. The purpose of altering the shape is to eliminate the distortions of the 3D content which occurred when observed from around the edges of the display body. Finally, an installation of depth cameras is considered to enable the possibility of replicating a 3D model of an object or a person in real-time using LuminantCube.

Acknowledgement

First and foremost, I would like to express my deepest appreciation to Prof. Hiroshi Shimoda and Asst. Prof. Hirotake Ishii for their most kindful guidance and support in doing this research. I have achieved great knowledge and experience in this two years in appreciation to their advices.

Second, I would like to thank Ryuta Endo and Yoshiki Ohashi for their unstinting effort in this research. If it were not for their work and support, I will not be able to achieve such achievements.

Third, I would like to thank Razana Husni and Huang Bingrong for their support in proofreading the thesis. For their helpful comments and feedbacks, I was able to finish this thesis.

Fourth, I would like to thank Takayoshi Kitamura for great advices, Daisuke Kamihigashi for treating me to a drink, Masanari Furuta, Hiroki Tokumaru, Yukin Wang and Hidehiro Kanagawa for being good rivals, Taro Kimura, Motoki Urayama, Shota Shimonaka, Kosuke Sugita and Yuta Tsuji for being great juniors, and Kimi Ueda for designing the *LuminantCube Team* Logo.

Finally, I am deeply grateful to my family, especially my parents for their generous support. Regardless of being able to meet each other once a year, they would always give me peace of mind every time we meet.

I am greatly happy to have studied for my master degree in Shimoda Lab.

Bibliography

[1] J. Hong, Y. Kim, Hee-Jin Choi, J. Hahn, J. H. Park, H. Kim, S. W. Min, N. Chen, B. Lee, Three-Dimensional Display Technologies of Recent Interest: Principles, Status, and Issues, Applied Optics, **50**(34), pp. H87-H115, (2011).

[2] H. Nagatani, Evaluation of the Safety of 3-Dimensional Image and Individuals' Binocular Vision Functions -Evaluation of Visual Safety, and Attempt to Investigate the Mechanism of Fatigue- , ITE Technical Report, **36**(43), pp. 29-34, (2012).

[3] S. Nagata, Visual Sensitivities to Cues for Depth Perception, Television, **31**(8), pp. 649-655, (1977).

[4] A. Yasuoka, M. Okura, Binocular Depth and Size Perception in the Peripheral Field, Vision, **23**(2), pp. 103-114, (2011).

[5] B. Rogers, M. Graham, Motion Parallax as an Independent Cue for Depth Perception, Perception, **8**, pp. 125-134, (1979).

[6] M. Graham, B. Rogers, Simultaneous and Successive Contrast Effects in the Perception of Depth From Motion Parallax and Stereoscopic Information, Perception, **11**, pp. 247-262, (1982).

[7] B. Rogers, M. Graham, Similarities Between Motion Parallax and Stereopsis in Human Depth Perception, Vision Research, **22**, pp. 261-270, (1982).

[8] M. A. Hogervorst, M. F. Bradshaw, R. A. Eagle, Spatial Frequency Turning for 3-D Corrugations From Motion Parallax, Vision Research, **40**, pp. 2149-2158, (2000).

[9] J. Geng, Three-Dimensional Display Technologies, Advances in Optics and Photonics, **5**, pp. 456-535, (2013).

[10] M. S. Landy, L. T. Maloney, E. B. Johnston, M. Young, Measurement and Modeling of Depth Cue Combination: in Defense of Weak Fusion, Vision Research, **35**(3), pp. 389-412, (1995).

[11] M. F. Bradshaw, P. B. Hibbard, A. D. Parton, D. Rose, K. Langley, Surface Orientation, Modulation Frequency and the Detection and Perception of Depth Defined by Binocular Disparity and Motion Parallax, Vision Research, **46**, pp. 2636-2644, (2006).

[12] T. Hatada, H. Sakata, Psychological Visual Perception and Display, Television, **31**(4), pp. 245-255, (1977).

[13] S. Yano, M. Emoto, T. Mitsuhashi, Two Factors in Visual Fatigue Caused by Stereoscopic Hdtv Images, Displays, **25**, pp. 141-150, (2004).

[14] T. Yamaga, M. Yoshizawa, N. Sugita, M. Abe, N. Homma, Assessment of Fatigue Caused by Accommodation Convergence Mismatch While View. 3D Scenography, The Society of Instrument and Control Engineers, (2014).

[15] D. M. Hoffman, A. R. Girshick, K. Akeley, M. S. Banks, Vergence-Accommodation Conflicts Hinder Visual Performance and Cause Visual Fatigue, Journal of Vision, **8**(3), pp. 1-30, (2008).

[16] T. Shibata, J. Kim, D. M. Hoffman, M. S. Banks, The Zone of Comfort: Predicting Visual Discomfort With Stereo Displays, Journal of Vision, **11**(8), pp. 1-29, (2011).

[17] M. Emoto, S. Yano, The Influence of the Dissociation of Vergence and Accomodation on Visual Fatigue in Watching Stereoscopic Images, ITE, **56**(3), pp. 447-454, (2002).

[18] H. Urey, E. Erden, State of the Art in Stereoscopic and Autostereoscopic Displays, Proceedings of the IEEE, pp. 540-555, (2011).

[19] S. Pastoor, M. Wopking, 3-D Displays: a Review of Current Technologies, Proceedings of IEEE Computer Society, pp. 54-63, (2007).

[20] D. Zhao, B. Su, G. Chen, H. Liao, 360 Degree Viewable Floating Autostereoscopic Display Using Integral Photography and Multiple Semitransparent Mirrors, Optics Express 9812, **23**(8), pp. 10.1364/OE.23.009812, (2015).

[21] S. Iwasawa, S. Yano, M. Kawakita, M. Sakai, Y. Haino, M. Sato, H. Ando, Implementation of Projector Array-Based Autostereoscopic Display, ITE Technical Report, **34**(41), pp. 29-32, (2010).

[22] H. Yamada, H. Yabu, K. Yoshimoto, H. Takahashi, Three-Dimensional Light Field Display With Overlaid Projection, IEEE Computer Society, (10.1109/IIH-MSP.2014.108 (2014)).

[23] Y. Xue, Y. Wang, Multi-User Autostereoscopic 2D/3D Switchable Flat-Panel Display, Journal of Display Technology, **10**(9), pp. 737-745, (2014).

[24] T. Zhao, X. Sang, X. Yu, X. Gao, P. Wang, Y. Liu, S. Xie, B. Yan, C. Yu, D. Xu, High Dense Views Auto-Stereoscopic Three-Dimensional Display Based on

Frontal Projection With Lla and Diffused Screen, Chinese Optics Letters, **13**(1), (011001.1-011001.3 (2015)).

[25] R. S. Brar, P. Surman, I. Sexton, R. Bates, W. K. Lee, K. Hopf, F. Neuman, S. E. Day, E. Willman, Laser-Based Head-Tracking 3D Display Research, Journal of Display Technology, **6**(10), pp. 531-543, (2010).

[26] K. Benzeroual, R. S. Allison, L. M. Wilcox, 3D Display Size Matters: Compensating for the Perceptual Effects of S3D Display Scaling, Proceedings of the IEEE Computer Vision and Pattern Recognition Workshops (CVPRW), pp. 45-52, (2012).

[27] S. F. Zang, Q. H. Wang, W. X. Zhao, J. Zhang, J. L. Liang, A Frontal Multi-Projection Autostereoscopic 3D Display Based on a 3D-Image-Guided Screen, Journal of Display Technology, **10**(10), pp. 882-886, (2014).

[28] H. G. Choo, M. Park, H. E. Kim, C. Bae, B. G. Chae, H. Kim, K. Moon, J. Kim, J. Hahn, Real-Time Pupil Tracking Backlight System for Holographic 3D Display, Chinese Optics Letters, **12**(6), pp. 060004-1 - 060004-4, (2014).

[29] P. C. Barnum, S. G. Narasimhan, T. Kanade, A Multi-Layered Display With Water Drops, ACM Transactions on Graphics, **29**(4), pp. 76:1-76:7, (2010).

[30] H. Gotoda, Implementation of an Auto Stereoscopic Dislay Using Multilayer Lcds, ITE Technical Report, **35**(35), pp. 1-4, (2011).

[31] C. Sun, X. Chang, M. Cai, J. Lie, An Improved Design of 3D Swept-Volume Volumetric Display, Journal of Computers, **9**(1), pp. 235-242, (2014).

[32] D. Teng, L. Liu, B. Wang, Generation of 360 Three-Dimensional Display Using Circular-Aligned Oled Microdisplays, Optics Express 2058, **23**(3), (10.1364/OE.23.002058).

[33] T. Yendo, T. Fujii, M. Tanimoto, M. P. Tehrani, The Seelinder: Cylindrical 3D Display Viewable From 360 Degrees, Journal of Visual Communication and Image Representation, **21**, (10.1016/j.vcir.2009.10.004).

[34] M. Gately, Y. Zhai, A Three Dimensional Swept Volume Display Based on Led Arrays, Journal of Display Technology, **7**(9), pp. 503-514, (2011).

[35] A. Jones, I. Mcdowall, H. Yamada, M. Bolas, P. Debevec, Rendering for an Interactive 360 Light Field Display, ACM Transactions on Graphics, **26**(3), pp. 40.1-40.10, (2007).

[36] Y. Takaki, S. Uchida, Table Screen 360-Degree Three-Dimensional Display Using a Small Array of High-Speed Projectors, Optics Express, **20**(8), pp. 8848-8861, (2012).

[37] S. Eitoku, T. Tanikawa, Y. Suzuki, Display Composed of Water Drops for Filling Space With Materialized Virtual Three-Dimensional Objects, Proceedings of the IEEE Virtual Reality Conference, pp. 165-172, (2006).

[38] A. Nakatani, I. Fujishiro, H. Ishikawa, H. Saito, Resource-Aware Rendering for Laser Plasma Scanning 3D Display Devices Using Surface Descriptors, TVRSJ, **17**(4), pp. 419-428, (2012).

[39] H. Ishikawa, H. Sato, Point Cloud Representation of 3D Shape for Laser-Plasma Scanning 3D Display, Proceedings of the IEEE Industrial Electronics, pp. 1913-1918, (2008).

[40] J. Watanabe, N. Sakamoto, A. Noritake, T. Maeda, S. Tachi, Study on Visual Persistence of Saccade-Induced Afterimage, ITE, **58**(12), pp. 1808-1814, (2004).

[41] H. Ishikawa, H. Saito, Object Representation Using Sequence for Laser Plasma 3D Display, ITE, **63**(5), pp. 665-672, (2009).

[42] R. Hirayama, H. Nakayama, T. Kakue, T. Shimobaba, T. Ito, Development of Volumetric Display Based on Multi-Bit Color Led, Proceedings of the IEEE Circuits and Systems (APCCAS), pp. 547-550, (2014).

[43] Y. Tokuda, K. Nishimura, Y. Suzuki, T. Tanikawa, M. Hirose, A Proposal for a Vortex Ring Display, Information Processing Society of Japan, **50**(12), pp. 2853-2862, (2009).

[44] A. Hirata, K. Suzuki, Three Dimensional Display-Types and Application to Television, Journal of the Institute of Television Engineers of Japan, **41**(7), pp. 610-618, (1987).

[45] M. Imura, A. Yagi, Y. Kuroda, O. Oshiro, Multi-Viewpoint Interactive Fog Display, The 21st International Conference on Artificial Reality and Telexistence, 170, (2011).

[46] S. K. Nayar, V. N. Anand, 3D Display Using Passive Optical Scatterers, Computer, **40**(7), pp. 54-63, (2007).

[47] I. Troitski, Laser-Induced Image Technology (Yesterdays, Today, and Tomorrow), Proceedings of SPIE, pp. 293-301, (2005).

[48] http://www.musashino-kikailaser.jp/images/laser01.pdf, (Last access, February 7th, 2016).

[49] G. Ye, A. State, H. Fuchs, A Practical Multi-Viewer Tabletop Autostereoscopic Display, IEEE ISMAR 2010 Science and Technology Proceedings, pp. 147-156, (2010).

[50] R. Horaud, B. Conio, O. Leboulleux, An Analytic Solution of the Perspective 4-Point Problem, Proceedings of the IEEE Computer Vision and Pattern Recognition, pp. 500-507, (1989).

[51] http://graphics.cs.msu.ru/en/node/909, (Last access, February 7th, 2016).

[52] T. Hatada, H. Sakata, Psychological Visual Perception and Display, Television, **31**(4), pp. 245-255, (1977).

[53] S. Aiba, Psychophysics of vision, Biophysics, **10**(6), pp. 259-267, (1970).

[54] R. Akizuki, T. Naemura, H. Ishikawa, H. Saito, 3 D content generation by fusing two graphics for Aerial 3D display, IEICE Technical Report, pp. 101-106, (2011).

[55] H. Ishikawa, Y. Sato, Relation between psychological scale in polyhedron recognition and 3-D object image entropy, IEICE Technical Report, pp. 41-48, (2000).

Appendix A Questionnaire

The original Japanese copy of the questionnaire is shown below.

Q1 大きさが段階的に大きくなっていき、最後に消える単純な立体物を模した３Ｄコンテンツがディスプレイの中央に表示されるので、その３Ｄコンテンツが消えるまで観察してください。次第に大きくなる立体物の形状を認識できた時点で、その名称を答えてください（例：球体、立方体など）。表示が消えるまでの間に、異なる形状に見えると判断された場合は、回答内容を変更してもかまいません。３Ｄコンテンツが表示されて消えるまでの手順を 6 回繰り返します。表示される形状は毎回ランダムに決定され、複数回同じ形状が表示される場合もあります。

Q2 ディスプレイ中央の水平面上に、直径と奥行き方向の位置がそれぞれ異なる２つの球体を左右に１つずつ配置した３Ｄコンテンツが表示されます。そして、左の球体は位置が固定され、右の球体は、上キーを押す度に一定距離奥に、下キーを押す度に一定距離手前に移動します。そこで、ご自身でキーボードの上下キーを自由に操作し、左右の球体の中心が奥行き方向で一致するよう、右側の球体を移動してください。この操作を、右の球体が左の球体よりも大きい場合と小さい場合を 2 回ずつ行います。どちらの場合が先に表示されるかはランダムに決定されます。また、右の球体の初期位置もランダムに決定されます。なお、1 回当たりの操作の制限時間は 1 分とします。

本設問はキーボードのエンターキーを押すとスタートし、再度エンターキー押すと終了します。左右の球が奥行き方向で一致したと判断した時に、２度目のエンターキーを押してください。これを４回繰り返します。

Q3 本実験における３Ｄコンテンツの観察を通して、どの程度目の疲労や酔いを感じたか口頭で答えてください。２つの質問を行います。まず、本実験におけるディスプレイの観察を通して、どの程度目の疲労を感じたかを、次の４段階でお答えください。☒ 全く感じなかった、☒少し感じた、☒感じた、☒非常に感じたその回答に至った理由があればお答えください。本実験におけるディスプレイの観察を通して、どの程度酔いを感じたかを、次の４段階でお答えください。☒全く感じなかった、☒少し感じた、☒感じた、☒非常に感じたその回答に至った理由があればお答えください。

Q4 表示されている動画の見え方や挙動について、30 秒程度で自由に説明してください。

Q5 実験全体について何か意見や感想などがあれば、お答えください。

Appendix B Projection Results of Primitive Shapes

The images of the 6 shapes used in Q1 acquired at each step, with Line Scan Method and Structured-Light Method are shown in the figures written below:

Line Scan Method

Sphere: Images acquired at each step are shown in Fig. B.1.

Cube: Images acquired at each step are shown in Fig. B.2.

Cuboid: Images acquired at each step are shown in Fig. B.3.

Pyramid: Images acquired at each step are shown in Fig. B.4.

Cone: Images acquired at each step are shown in Fig. B.5.

Cylinder: Images acquired at each step are shown in Fig. B.6.

Structured-Light Method

Sphere: Images acquired at each step are shown in Fig. B.7.

Cube: Images acquired at each step are shown in Fig. B.8.

Cuboid: Images acquired at each step are shown in Fig. B.9.

Pyramid: Images acquired at each step are shown in Fig. B.10.

Cone: Images acquired at each step are shown in Fig. B.11.

Cylinder: Images acquired at each step are shown in Fig. B.12.

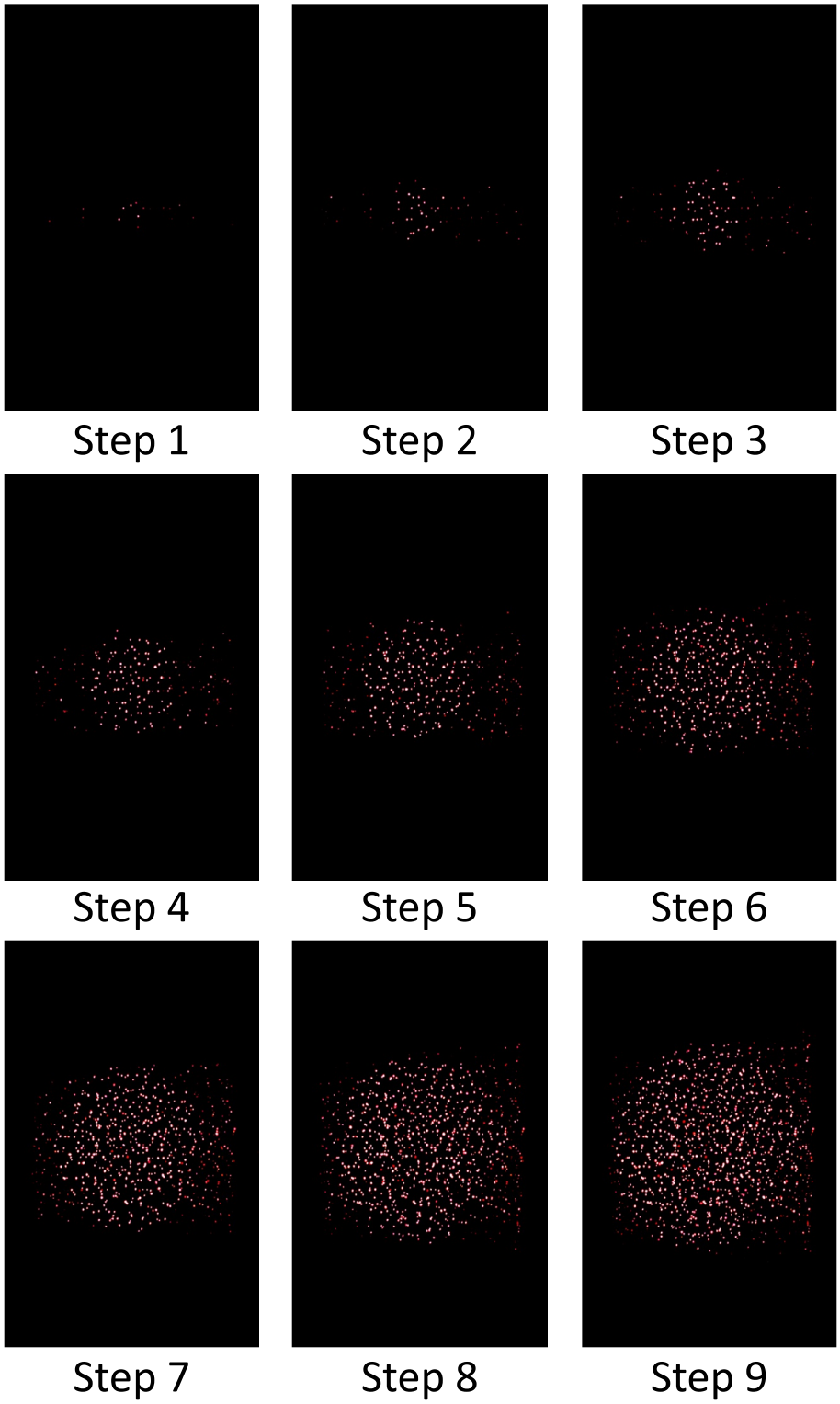

Fig. B.1: Images acquired at each step of the size increase of a sphere using Line Scan Method.

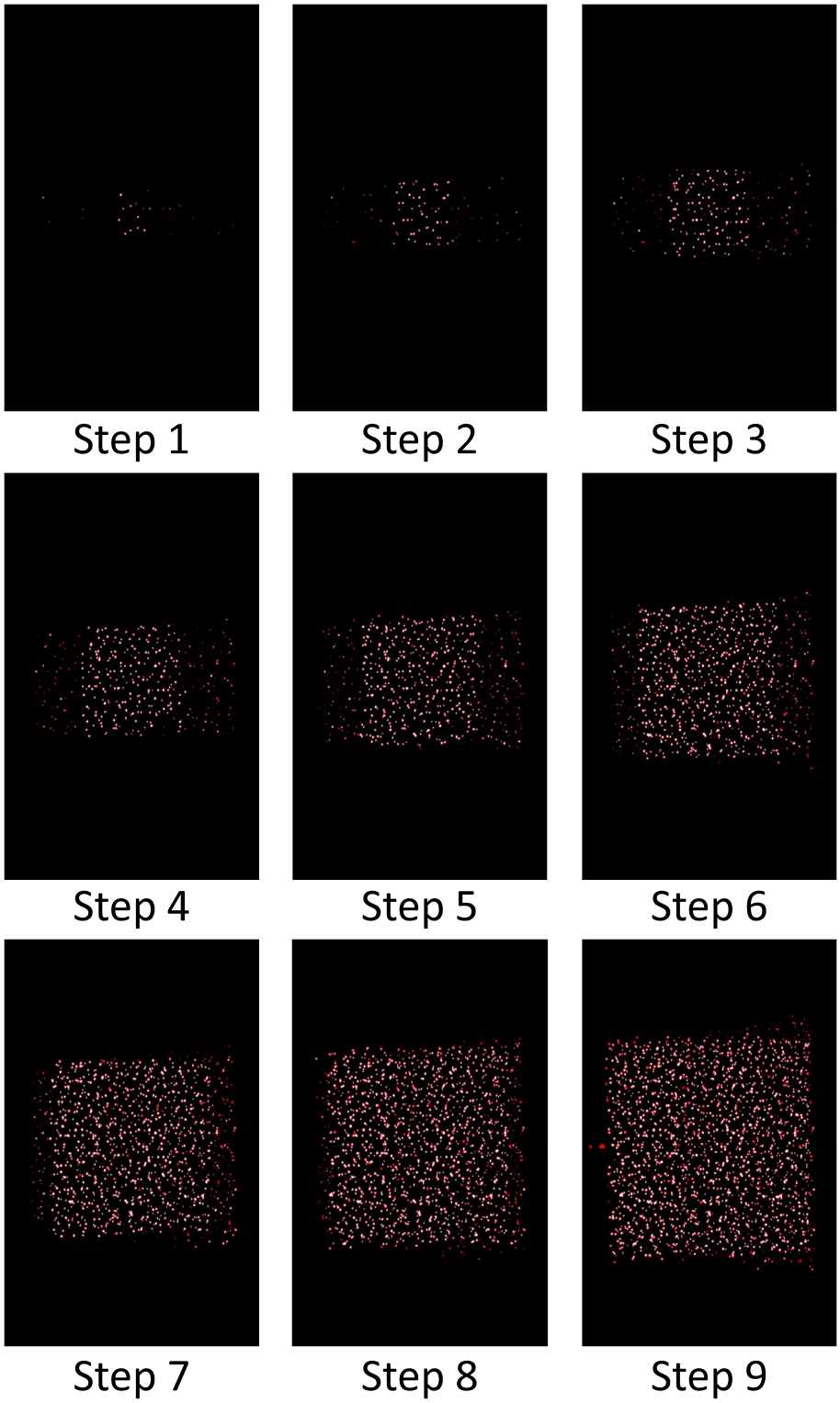

Fig. B.2: Images acquired at each step of the size increase of a cube using Line Scan Method.

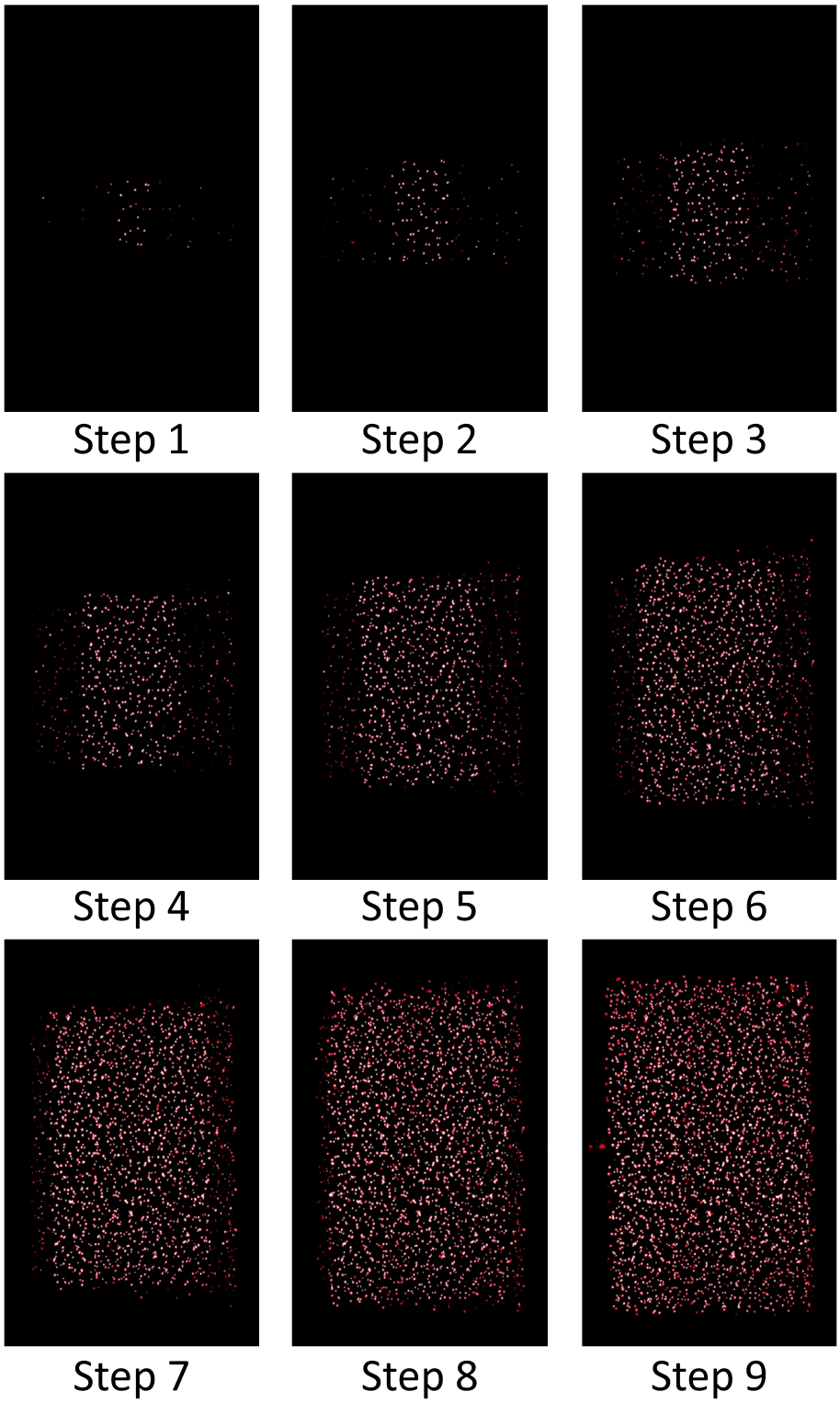

Fig. B.3: Images acquired at each step of the size increase of a cuboid using Line Scan Method.

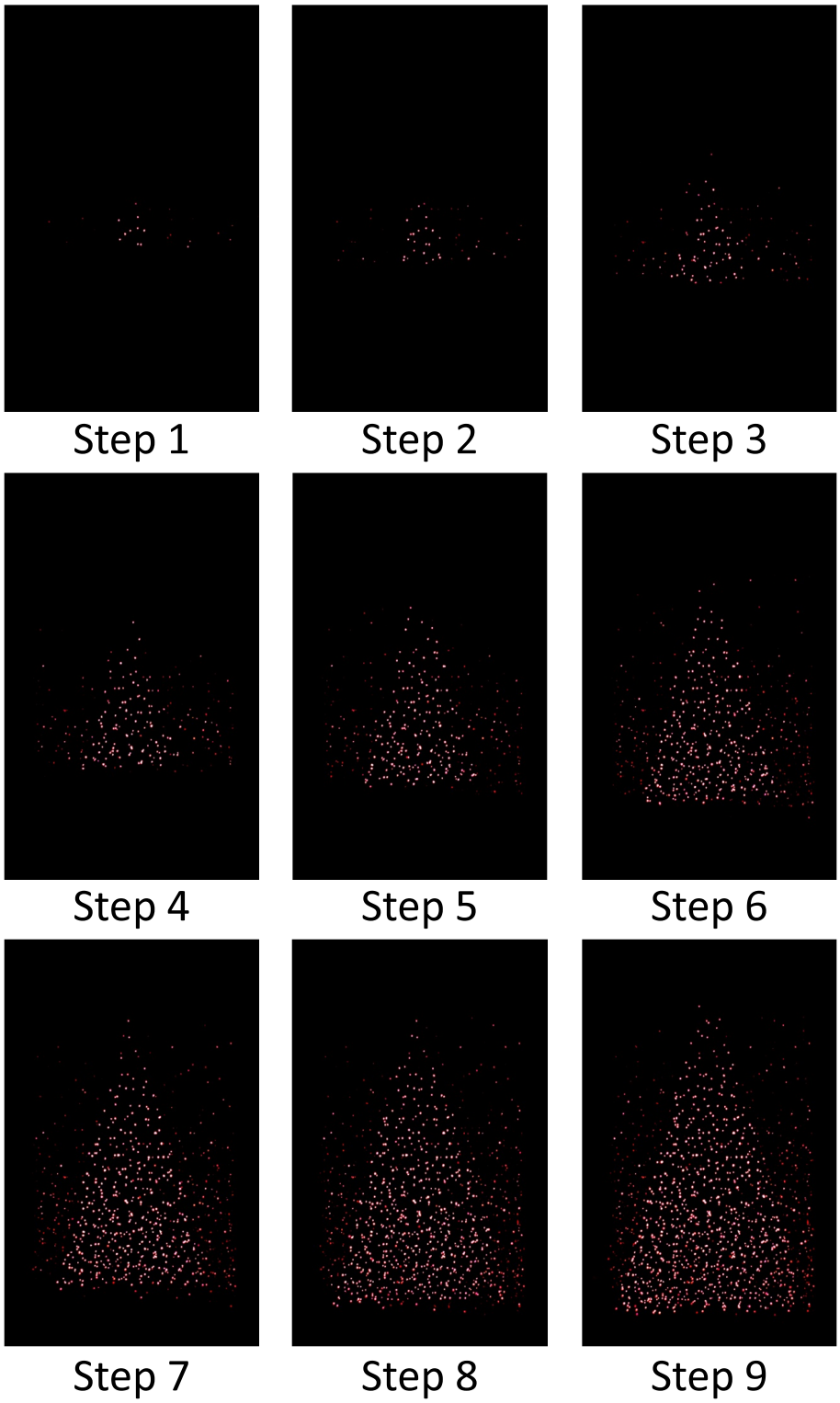

Fig. B.4: Images acquired at each step of the size increase of a pyramid using Line Scan Method.

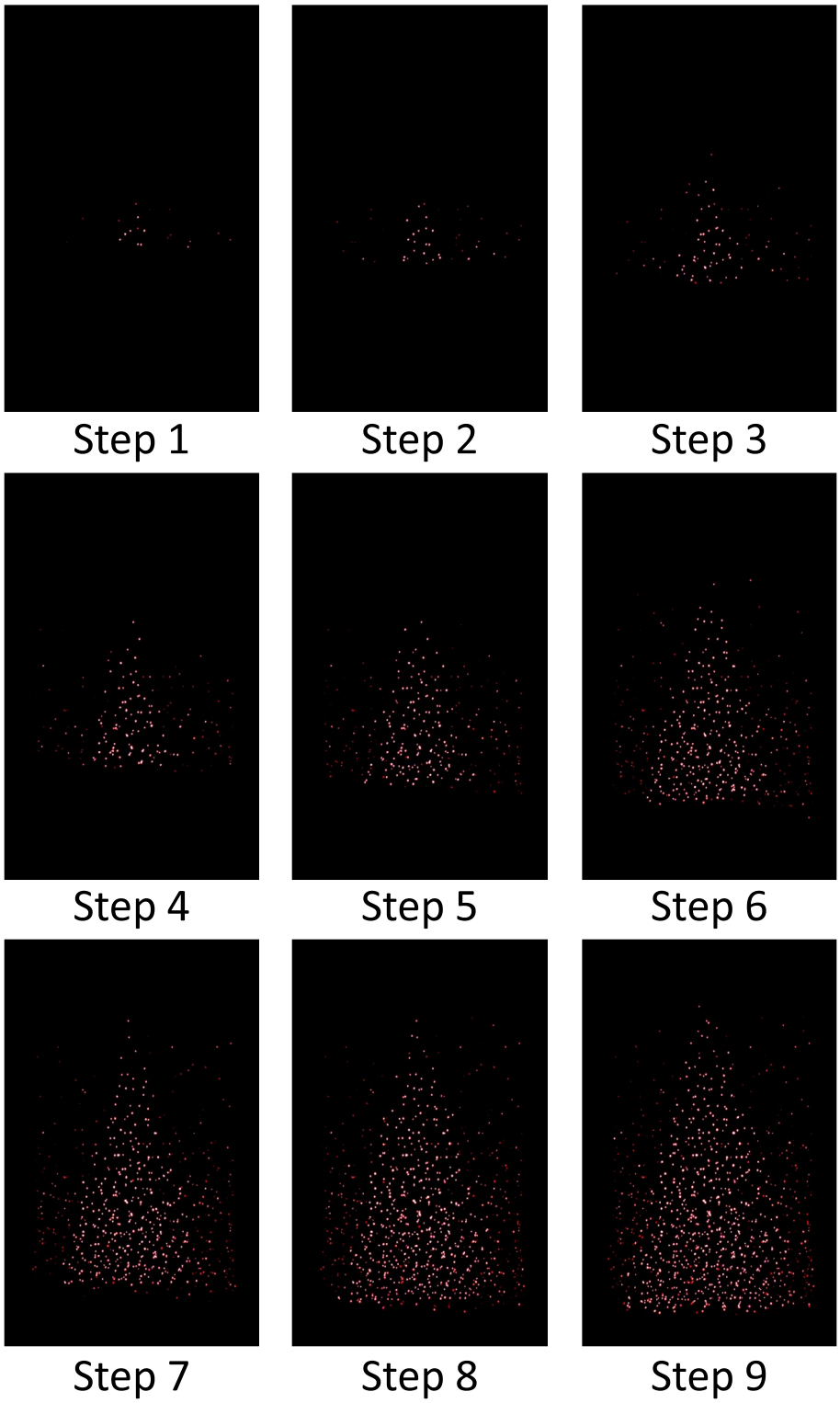

Fig. B.5: Images acquired at each step of the size increase of a cone using Line Scan Method.

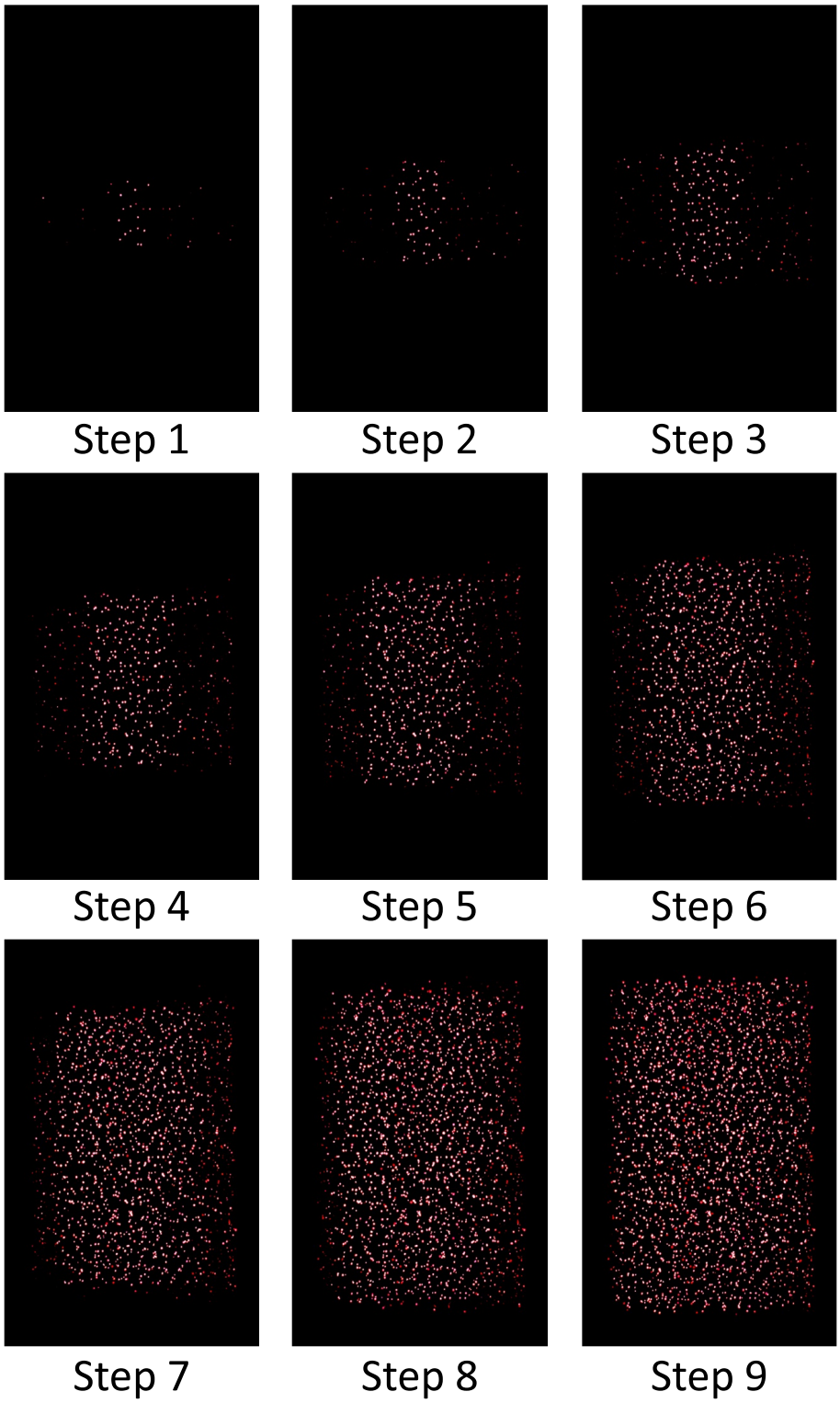

Fig. B.6: Images acquired at each step of the size increase of a cylinder using Line Scan Method.

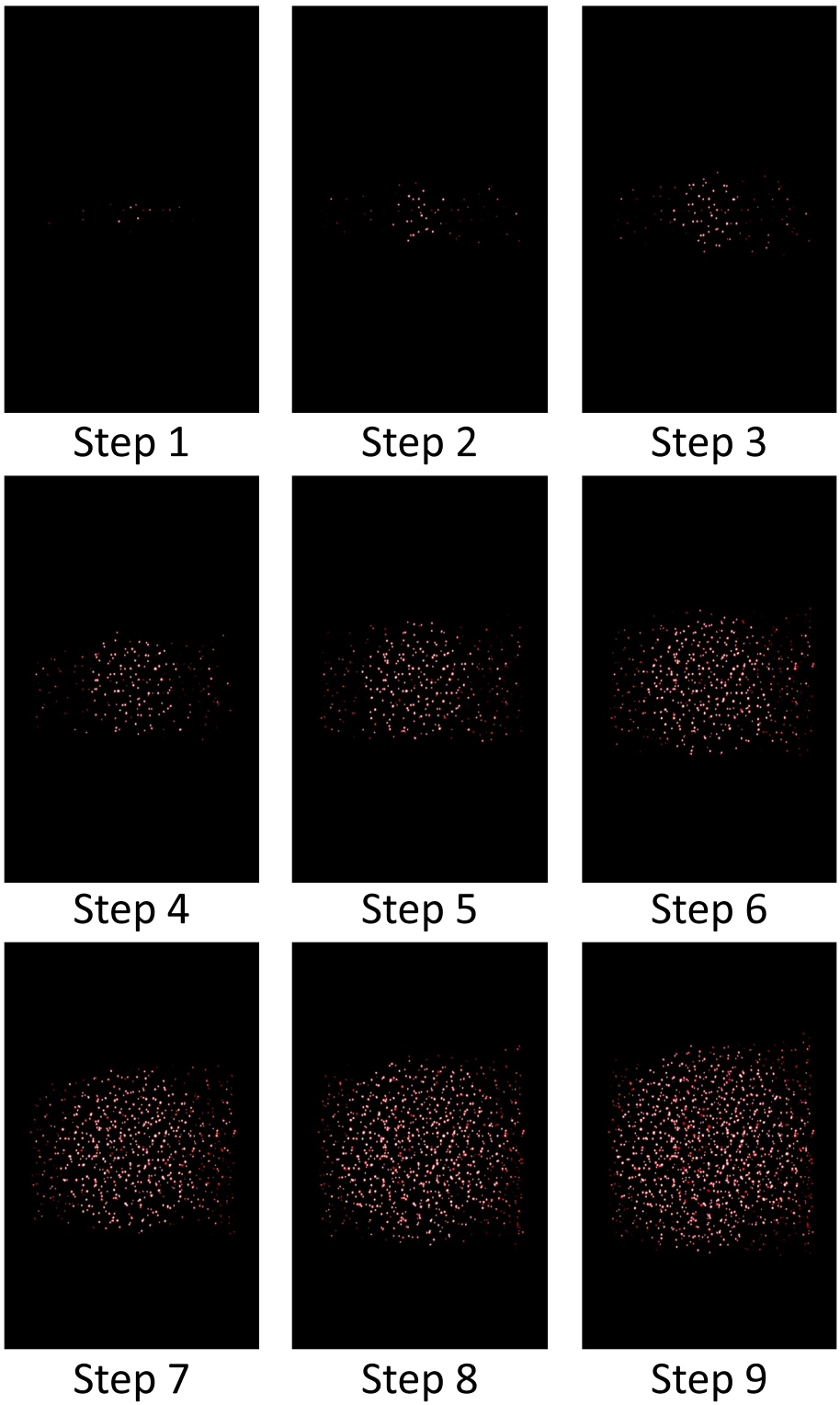

Fig. B.7: Images acquired at each step of the size increase of a sphere using Structured-Light Method.

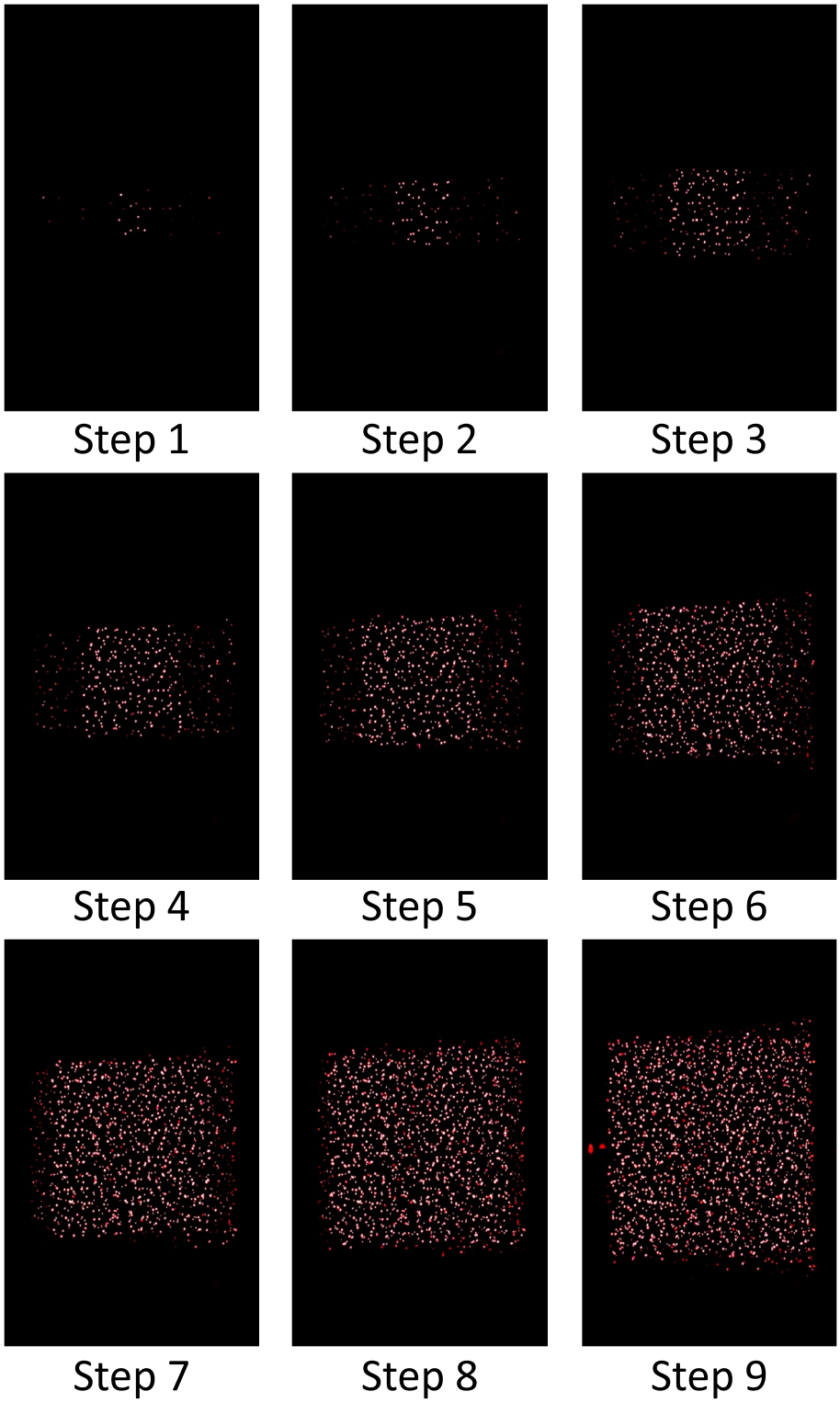

Fig. B.8: Images acquired at each step of the size increase of a cube using Structured–Light Method.

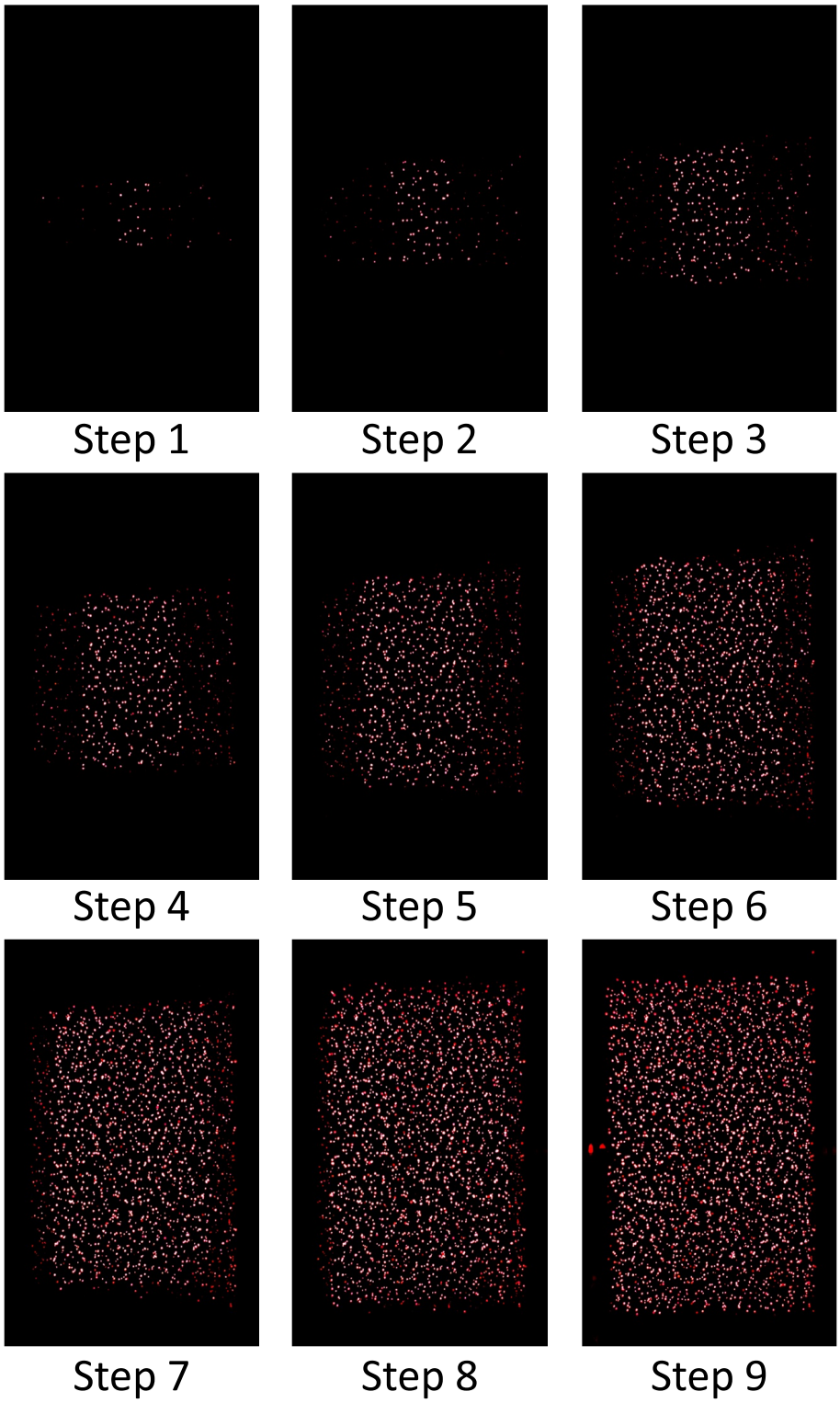

Fig. B.9: Images acquired at each step of the size increase of a cuboid using Structured-Light Method.

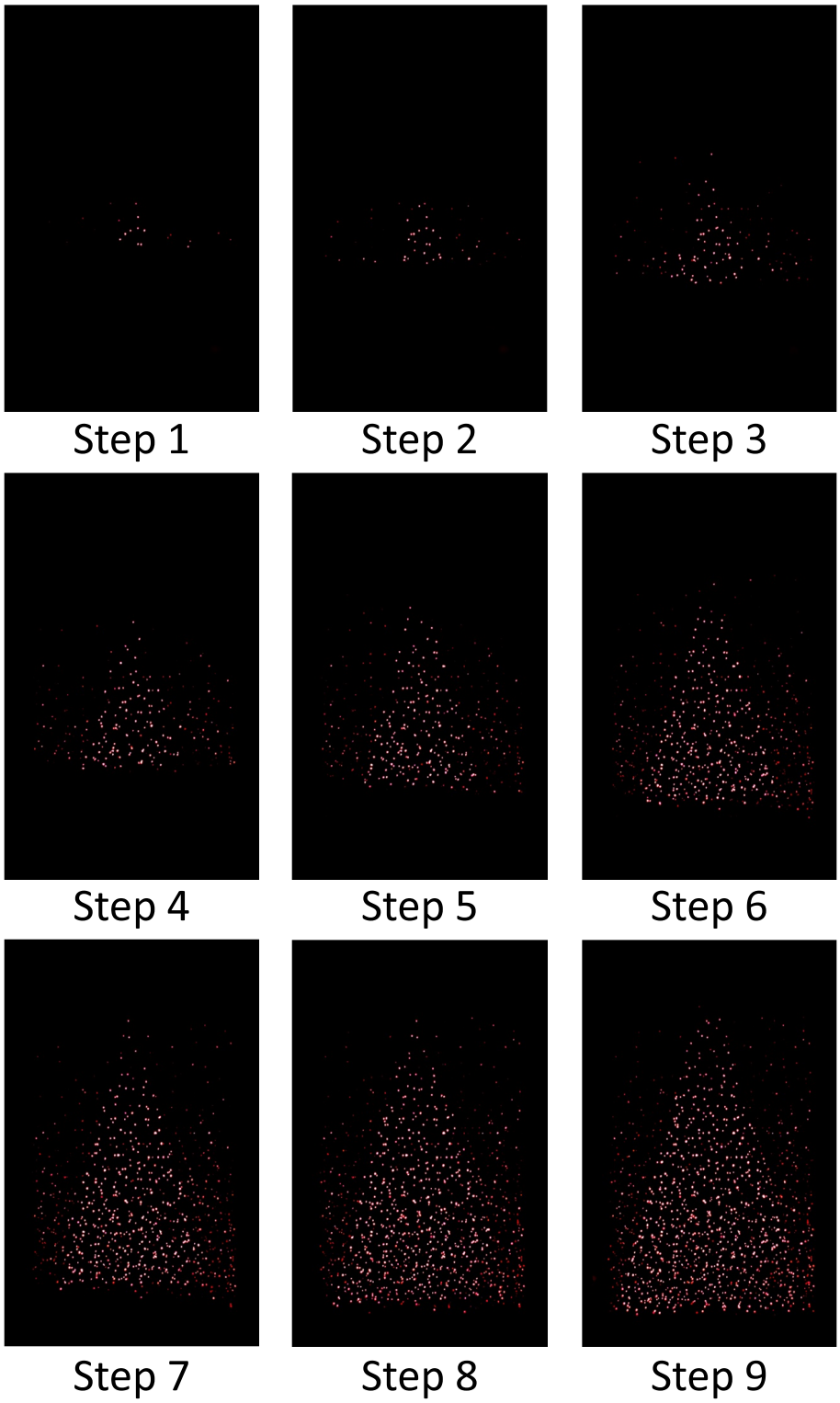

Fig. B.10: Images acquired at each step of the size increase of a pyramid using Structured-Light Method.

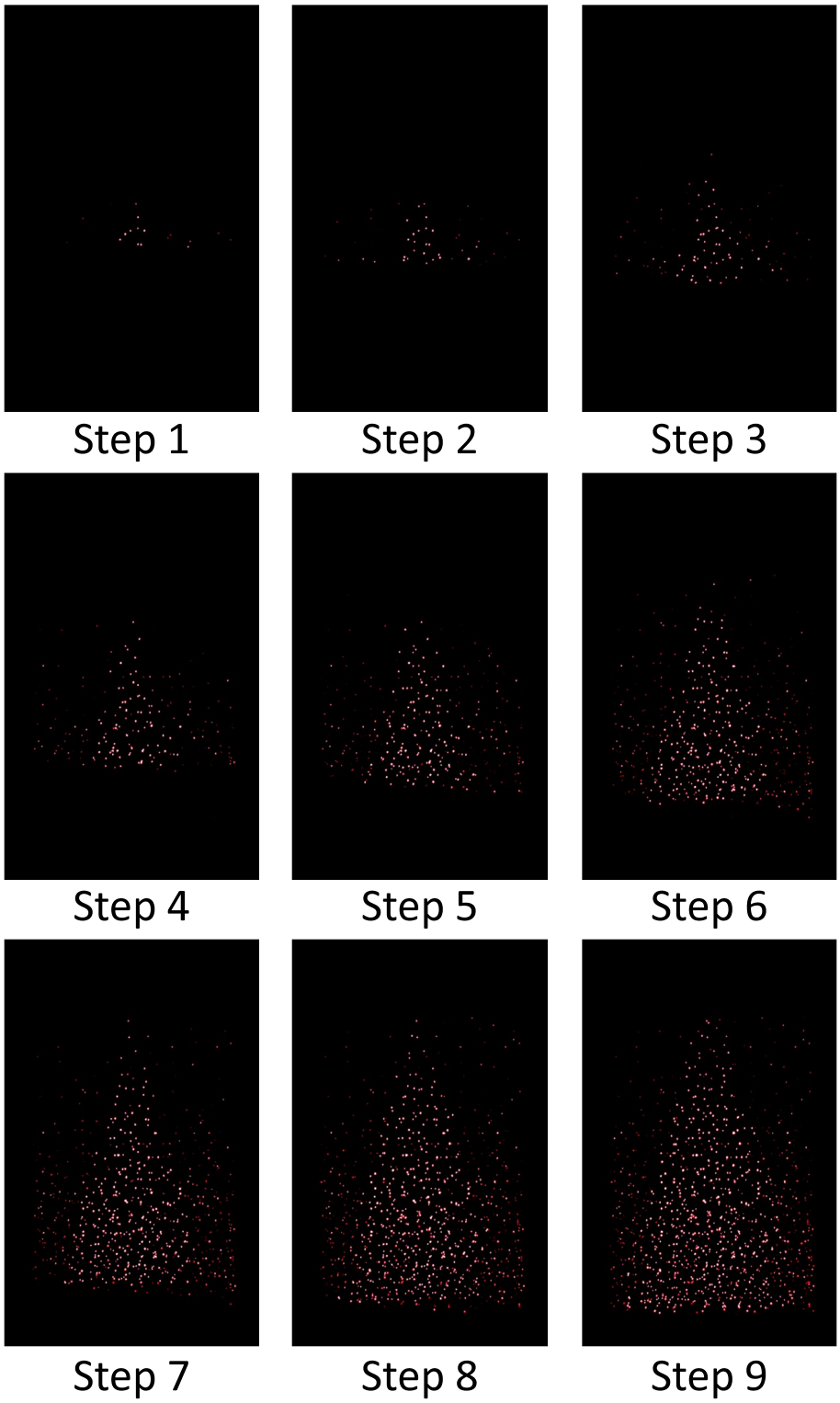

Fig. B.11: Images acquired at each step of the size increase of a cone using Structured-Light Method.

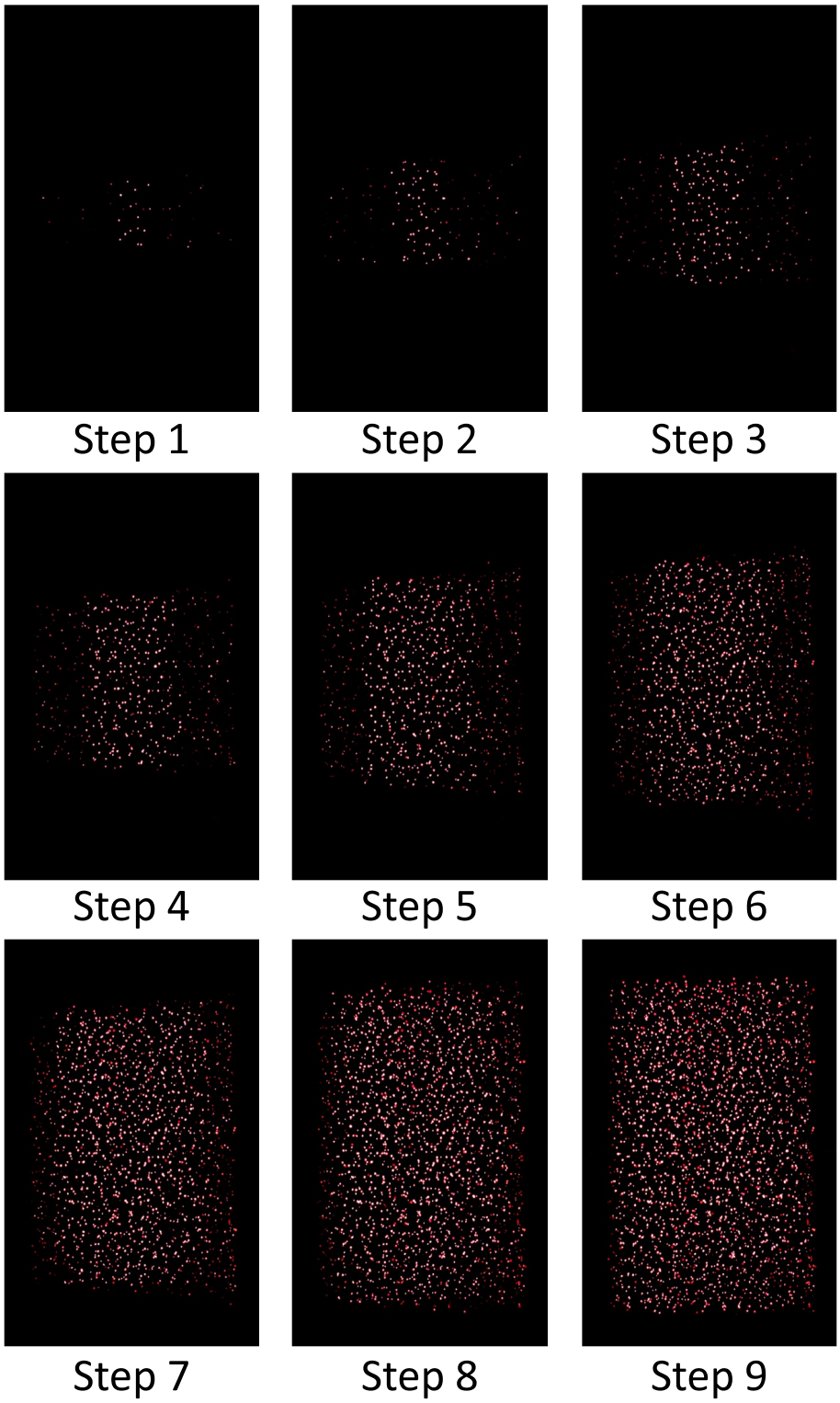

Fig. B.12: Images acquired at each step of the size increase of a cylinder using Structured-Light Method.

Appendix C Descriptions for the questionnaire

The original Japanese copy of the descriptions for Q3, Q4 and Q5 of the questionnaire are shown in Table C.1, Table C.2 and Table C.3, respectively.

Table C.1: Descriptions for the cause of visual fatigue and sickness in Q3 of each participant

被験者番号	眼の疲労の原因	酔いの原因
1	問1で、表示されている立体物全体を見ようとするも、1点1点にピントがあってしまった。全体と発光点単位でピントを調節することになり疲れた。	-
2	奥行きを合わせる問いで、左と右の大きさが違うから目を凝らす必要があった。それで少しつかれた。	点滅して形状が変わるからそれで少し酔いを感じたかも(しれない)。
3	-	提示時間が短いから疲労は感じなかった。だけど、問2で自分で球を操作した時に、発光のONとOFFが変化する点だけに着目してしまうと酔った。どの点が光っているか光っていないのかを意識した時に、少し酔った。
4	-	-
5	光を注視し続けることに少し疲れた。	-
6	-	照射している物体の周りに、明るくない点が沢山見えて、その影響で酔った。
7	-	-
8	-	-
9	コンテンツのせいか、部屋が乾燥しているせいか分からないが、少し疲労を感じた。	-
10	-	-

Table C.2: Descriptions for Q4 of each participant

被験者番号	回答
1	雪が降っている中に雪だるまがいる。赤いバケツをかぶっている。雪がどんどん、雪だるまがうまるように積もっていく。最後は赤いバケツがギリギリうまるくらいまで積もった
2	水色の点が上のほうでぐるぐるしてる。下のほうにも青い点が上にたまっていってる。真ん中に赤い球がある。
3	直方体がある。上半分が点滅、同時に点滅しているのではなく、構成している点が回りながら点滅している。時計回りに。赤い部分が直方体の真ん中にある。
4	真ん中に赤い物体が見える。下の方に雪だるまのようなものが見える。大きい物体の上に小さい物体が乗っている。全体的に下のほうが濃度が高くて、だんだん下の方の濃度が上がっていっているなんとなく雪が積もっていっているように見える。赤い所までつもったようにみえる。
5	直方体がある。上の1/4が点滅、パラパラしている。右の方も点滅しているようにみえる。真ん中に赤い球が見える。下から点が上がってきている。左の中央に球が見える。
6	真ん中の少し上に赤い球体がある。左下に、雪だるまがある。上の方で雪か雨のようなものが降っている。下の方が段々積もっていく。
7	真ん中に赤い球体が浮かんでいる。左のほうに雪だるまのような物体がある。雪がどんどん積もっていくように見える。上の方にキラキラ光っているのが見える。
8	雪だるまがいて雪が降っているように見える。真ん中に赤い塊がある。下の白いところはあまり動いていないけど、上のほうの白い部分は動いている。下の方がどんどん積もっているようにみえる
9	雪だるまがある。雪が降っている。雪が積もっていっている。雪だるまの下のほうが埋もれていく感じ。
10	下に緑と白い光がある。中心の少しうえに赤い球か丸がある。上の方は点滅をしている。

Table C.3: Descriptions for Q5 of each participant

被験者番号	回答
1	問1の4問目はすごく迷った。立体物の表示は角の有無を判断するのが難しかった。動画の表示の時は、「モノ」が表示されていたため、脳内で補完できたためわかりやすかったし答えやすかった。
2	問1が、輪郭がハッキリしない形状がいくつかあった。円錐と正四面体の区別がつきにくかったから高さで判断した。問2は、左右の大きさが違うから奥行きを合わせるのが難しかった。
3	なんとなく、点で立体をとらえるということがいがいと難しい。装置云々ではなくて、人間の知覚の仕組みとして難しいのかなと感じた。本来見えにくい状態の中では見えやすいと感じた。直方体と円柱や四角錐と円錐などの差がわかりにくかった。手前は左右の端の違いがみえにくかった。
4	綺麗でした。特に見え方に問題はなかった。
5	最初のデモで表示される立体の大きさが異なる事が気になった。大きさを統一したほうがわかりやすい気がした。
6	酔いの原因。小さい形状から大きい形状に変化する間、立体物の周りに関係ない発光点が見えた。それをなくせたらもっとハッキリ見えてわかりやすいのかもと感じた。ディスプレイがもっと大きくなれば、もっと印象に残る気がした。
7	特に無し。
8	円錐と四角錐の違いがわからなかった。
9	すごいなー。円錐と四角錐とかの底面の形が認識しづらかった。2次元の平面として認識しづらかった。問2くらいで、円柱かと直方体かで迷ったけど、あれ円柱だったな。
10	特に無し